CHAPTER 2

Halogenated Very Short-Lived Substances

Lead Authors:
K.S. Law
W.T. Sturges

Coauthors:
D.R. Blake
N.J. Blake
J.B. Burkholder
J.H. Butler
R.A. Cox
P.H. Haynes
M.K.W. Ko
K. Kreher
C. Mari
K. Pfeilsticker
J.M.C. Plane
R.J. Salawitch
C. Schiller
B.-M. Sinnhuber
R. von Glasow
N.J. Warwick
D.J. Wuebbles
S.A. Yvon-Lewis

Contributors:
A. Butz
D.B. Considine
M. Dorf
L. Froidevaux
L.J. Kovalenko
N.J. Livesey
R. Nassar
C.E. Sioris
D.K. Weisenstein

CHAPTER 2

HALOGENATED VERY SHORT-LIVED SUBSTANCES

Contents

SCIENTIFIC SUMMARY

Definition of Halogenated Very Short-Lived Substances (VSLS)

- Very short-lived substances (VSLS) are defined as trace gases whose local tropospheric lifetimes are comparable to, or shorter than, tropospheric transport time scales, such that their tropospheric distributions are non-uniform. In practice, VSLS are considered to have atmospheric lifetimes of less than 6 months. We consider only halogenated VSLS, i.e., those that contain bromine, chlorine, or iodine. We consider VSLS to include very short-lived (VSL) source gases (SGs), halogenated organic and inorganic product gases (PGs) arising from SG degradation, and other sources of tropospheric inorganic halogens.

Importance of VSLS for Stratospheric Halogen and Ozone Trends

Bromine

- **Our quantitative understanding of how halogenated very short-lived substances contribute to halogen levels in the stratosphere has improved significantly since the last Assessment (WMO, 2003), with brominated VSLS believed to make a significant contribution to total stratospheric bromine and its effect on stratospheric ozone. Various lines of evidence show that brominated VSLS contribute about 5 ppt (with estimates ranging from 3 to 8 ppt) to total stratospheric inorganic bromine (Br_y)**:
  - Estimates of total stratospheric Br_y derived from different observations of bromine monoxide (BrO) relevant to the late 1990s are about 18 to 25 parts per trillion (ppt). This is greater than the 16 to 17 ppt of bromine delivered to the stratosphere by "long-lived" brominated source gases (i.e., the halons and methyl bromide, CH_3Br) during this period.
  - Measurements of organic brominated very short-lived source gases (VSL SGs) in the tropical upper troposphere amount to about 3.5 ppt. Product gases (from SG degradation) and other sources of tropospheric inorganic bromine may also contribute comparable amounts.

- **The inclusion of additional stratospheric Br_y from VSLS in models leads to larger ozone destruction at midlatitudes and polar regions compared with studies including only long-lived bromine source gases.** In both regions, the enhanced ozone loss occurs in the lower stratosphere via interactions of this bromine with anthropogenic chlorine. Midlatitude ozone loss is most enhanced during periods of high aerosol loading. Ozone loss through cycles involving bromine and odd-hydrogen (HO_x) is also enhanced at midlatitudes under all conditions, becoming comparable with ozone loss by HO_x cycles alone. This additional amount of stratospheric bromine has not, to date, been routinely included in model calculations of midlatitude ozone depletion.

- **Levels of stratospheric Br_y continue to show evidence for a trend that is consistent with that of tropospheric total bromine.** Further studies are required to determine if the recent decline in tropospheric bromine is reflected in stratospheric bromine abundance.

Iodine

- **It is unlikely that iodine is important for stratospheric ozone loss in the present-day atmosphere.** There is little evidence for inorganic iodine, in the form of iodine monoxide (IO), in the lower stratosphere at concentrations above about 0.1 ppt. This difference in behavior compared with bromine may be partly attributed to the short photochemical lifetime of iodine SGs, their lower abundance, and aerosol uptake of iodine oxides.

Chlorine

- **The sum of the chlorine content from VSL SGs in the tropical upper troposphere is currently estimated to be about 50 ppt, on the basis of available observations.** While a 50 ppt contribution to total inorganic stratospheric chlorine (Cl_y) from VSLS represents only 1 to 2% of Cl_y from long-lived source gases (~3500 ppt), it would represent a significant contribution compared with the background Cl_y from methyl chloride of about 550 ppt (Chapter 1).

- **Phosgene ($COCl_2$), which can be produced from chlorinated VSL SGs as well as long-lived chlorine gases, has been observed at levels of around 20 to 25 ppt in the tropical upper troposphere.** The contribution of this gas to stratospheric Cl_y (up to about 40 to 50 ppt) is not currently included in most models.

- **Analyses of upper stratospheric hydrogen chloride (HCl) measurements from satellite instruments are generally consistent with a possible contribution of VSLS to stratospheric Cl_y.** Further improvements in HCl measurement accuracy are required to quantify this contribution.

Sources and Trends of Halogenated Very Short-Lived Source Gases

Bromine

- **The majority of known brominated VSL SGs are of natural origin. A few brominated VSLS have almost exclusively anthropogenic sources, notably n-propyl bromide (n-PB).** Some have small contributions from anthropogenic sources, e.g., certain brominated trihalomethanes.

- **Most brominated VSL SGs are emitted from the ocean, with higher emissions in tropical coastal regions.** Sea surface supersaturations of some gases, due to production by marine microorganisms, have been found to be elevated in the tropical open ocean. High concentrations in air have been observed near coasts over tropical and temperate waters.

- **Inorganic tropospheric sources of bromine, such as sea salt and volcanoes, may also contribute to inorganic bromine in the free troposphere.** Some fraction of this contribution could be subsequently transported to the stratosphere.

- **There is no evidence for a trend in the sum of brominated VSL SGs during the latter half of the 20th century**. This is according to trend reconstructions from firn air studies, and reflects their predominantly natural origins. The exceptions are some trihalomethane species, which have increased slightly in the Northern Hemisphere, possibly due to small anthropogenic sources.

Iodine

- **Iodinated VSLS are exclusively of natural origin in the present-day atmosphere, although the possibility of deliberate future anthropogenic use of new SGs exists.** A notable example is the proposed use of trifluoroiodomethane (CF_3I).

- **Iodinated VSL SGs are emitted from the ocean, with higher emissions in tropical ocean regions.** Emissions in the marine boundary layer are dominated by iodomethanes such as methyl iodide (CH_3I) and chloroiodomethane (CH_2ClI), which are produced both by marine organisms and by abiotic photochemical processes in surface waters. There is some evidence for enhanced marine emissions of iodinated VSL SGs in the tropics and subtropics, and also in regions of high productivity in coastal zones.

Chlorine

- **Chlorinated VSL SGs originate largely from anthropogenic emissions, although natural sources also contribute.** Their principal emissions are, therefore, more likely to be located at northern midlatitudes.

- **There is evidence for significant recent declines in concentrations of some chlorinated VSL SGs**, notably chloroform, dichloromethane, and tetrachloroethene.

Transport, Lifetimes, and Sinks of Halogenated VSLS

- **The predominant pathways for VSLS transport into the upper troposphere are likely to be in tropical convection regions, co-located with high emissions of VSLS over tropical oceans.** The fraction of a halogenated VSL SG that reaches the stratosphere via the source gas injection (SGI) pathway depends on its local chemical lifetime relative

to local transport time scales. Local SG lifetimes depend strongly on distributions of photochemical sinks and emission patterns and, as such, this limits the value of using a single "global" lifetime, as has often been used previously.

- **The amount of VSL PGs entering the stratosphere depends on the locations of their tropospheric production and loss processes.** The fraction of halogenated organic and inorganic PGs (produced from the decomposition of VSL SGs) that enters the stratosphere via the product gas injection (PGI) pathway depends on the location in the troposphere where the "parent" SG decomposes, and on subsequent loss processes such as (possibly irreversible) uptake of the PG on to aerosol/cirrus, or uptake of soluble species in precipitating clouds.

- **Many more data have become available on Henry's Law constants, uptake coefficients, and heterogeneous reactivity for a number of relevant surfaces and for a wide range of PGs.** Many uncertainties, however, still remain. Furthermore, incorporation of this knowledge into large-scale models is often lacking, thus limiting assessment of the location-dependent lifetimes and distributions of VSL PGs.

- **The impact of halogens from VSL SGs on column ozone is likely to be greatest in the extratropics. The dominant transport pathway is likely to be via quasi-horizontal transport from the tropical upper troposphere into the extratropical lowermost stratosphere.** While transport time scales via this pathway, and back to the troposphere, are relatively short (a few months), the short chemical lifetime of VSL SGs means that they will be fully degraded into inorganic halogen before they can be transported back into the troposphere. Quasi-horizontal transport from the tropical upper troposphere is highly seasonal, being much larger in the summer than winter.

- **Recent model simulations continue to suggest that, depending on lifetime and location of emissions, less than 1% of the VSL SG flux emitted at the surface enters the stratosphere via the SGI pathway, and a larger amount (up to a few percent) enters via the PGI pathway.** Studies are limited, however, by the ability of current global models to accurately simulate deep convection and transport into the lower stratosphere.

Ozone Depletion Potentials (ODPs) of Halogenated VSL SGs

- **There are no new evaluations for the ODP of n-propyl bromide (0.1 for tropical emissions, and 0.02-0.03 for emissions restricted to northern midlatitudes).**

- **New analyses suggest ODPs for CF_3I ranging from 0.011 to 0.018 for surface emissions at midlatitudes and in the tropics, respectively, which are higher than found previously (<0.008).** The model studies do not include uptake of iodine on aerosols, the inclusion of which could result in lower calculated values. If CF_3I were to be used for fire fighting/inhibition on aircraft, then it could be emitted at higher altitudes and the corresponding ODP would be larger.

- **New analyses confirm previous estimates that the ODP of a chlorinated VSL SG with a lifetime of ~25 days, one chlorine atom, and similar molecular weight to CFC-11, is about 0.003.**

Future Considerations for Halogenated VSLS

- **Possible future changes in anthropogenic VSLS.** If anthropogenic emissions increased, or if presently unused halogenated VSL SGs were to come into widespread commercial use, then halogenated VSLS would become of increased importance in affecting the future behavior of stratospheric ozone.

- **Delivery of VSLS to the stratosphere may change in the future in response to circulation changes.** The impact of natural halogenated VSLS might also be influenced by changes in the atmospheric circulation, which could, for example, increase the rate of delivery of VSL SGs and PGs into the stratosphere.

- **Natural VSLS emissions may respond to future changes in climate processes.** Natural sources could respond to changes in, for example, carbon dioxide (CO_2), land use, wind speed, and temperature. Our knowledge about these potential effects, and many other relevant feedbacks, is very limited at present.

2.1 INTRODUCTION

An important goal of previous Assessments was to quantify the impact of halogen-containing source gases on stratospheric ozone (e.g., WMO, 2003, 1999). In the last Assessment (WMO, 2003), the possible contribution of very short-lived substances (VSLS) was examined in detail in Chapter 2 (Ko and Poulet et al., 2003) and an approach for determining their Ozone Depletion Potentials (ODPs) was presented. VSLS are defined as substances that have atmospheric lifetimes comparable to, or less than, average tropospheric transport time scales of about 6 months. We consider halogenated very short-lived (VSL) organic source gases (SGs), and the halogenated organic and inorganic product gases (PGs) arising from the atmospheric degradation of VSL SGs, and also inorganic tropospheric halogen sources such as sea salt. Note that, in contrast to WMO (2003), sulfur-containing VSLS (e.g., dimethyl sulfide (DMS), and sulfur dioxide (SO_2)) are dealt with in Chapter 5 of this Assessment. Halogen atoms bound in SGs and intermediate degradation products are referred to as organic halogen, and the final products are referred to as inorganic halogen (containing no carbon) (e.g., hydrogen chloride (HCl), hydrogen bromide (HBr), chlorine monoxide (ClO), bromine monoxide (BrO), and iodine monoxide (IO)). Some important acronyms used in this chapter are defined in Box 2-1 below.

This chapter assesses the contribution of halogenated VSLS to the halogen loading in the stratosphere, as well as their possible contribution to past, present, and future stratospheric ozone loss, and considers the ODPs of substances that are, or might be, released as a result of human activities. Table 2-1 provides a list of the VSL SGs discussed in this chapter, together with an estimation of their local photochemical lifetimes and an indication of whether these gases have predominantly natural or anthropogenic origins and/or are proposed for new commercial applications. The majority of currently observable VSL SGs are thought to be partly or wholly of natural origin. A few halogenated VSLS have predominantly anthropogenic origins (e.g., n-propyl bromide (n-C_3H_7Br), 1,2-dibromoethane (CH_2BrCH_2Br), dichloromethane (CH_2Cl_2), tetrachloroethene (C_2Cl_4), and, to a lesser extent, chloroform ($CHCl_3$)). Currently, among the compounds listed in Table 2-1, only bromochloromethane (CH_2BrCl) is considered by the Montreal Protocol. In the light of observed

Box 2-1. Definition of Acronyms in Chapter 2

VSLS	Very Short-Lived Substances – organic and inorganic gases with lifetimes of less than 0.5 years
VSL	Very Short-Lived
SG/SGI	Source Gas / Source Gas Injection – refers to a halogenated organic source gas and its injection into the stratosphere
PG/PGI	Product Gas / Product Gas Injection – refers to the sum of the halogenated organic and inorganic degradation products for a particular source gas and their injection into the stratosphere
CFC	Chlorofluorocarbon
HCFC	Hydrochlorofluorocarbon
Br_x	Inorganic bromine oxides and radicals (e.g., BrO, atomic bromine (Br), bromine nitrate ($BrONO_2$))
Br_y	Total inorganic bromine (e.g., HBr, Br_x) resulting from degradation of bromine-containing organic-source gases (halons, methyl bromide, VSLS), and natural inorganic bromine sources (e.g., volcanoes, sea salt, and other aerosols)
Br_y^{VSLS}	The component of stratospheric Br_y from the degradation of brominated organic VSL SGs and tropospheric inorganic bromine sources (also called "additional" stratospheric Br_y)
$Br_y^{CH3Br+Halons}$	The component of stratospheric Br_y from the degradation of methyl bromide (CH_3Br) and halons
Cl_y	Total inorganic stratospheric chlorine (e.g., HCl, ClO) resulting from degradation of chlorine-containing source gases (CFCs, HCFCs, VSLS), and natural inorganic chlorine sources (e.g., sea salt and other aerosols)
Cl_y^{VSLS}	The component of stratospheric Cl_y from the degradation of chlorinated organic VSL SGs and tropospheric inorganic chlorine sources
I_y	Total inorganic stratospheric iodine (e.g., IO, iodine dioxide (OIO), hypoiodous acid (HOI)) resulting from degradation of iodine-containing source gases (VSLS), and natural inorganic sources (e.g., sea salt and other aerosols)
ODP	Ozone Depletion Potential
EESC	Equivalent Effective Stratospheric Chlorine

Table 2-1. Halogenated VSL source gases considered in this Assessment. New additions since WMO (2003) are shown in boldface; other compounds were assessed in WMO (2003).

Source Gas	Formula	Local Lifetime [a] (days)	Atmospheric Source [b]
Bromochloromethane	CH_2BrCl	150	N
Dibromomethane	CH_2Br_2	120	N
Bromodichloromethane	$CHBrCl_2$	78	N(A)
Dibromochloromethane	$CHBr_2Cl$	69	N(A)
1,2-Dibromoethane (ethylene dibromide, EDB)	CH_2BrCH_2Br	55	A
Bromoethane (ethyl bromide)	C_2H_5Br	34	A
Tribromomethane (bromoform)	$CHBr_3$	26	N(A)
1-Bromopropane (n-propyl bromide)	n-C_3H_7Br	13	A
Phosphorous tribromide ("PhostrEx")	PBr_3	<0.01	A[c]
Iodomethane (methyl iodide)	CH_3I	7	N
Trifluoroiodomethane	CF_3I	4	A[c]
Iodoethane (ethyl iodide)	C_2H_5I	4	N
2-Iodopropane (isopropyl iodide)	i-C_3H_7I	1.2	N
1-Iodopropane (n-propyl iodide)	n-C_3H_7I	0.5	N
Chloroiodomethane	CH_2ClI	0.1	N
Bromoiodomethane	CH_2BrI	0.04	N
Diiodomethane	CH_2I_2	0.003	N
Trichloromethane (chloroform)	$CHCl_3$	150	AN
Dichloromethane (methylene chloride)	CH_2Cl_2	140	A(N)
Tetrachloroethene (perchloroethylene, PCE)	C_2Cl_4	99	A
1,2-Dichloroethane	CH_2ClCH_2Cl	70	A
Chloroethane (ethyl chloride)	C_2H_5Cl	30	AN
Trichloroethene (trichloroethylene; TCE)	C_2HCl_3	4.6	A

[a] Local lifetimes are calculated as $(\tau_{local})^{-1} = (\tau_{OH})^{-1} + (\tau_J)^{-1}$, with [OH] = 1×10^6 molec cm^{-3}, T = 275 K, and a globally and seasonally averaged solar flux for 5 km altitude. See Section 2.3.2.

[b] N ≡ entirely natural atmospheric sources; A ≡ entirely anthropogenic atmospheric sources; AN ≡ combination of natural and anthropogenic atmospheric sources (a minor component shown in parentheses).

[c] Proposed application.

and predicted decreases in anthropogenic chlorofluorocarbons (CFCs), halons, etc., it is important to quantify the contribution of these VSLS to the natural background halogen loading in the stratosphere. Possible changes in the emissions of naturally occurring compounds, for example as a result of changing climatic factors, also need to be assessed.

In order to quantify the contribution of halogenated VSLS to halogen loading and ozone loss in the stratosphere, it is necessary to quantify the amount of VSLS entering the stratosphere directly via the SG injection (SGI) pathway, the degradation of SGs in the troposphere, transport of organic and inorganic PGs into the stratosphere via the PG injection (PGI) pathway, and also injection of inorganic tropospheric halogen. The contribution to, for example, total inorganic bromine (Br_y) in the stratosphere, which derives from the sum of VSL SGs (via the SGI and PGI pathways) and tropospheric inorganic halogen, is denoted Br_y^{VSLS}. The impact of such VSLS-derived inorganic halogen on stratospheric ozone loss will depend on the abundance of different halogen radicals and their efficiency at destroying ozone. Note that one atom of iodine is much more efficient at removing ozone than bromine, which in turn is more efficient than chlorine, as expressed by so-called α-factors (see Chapter 8 and Section 2.6.1 for further discussion).

Figure 2-1 shows a schematic of the processes influencing the transport, degradation, and loss of VSL SGs and PGs in the troposphere and stratosphere. It is an updated version of Figure 2-2 in Chapter 2, WMO (2003).

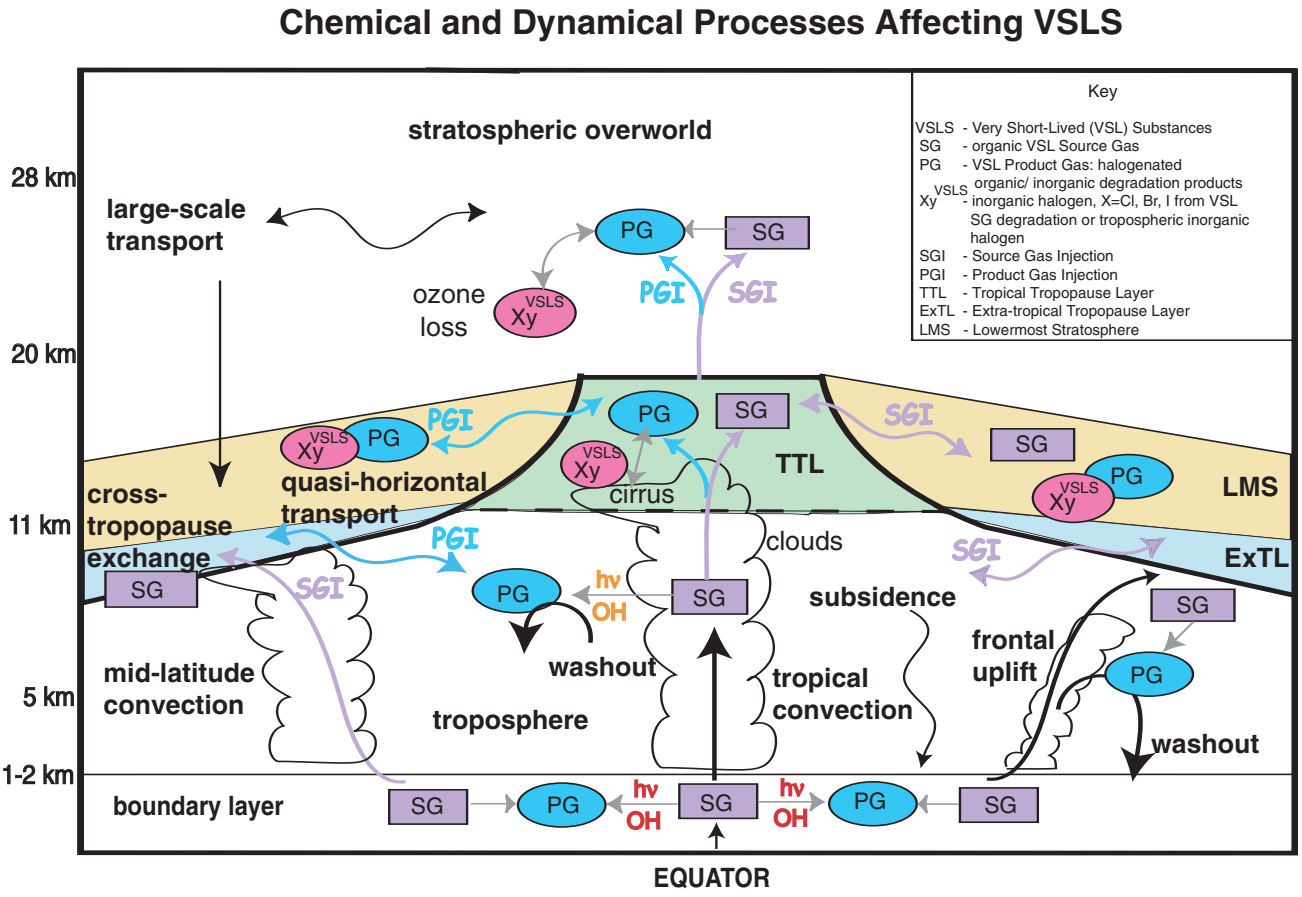

Figure 2-1. Schematic showing principal chemical and dynamical pathways transporting VSL source gases (SG) and organic/inorganic product gases (PG). Stratospheric halogen loading is maintained by transport of source gases followed by their degradation in the stratosphere (the SGI pathway), and transport of intermediate products and inorganic halogens produced in the troposphere (the PGI pathway). Tropospheric inorganic halogens can derive from degradation of VSL SGs, or from inorganic halogen sources. This figure is an update to Figure 2-2 in WMO (2003); courtesy of K.S. Law (Service d'Aéronomie/CNRS, France) and P.H. Haynes and R.A. Cox (University of Cambridge, U.K.).

In terms of chemical processes affecting VSLS, it is the degradation and loss of intermediate products, and inorganic multiphase heterogeneous chemistry, that remain the largest uncertainties in our knowledge about the fate of VSLS. The most efficient transport pathway is in the tropics, where there is rapid transport of air from the surface to the tropical tropopause layer (TTL) by deep convection, followed by transport of a small fraction into the stratosphere. Quasi-horizontal transport of air from the TTL into the lowermost stratosphere (LMS), as well as direct transport of air from the surface at midlatitudes either by frontal processes or deep convection, also need to be considered.

Given that VSL SGs and PGs have, by definition, shorter photochemical lifetimes than the large-scale transport time constant in the troposphere of roughly 6 months, mixing ratios (molar fractions) of both SGs and PGs (unless the latter are long-lived) are not uniform in the troposphere, and significant vertical as well as horizontal gradients can exist. Therefore, the amount of halogen entering the stratosphere may be sensitive to, among other factors, the location and timing of emission of VSL SGs, chemical degradation to produce organic and inorganic PGs, tropospheric transport processes, and location/altitude of removal of inorganic degradation products by wet deposition or other heterogeneous processes. Measured ratios of boundary layer (BL) to upper tropospheric (UT) mixing ratios of VSL SGs can provide an indication of the fraction available to be transported into the stratosphere. It has been noted previously that brominated and iodinated VSL SGs have been observed at mixing ratios of a few parts per trillion (ppt or pmol mol^{-1}) at the surface (WMO,

2003). An estimate was also given for the tropospheric abundance of chlorinated VSL SGs ranging from 50 to 100 ppt. This value also included phosgene (carbonyl dichloride, $COCl_2$), produced from the degradation of VSL SGs and long-lived chlorine gases. Apart from phosgene, very few measurements of organic VSL PGs are available in the free troposphere or stratosphere. Measurements of inorganic halogen are available and represent the final degradation products of halogen-containing sources gases (e.g., CFCs, halons, VSLS) as well as direct emission of inorganic halogens (e.g., sea salt, volcanoes).

The different radical families that are important for ozone loss in the midlatitude stratosphere are shown in Figure 2-2. At the levels of total inorganic iodine used in these model calculations (I_y = 0.1 ppt), which are representative of upper limits based on rather limited observa-

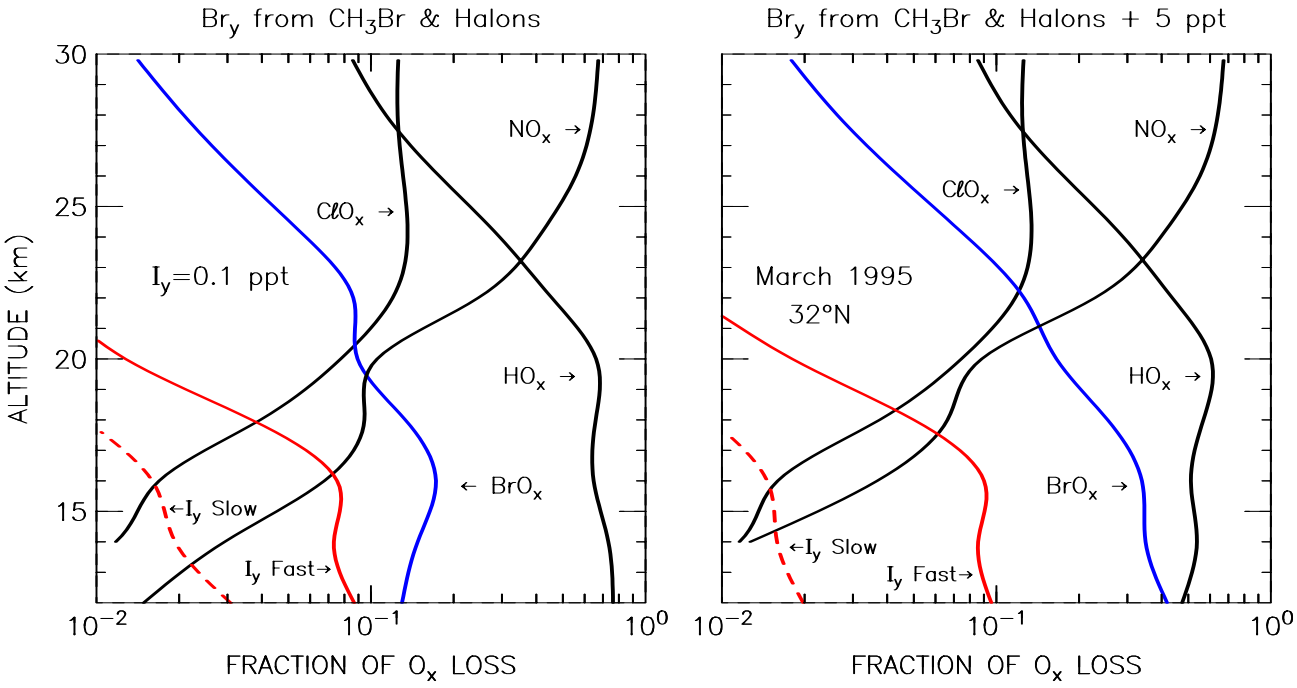

Figure 2-2. Calculated fractional contribution to odd oxygen (O_x) loss by catalytic cycles involving nitrogen (NO_x), hydrogen (HO_x), chlorine (ClO_x), bromine (BrO_x), and iodine (I_y Fast and Slow; see below) radicals for March 1995, 32°N. Jet Propulsion Laboratory (JPL) kinetics (Sander et al., 2006) were used, except for the rate constant of IO + HO_2, for which the expression given by Knight and Crowley (2001) representing all available data, 1.4×10^{-11}exp(554/T), was used (this is the same rate constant as given by the February 2006 International Union of Pure and Applied Chemistry (IUPAC) evaluation, posted at http://www.iupac-kinetic.ch.cam.ac.uk/). Total inorganic stratospheric iodine was set equal to 0.1 ppt, the upper limit reported by Bösch et al. (2003) and Butz (2006). For the left-hand panel, other model inputs are the same as given in Table 4 of Wennberg et al. (1997), which assumed stratospheric Br_y derived only from the breakdown of CH_3Br and halons. For the right-hand panel, 5 ppt has been added to Br_y at all altitudes, representing Br_y^{VSLS} (see text and Section 2.5). The ClO_x curve represents loss from the ClO + O and ClO + HO_2 cycles, plus other minor cycles that involve ClO, but not BrO or IO. The BrO_x curve represents loss from the BrO + ClO and BrO + HO_2 cycles, plus other minor cycles that involve BrO, but not IO. Two model curves are given to represent loss by all cycles that involve IO in the rate-limiting step. The "I_y Fast" curve uses the rate constant for IO + BrO given by Rowley et al. (2001) and assumes all products of this reaction lead to catalytic loss of ozone. The "I_y Slow" curve uses the JPL rate constant for IO + BrO and assumes that production of OIO results in a null cycle. These two curves are shown to illustrate the sensitivity of iodine-induced ozone loss to the rate constant of IO + BrO and to the fate of OIO (e.g., photolysis of OIO to O + IO leads to a null cycle, whereas photolysis to I + O_2 leads to O_3 loss). If the temperature-independent rate constant for IO + HO_2 given by JPL is used, the fractional contribution to ozone loss by iodine in the LMS is about a factor of two less than illustrated. Adapted from Wennberg et al. (1997); see also the extensive discussion of iodine kinetics in Bösch et al. (2003).

tions in the stratosphere (Bösch et al., 2003; Butz, 2006), loss of ozone by iodine is unlikely to be a driving factor for present-day midlatitude ozone loss. Note that the efficiency of ozone loss by iodine is sensitive to unresolved details of the photochemical mechanism, regarding the rate constant of the IO + BrO reaction and different decomposition products resulting from iodine dioxide (OIO) photolysis ("I_y Fast" versus "I_y Slow" in Figure 2-2; see caption). The likely relatively small contribution of iodine to stratospheric ozone loss is in contrast to bromine, which has been observed regularly in the stratosphere at levels significantly higher than can be supplied solely by the longer lived brominated gases (CH_3Br and halons) and at sufficient concentrations in the lower stratosphere to make a difference to present-day ozone.

A key question for this chapter, then, is to what extent brominated VSLS contribute to stratospheric Br_y. The contributions of chlorinated and iodinated VSLS to stratospheric Cl_y and I_y budgets are also considered. Figure 2-3, which is an updated version of Figure 1-8, Chapter 1, WMO (2003), shows Br_y estimated from balloonborne BrO observations adjusted to the time when the measured air masses were last in the troposphere (see Figure 2-3 caption for further details). In the late 1990s, this amounted to about 18 to 25 ppt of Br_y. Also shown are observed trends in surface mixing ratios of bromine-containing halons and methyl bromide (CH_3Br) since 1980 (see Chapter 1 for details). Note that the trends of CH_3Br have not been corrected to account for vertical gradients in the troposphere, so that this contribution to stratospheric Br_y may be overestimated, and therefore Br_y^{VSLS} underestimated. It can be seen that there is an apparent discrepancy between Br_y from halons plus CH_3Br, and Br_y inferred from BrO data. In WMO (2003), this discrepancy, denoted "additional" stratospheric bromine, was attributed to either direct injection into the stratosphere of inorganic bromine from the troposphere as well as from degradation of organic VSLS, or to possible calibration errors in the measurement of either BrO or the organic source gases. Since the last Assessment, there have been many studies focused on quantification of this "additional" bromine (Br_y^{VSLS}). Figure 2-3 shows possible contributions of Br_y^{VSLS} varying between 3, 5, and 7 ppt, as indicated by the thin blue lines. If 5 ppt of Br_y^{VSLS} is incorporated into a photochemical model, then ozone loss in the lower stratosphere from reactions involving BrO occurs at a rate approaching that due to the traditionally considered hydrogen oxide cycles alone (see Figure 2-2).

The structure of this chapter is as follows. Section 2.2 discusses the emissions, observations, and trends of VSL SGs, including vertical distributions at different locations, and their likely mixing ratios in the upper troposphere. Section 2.3 provides an update to our knowledge about the atmospheric chemistry of halogenated VSL SGs and PGs (organic and inorganic), wet removal of PGs, and a discussion about the geographical variability of chemical lifetimes. The role of heterogeneous chemistry in the inorganic halogen budget is also discussed. Section 2.4 revisits our understanding of transport processes that are important for the transport of VSL SGs and PGs to the stratosphere via the SGI and PGI pathways in both the tropics and extratropics. The ability of current models to simulate the distributions of short-lived gases is also examined, since these are the tools used to estimate the impact of VSLS on stratospheric halogen loading, ozone loss, and their ODPs. Section 2.5 presents an assessment of the contribution of VSL SGs and PGs to stratospheric halogen budgets. Model estimates of the SGI and PGI fraction entering the stratosphere are also discussed. The possible contribution of VSLS (bromine) to stratospheric ozone loss, and an update of ODPs for VSLS, are discussed in Section 2.6. Finally Section 2.7 summarizes recent evidence for, and speculates on, possible future changes in halogenated VSLS that could affect future stratospheric halogen loadings and ozone loss.

2.2 SOURCES, DISTRIBUTIONS, AND TRENDS OF VSLS

2.2.1 New Observations of the Distributions and Abundances of VSL Source Gases

Since the last Assessment (WMO, 2003), a number of shipboard, atmospheric, firn air, and coastal observations have provided new information that either adds to or constrains earlier estimates of atmospheric mixing ratios of VSL SGs, which are known to exhibit significant geographical variation. Table 2-2 provides updated information since the last Assessment on VSL SG mixing ratios in the atmosphere and, in particular, it assesses the subset of relevant observations required to arrive at an estimated range of mixing ratios in the tropical marine boundary layer and tropical upper troposphere for each source gas. It suggests mean tropical boundary layer mixing ratios of 8.4, 1.2, and 81 ppt for total bromine, iodine, and chlorine, respectively, in VSL SGs; and corresponding mixing ratios in the tropical upper troposphere of 3.5, 0.08, and 55 ppt. It is clear from these observations that many of the chlorinated and brominated compounds are delivered efficiently from the boundary layer to the upper troposphere. Bromoform ($CHBr_3$) and dibromomethane (CH_2Br_2) contribute the most VSL organic bromine

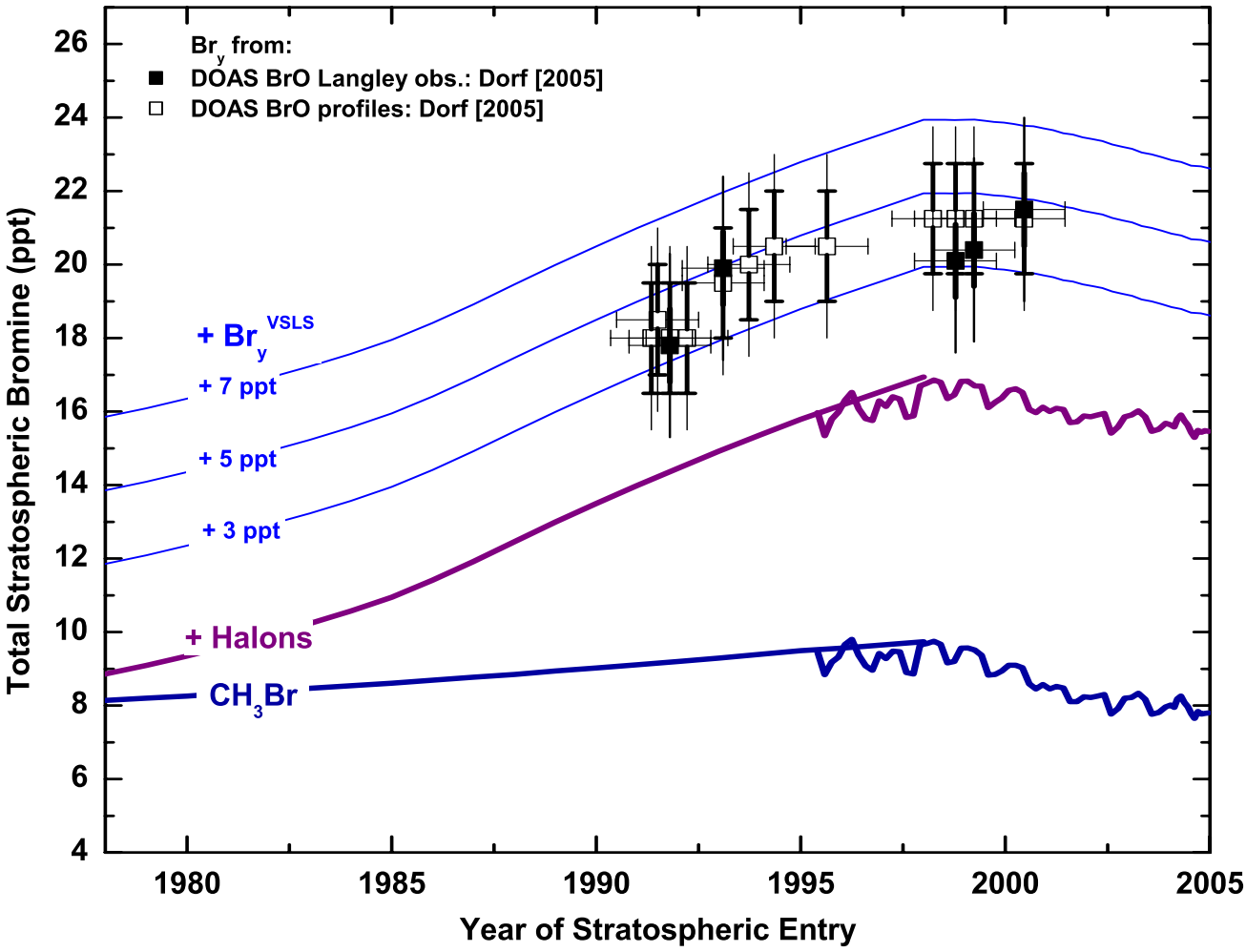

Figure 2-3. Trends (solid lines) of expected total inorganic stratospheric bromine (Br_y) due to measured tropospheric abundances of bromine from methyl bromide (CH_3Br; thick blue lines), the sum of CH_3Br plus halons (thick purple lines), and this sum together with assumed additional bromine (3, 5, and 7 ppt) derived from VSLS and/or inorganic tropospheric bromine sources (thin blue lines). This figure is an update of Figure 1-8 from the last Assessment (WMO, 2003). The smooth thick blue and purple lines prior to 1995 are based on a combination of Antarctic firn air reconstructions and ambient air measurements from a number of studies, adjusted to represent mean global abundances (references in WMO, 2003), and updated here with mean ambient air measurements (non-smooth blue and purple lines post-1995) from NOAA global monitoring stations (Montzka et al., 2003; updated). There may be small calibration differences between the different studies (see, for example, Fraser et al., 1999). The points (open and filled squares) are total inorganic bromine derived from stratospheric balloon measurements of BrO and photochemical modeling to account for BrO/Br_y partitioning. The filled black squares are from the slopes of Langley plot BrO observations above balloon float altitude, while the open squares are lowermost stratospheric BrO measurements (Dorf, 2005, and Dorf et al., 2006a, and references therein; together with more recent data as described in Section 2.5.2.1). Bold/faint error bars correspond to the precision/accuracy of the estimates, respectively (Dorf, 2005). For stratospheric data, the date corresponds to the time when that air was last in the troposphere, i.e., sampling date minus mean age of air in the stratosphere. No correction has been made for gradients of CH_3Br in the troposphere (see text for discussion). Preindustrial levels of CH_3Br of 5.8 and 5.5 ppt have been inferred by Saltzman et al. (2004) from Antarctic ice cores and by Trudinger et al. (2004) from Antarctic firn air, respectively, whereas preindustrial levels of the halons have been reported to all be below detection limits in Arctic and Antarctic firn air by Reeves et al. (2005). Adapted from Dorf (2005); see also Dorf et al. (2006b).

Table 2-2. Reported mixing ratios of VSL source gases in the troposphere (global and hemispheric values), at 10 km in the tropics, and best estimates from this Assessment of median mixing ratios in the tropical marine boundary layer [MBL] (<1 km), and tropical upper troposphere [UT]. All mixing ratio values are in parts per trillion (ppt). New information since WMO (2003) is indicated in boldface.

Species	Reported Tropospheric Mixing Ratio [a]	Reported 10-km Tropical Mixing Ratio [a]	Estimated Tropical [MBL] Mixing Ratio and Range	Estimated Tropical [UT] Mixing Ratio and Range	Estimated Ratio of Tropical [UT]/[MBL]
CH_2BrCl			**0.47 (0.38-0.59)[c]**	**0.32 (0.26-0.35)[c]**	**0.7**
CH_2Br_2	0.8-3.4	0.6-0.9	**1.1 (0.7-1.5)[b,c,f]**	**0.9 (0.7-1.0)[b,c,e]**	**0.8**
$CHBr_2Cl$	0.1-0.5	0.04-0.11	**0.30 (0.06-0.76)[b,g,i]**	**0.08 (0.03-0.12)[b,c]**	**0.3**
$CHBrCl_2$	0.12-0.6	0.04-0.11	**0.33 (0.14-0.91)[b,c,g,j]**	**0.12 (0.05-0.15)[b,c]**	**0.4**
$CHBr_3$	0.6-3.0	0.4-0.6	**1.6 (0.5-2.4)[b,c,f,g]**	**0.37 (0.13-0.7)[b,c,e]**	**0.2**
CH_3I	0.1-2.0	0.05-0.2	**0.8 (0.3-1.9)[b,c,f]**	**0.08 (0.02-0.18)[b,c]**	**0.1**
CH_2ClI			**0.35[g]**		
CH_2Cl_2			**17.5 (9-39)[b,c,f]**	**13.2 (9-19)[b,c,e]**	**0.75**
$CHCl_3$	NH, 10-15 **12.4 (9.8-14.5)[k]** SH, 5-7 **8.0 (6.5-9.1)[k]**	3.1 ±0.7	**7.8 (5.2-13.3)[b,c,f,k]**	**6.0 (4.8-7.5)[b,c,e]**	**0.78**
C_2HCl_3	NH, 1-5 SH, 0.01-0.1	0-0.1	**0.5 (0.05-2)[b,c,d]**	**0.14 (0.02-0.3)[b,c,d,e]**	**0.3**
C_2Cl_4	NH, 5-15 **5.3 (3.3-7.3)[k]** SH, 0.7-1.5 **1.5 (1.1-1.6)[k]**	1-3	**1.8 (1.2-3.8)[b,c,f,k]**	**1.3 (0.9-1.6)[b,c,e]**	**0.7**
C_2H_5Cl	**NH, 2.6[l]** **SH, 1.6[l]**		**5.0 (2.7-5.9)[d]**	**1.5 (1.0-1.8)[d]**	**0.3**
CH_2ClCH_2Cl	NH, 20-40 SH, 5-7	14.9 ±1.1	**3.7 (0.7-14.5)[b,c,h]**	**1.8 (0.7-3.3)[b,c,e,h]**	**0.5**
$COCl_2$				**22.5 (20-25)[m]**	
Total Cl			**81 (75-99)[n]**	**55 (52-60)[n,o]**	
Total Br			**8.4 (6.9-9.6)[n]**	**3.5 (3.1-4.0)[n]**	
Total I			**1.2 (0.7-2.3)[n]**	**0.08 (0.02-0.18)[n]**	

NH = Northern Hemisphere, SH = Southern Hemisphere.

[a] Kurylo and Rodríguez et al. (1999), except as noted.

[b] Transport and Chemical Evolution Over the Pacific (TRACE-P), Pacific Exploratory Missions (PEM) "Tropics A"/"Tropics B," Tropospheric Ozone Production about the Spring Equinox (TOPSE); Blake et al. (1999a,b, 2001, 2003a,b).

[c] 10-14 km tropical upper troposphere data from the Biomass Burning and Lightning Experiment-B (BIBLE-B) (Choi et al., 2003; Kondo et al., 2002).

[d] TRACE-P data only.

[e] 10-17.5 km non-stratospheric data from the Preliminary Aura Validation Experiment (preAVE; ozone < 75 ppt) (ftp://espoarchive.nasa.gov/archive/pre_ave/data/wb57).

[f] Cruise data (Butler et al., 2006).

[g] Chuck et al. (2005).

[h] TRACE-P and PEM-Tropics A only (see above).

[i] High value from Chuck et al. (2005) increased mean from 0.15 to 0.30.

[j] High value from Chuck et al. (2005) increased mean from 0.19 to 0.33.

[k] 2002-2004 surface (Simpson et al., 2004; Blake, 2005).

[l] Low et al. (2003).

[m] Toon et al. (2001).

[n] Sum of medians and the root mean square (rms) range determined from data for individual compounds shown in the table.

[o] $COCl_2$ is not included in Total Cl, as part of it may be derived from long-lived species (see text).

(>80%) to both the marine boundary layer and the upper troposphere. Similarly chloroform ($CHCl_3$) and dichloromethane (CH_2Cl_2) contribute most of the VSL organic chlorine (~80%) to the marine boundary layer and the upper troposphere. There are few observations of measurable iodine source gases in the upper troposphere or lower stratosphere.

As discussed later in this chapter, many of the compounds listed in Table 2-2 are converted to inorganic forms, but few of these have been measured in the upper troposphere. A notable exception is phosgene ($COCl_2$) which may account for an additional c. 45 ppt of chlorine (Cl) in the tropical upper troposphere although, as discussed in Section 2.3.3, part of the phosgene might be associated with the decomposition of long-lived source gases in either the troposphere or stratosphere.

The abundances, distributions, and sources of these short-lived, potentially ozone-depleting gases are considered in more detail below.

2.2.1.1 Bromine and Iodine

Atmospheric mixing ratios of many brominated and iodinated VSLS are typically higher where marine influence is significant. They tend to be highest near coastal areas, oceanic fronts, and in the tropics or subtropics (e.g., Quack and Wallace, 2003; Carpenter, 2003; Chuck et al., 2005; Yokouchi et al., 2005b; Butler et al., 2006). The tropics, including coastal areas, are significant in that they comprise the main region where deep convection occurs, and are therefore the most likely location for transport of gases emitted at the surface to be carried to the upper troposphere and lower stratosphere.

Carpenter et al. (2003) compared atmospheric measurements of a range of reactive organic halogens at Mace Head, Ireland (September, 1998) and Cape Grim, Tasmania (January-February, 1999). Mixing ratios of methyl iodide (CH_3I), chloroiodomethane (CH_2ClI), dibromochloromethane ($CHBr_2Cl$), $CHBr_3$, and CH_2Br_2 at Cape Grim were on average only 25-50% of those at Mace Head, Ireland, which is more strongly influenced by emissions from local macroalgae (seaweeds). Average total VSL bromine abundances at Cape Grim and Mace Head during these campaigns were 18 ppt and 39 ppt as bromine (Br), respectively. These amounts are much higher than the global averages of 2.4-3.5 ppt reported in the last Assessment, and reflect the intense emissions from coastal waters. Bromoform contributed 45% and 54% of the total VSL bromine at these two sites, respectively, and accounted for most of the variability. Peters et al. (2005) noted extremely high values of CH_3I, $CHBr_3$, and other VSLS over seaweed beds in northern Europe. These values, as high as 1830 ppt for CH_3I and 393 ppt for $CHBr_3$, have not been reported by any other investigations, the closest being 40 ppt of $CHBr_3$ reported by Yokouchi et al. (2005b). Other iodinated VSLS have been observed in such coastal environments, including diiodomethane (CH_2I_2), bromoiodomethane (CH_2BrI), iodoethane (C_2H_5I), and 1-iodopropane (n-C_3H_7I), but at smaller concentrations (Carpenter et al., 2003; Peters et al., 2005).

Quack and Wallace (2003), summarizing global air and seawater mixing ratios of $CHBr_3$ by oceanic region, showed that background mixing ratios of $CHBr_3$ in marine boundary layer air are generally in the range 0.5-1.5 ppt. This is consistent with data in Butler et al. (2006), but it is about half of the range of 1.3-3.9 ppt reported by Chuck et al. (2005) for the open ocean. This difference may have resulted from natural temporal and spatial variability, but it may also be due to differences in calibration scales, which underscores the need for intercalibration of these gases among laboratories. Quack and Wallace (2003) and Butler et al. (2006) showed high and variable coastal marine boundary layer $CHBr_3$ mixing ratios ranging between 1 and 8.3 ppt, and levels in the open ocean ranging between 0.4 and 2.5 ppt. These levels are consistent with the previous Assessment (WMO, 2003). Yokouchi et al. (2005b) recently reported over 40 ppt of $CHBr_3$ (i.e., >120 ppt as Br) in the first study of air over tropical coastal waters, suggesting that such areas may be particularly important in delivering halogenated VSLS to the stratosphere.

Seasonality in mixing ratios of VSLS is evident over most of the ocean (Butler et al., 2006) and is particularly marked in coastal areas. Cohan et al. (2003) and Cox et al. (2005) reported high frequency, in situ observations at Cape Grim. Average background levels of CH_3I for 1998-2001 were 1.4 ppt (Cox et al., 2005). Mixing ratios peaked during the summer (amplitude 0.47 ppt) despite faster photolytic loss, suggesting that the local oceanic emissions were a significant source of this gas (Cohan et al., 2003). Carpenter et al. (2005) found a strong, broad seasonal range of $CHBr_3$ (1.8-5.3 ppt) at Mace Head, noting higher values in the summer, and identifying both terrestrial and marine sources.

Although organic VSL source gases predominate in the marine boundary layer, it is possible that small amounts of inorganic bromine or iodine in the boundary layer could also be rapidly convected to the lower stratosphere. Recent observations suggest that bromine monoxide (BrO) in the marine boundary layer, whether from organic or inorganic sources, is on the order of 0-2 ppt (Leser et al., 2003; Saiz-Lopez et al., 2004a), with higher values observed locally. High amounts of iodine monoxide (IO) are routinely observed in the marine

boundary layer near macroalgae, with values as high as 7-8 ppt having been reported along the coasts of Ireland and France (Saiz-Lopez and Plane, 2004; Saiz-Lopez et al., 2004b; Peters et al., 2005). Saiz-Lopez and Plane (2004) suggest that emission of molecular iodine (I_2) from macroalgae may be the dominant source of IO. Although VSLS produced at midlatitudes are not as likely to be convected into the upper troposphere as are VSLS produced in tropical regions, this still underscores the potential contribution of VSLS from coastal regions.

2.2.1.2 CHLORINE

Cox et al. (2005) reported background mixing ratios of 6.3 ppt for $CHCl_3$ at Cape Grim (1998-2000), and Simmonds et al. (2006) reported 8.7 ppt for CH_2Cl_2 also at Cape Grim (1998-2004). Observed elevated levels of $CHCl_3$ (55 ppt) were attributed to local natural sources, while elevated levels of CH_2Cl_2 (up to 70 ppt above background) were attributed to anthropogenic sources. Data referenced in Butler et al. (2006) show higher tropical marine air mixing ratios of CH_2Cl_2 (18.8 ppt), but similar tropical mixing ratios of $CHCl_3$ (7.4 ppt) to those observed at Cape Grim. Numerous studies (e.g., Prinn et al., 2000; Thompson et al., 2004; Simmonds et al., 2006) show higher Northern Hemispheric mixing ratios of both of these gases, which suggest greater emissions in the Northern Hemisphere and are consistent with a large anthropogenic source.

Low et al. (2003) reported the first calibrated measurements of atmospheric chloroethane (C_2H_5Cl). The median mixing ratios observed at a clean California coastal site were 3.3 and 0.3 ppt for C_2H_5Cl and C_2H_5Br, respectively. No significant correlation was found between the atmospheric concentrations of the methyl halides and the ethyl halides, suggesting different source-sink relationships. These results, combined with data from the Transport and Chemical Evolution over the Pacific experiment (TRACE-P), suggest an average global mixing ratio for C_2H_5Cl of 2.6 ppt. Using these data with an average hydroxyl radical (OH) lifetime of ~1 month, the global burden and required annual source of C_2H_5Cl to the atmosphere are 25 Gg (1 Gg = 10^9 g), and 300 Gg yr^{-1}, respectively (Redeker et al., 2003).

2.2.2 Terrestrial Emissions

Terrestrial emissions of brominated or iodinated VSLS are generally thought to be smaller than from the ocean (Table 2-3). Emissions from many terrestrial sources, such as rice cultivation, fires, and wastewater effluents, are anthropogenically influenced. Several evaluations of fluxes from rice paddies, using both new data and modeling techniques, indicate that rice paddies remain a significant source of CH_3I to the atmosphere. Lee-Taylor and Redeker (2005) re-evaluated the global fluxes of CH_3I from rice cultivation, including the effects of temperature, seasonality, and soil moisture. Their best estimate was 16 to 29 Gg yr^{-1} of CH_3I. This range is similar to the previous estimate of Muramatsu and Yoshida (1995), but is considerably lower than the earlier estimates of Redeker et al. (2000) and Redeker and Cicerone (2004). Redeker and Cicerone (2004) did note that CH_3I emissions from paddies were positively correlated with temperature, essentially doubling with an increase of 10 degrees (25-35°C).

The first measurements of emissions of C_2H_5Cl, $CHBr_3$, and bromodichloromethane ($CHBrCl_2$) from rice paddies, or any other terrestrial ecosystem, were reported by Redeker et al. (2003). Integrated seasonal emissions of C_2H_5Cl were 0.60 ± 0.50 milligrams (1 mg = 10^{-3} g) per meter squared (mg m^{-2}), about 25 micrograms (1 µg = 10^{-6} g) m^{-2} for $CHBr_3$, and 2.9 µg m^{-2} for $CHBrCl_2$. Redeker et al. (2003) extrapolated their findings to the global coverage of rice and calculated an annual emission of about 1 Gg of C_2H_5Cl, which is insignificant compared with annual global emissions of c. 300 Gg yr^{-1}.

Evidence for direct terrestrial input of inorganic and organic halogens into the lower troposphere comes from studies of volcanoes and salt flats. Bureau et al. (2000) estimated the bromine yield of recent volcanic eruptions based on laboratory examination of ejected gases, and Bobrowski et al. (2003) measured enhanced BrO in a volcanic plume. Both authors suggest that these emissions could contribute to stratospheric bromine. Bobrowski et al. (2003) further estimated that volcanoes might emit c. 30 Gg BrO yr^{-1} into the lower atmosphere. Afe et al. (2004), however, showed that space-based measurements of column BrO are not correlated with enhancements of column sulfur dioxide in volcanic plumes, casting some doubt on the latter hypothesis. Volcanic perturbation to stratospheric bromine is not commonly considered in ozone assessment simulations.

Stutz et al. (2002) recorded elevated levels of BrO (6 ± 0.4 ppt) and ClO (15 ± 2 ppt) associated with mobilization of halogens from salt near the Great Salt Lake in the U.S. However, no flux estimates were provided, and it is not clear how widespread this phenomenon may be. Similarly, Zingler and Platt (2005) reported IO abundances of 0.3-2 ppt, and occasionally more than 10 ppt, over Dead Sea salt flats, apparently from inorganic sources. It is unlikely, however, that these emissions could contribute significantly to stratospheric halogen loading.

Table 2-3. Estimated local lifetimes, burdens, removal rates, and sources for some halogenated VSLS. New information since WMO (2003) is indicated in boldface.

Compound	Local Lifetime (days)	Estimated Burden (Gg)	Estimated Removal Rate (Gg yr^{-1})	Estimated Source from Inventory or Estimate of Biogeochemical Cycle (Gg yr^{-1})
CH_2BrCl	150[a]	1.2 (Br), 0.5 (Cl)[1]	2.9 (Br), 1.3 (Cl)[c]	
CH_2Br_2	120[a]	18-22 (Br)[b]	55-67 (Br)[c]	
		19 (Br)[1]	58 (Br)[c]	
$CHBrCl_2$	78[a]	1.3-1.5 (Br)[b]	6.1-7.0 (Br)[c]	**17 (Cl) open ocean[15,h]**
		1.2-1.3 (Cl)	5.4-6.2 (Cl)	**19 (Br) open ocean[15,h]**
		1.2 (Br), 1.1 (Cl)[1]	5.5 (Br), 4.9 (Cl)[c]	
$CHBr_2Cl$	69[a]	0.8-2.2 (Br), 0.2-0.5 (Cl)[b]	4.2-12 (Br), 0.9-2.7 (Cl)[c]	**5 (Cl) open ocean[15,h]** **23 (Br) open ocean[15,h]**
		2.3 (Br), 0.5 (Cl)[1]	12 (Br), 2.7 (Cl)[c]	
$CHBr_3$	26[a]	11-18 (Br)[b]	150-250 (Br)[c]	209 (47-370) (Br)[3]
		14 (Br)[1]	200 (Br)[c]	**800 (240-1760) (Br)[9]**
			285[2, d]	**28 (20-112) (Br) industry[9]**
CH_3I	5[e]	1.7-2.2 (I)[b]	120-160 (I)[c]	90-450 (I)[4]
	6[f]	4.8 (I)[f]	214 (I)[f]	**272 (I) total[10]**
				191 (I) net ocean (incl. 66 anthropogenic)[10]
				180 (I) open ocean[15,h]
C_2H_5I	4[a]	0.5 (I)	46 (I)[c]	
CH_2ClI	**0.1[a]**			**95 (I) open ocean[15,h]**
				27 (Cl) open ocean[15,h]
CH_2Cl_2	140[a]	83-250 (Cl)[b]	220-650 (Cl)[c]	487 (Cl) industrial[5]
	180[6, e]	250 (Cl)[6]	650 (Cl)[c]	160 (Cl) ocean
			500 (Cl)[6,d]	49 (Cl) biomass burning[16,i]
$CHCl_3$	150[a]	66-130 (Cl)[b]	160-320 (Cl)[c]	564 (Cl)[6]
	183[7,e]	210 (Cl)[7]	511 (Cl)[c]	**588 (392-784) (Cl)[11]**
			470 (350-600)[7,e]	**320 (240-400) (Cl) seawater[11]**
			412 (Cl)[6,d]	**196 (107-285) (Cl) soil[11]**
C_2HCl_3	4.6[a]	3.1 (Cl)[b]	260 (Cl)[c]	95 (Cl) industry[5]
	5.5[6,e]	5.30 (Cl)[6]	440 (Cl)[c]	20 (Cl) ocean[6]
			350 (Cl)[6,e]	3 (Cl) fossil fuel[6]
C_2Cl_4	99[a]	17-85 (Cl)[b]	63-310 (Cl)[c]	313 (Cl) industry[5]
	133[6,e]	160 (Cl)[6]	590 (Cl)[c]	16 (Cl) ocean[6]
			440 (Cl)[6,e]	2 (Cl) fossil fuel[6]
				222 (210-235) (Cl)[12,g]
C_2H_5Cl	**~ 30[13]**	**14 (Cl)[13]**	**165 (Cl)[c]**	
	~ 24[14]	**4.6-7.3 (Cl)[14]**	**70-110 (Cl)[c]**	
CH_2ClCH_2Cl	70[a]	5-26 (Cl)[b]	26-130 (Cl)[c]	700[8]

References: [1]Kurylo and Rodríguez et al. (1999); [2]Dvortsov et al. (1999); [3]Carpenter and Liss (2000); [4]Singh et al. (1983), Liss and Slater (1974), Moore and Groszko (1999); [5]McCulloch et al. (1999); [6]Keene et al. (1999); [7]Khalil and Rasmussen (1999); [8]Khalil (1999); [9]Quack and Wallace (2003); [10]Bell et al. (2002); [11]McCulloch (2003); [12]Simpson et al. (2003); [13]Redeker et al. (2003); [14]Low et al. (2003); [15]Chuck et al. (2005); [16]Lobert et al., (1999).

[a] From Table 2-4 of Ko and Poulet et al. (2003).

[b] Burden estimated using Equation 2.3 and the median BL mixing ratios from Table 2-7 in Ko and Poulet et al. (2003), and the estimated scale height from Table 2-10 in Ko and Poulet et al. (2003).

[c] From estimated lifetime and estimated burden, i.e., (column 3)/(column 2). The range reflects the range in the estimated burden.

[d] From two-dimensional (2-D) model.

Table 2-3, continued.

[e] Burden estimated from information given in Ko and Poulet et al. (2003): Equation 2.3, Table 2-7 (median BL mixing ratios), Table 2-10 (estimated scale heights).
[f] From three-dimensional (3-D) model simulation of Bell et al. (2002).
[g] Estimate for 2002.
[h] Estimated using data from Chuck et al. (2005). The surface ocean during the Chuck et al. study was generally a sink for $CHBr_3$.
[i] May be a less significant and more uncertain source than estimated here, although no new global emission estimates are available (Simmonds et al., 2006; Scheeren et al., 2002).

2.2.3 Oceanic Emissions

Numerous studies evaluating the oceanic production, degradation, and emission of VSLS suggest high spatial and temporal variability, with emissions generally high in the tropics and near ocean fronts, and highest in coastal regions (Figure 2-4). These studies continue to suggest that oceanic emissions constitute by far the largest source of brominated and iodinated VSLS to the atmosphere, making up 90-95% of the total global flux of these gases. The potential for spatially and seasonally dependent variability is shown clearly in the work of Cohan et al. (2003), where model results indicate that the mean oceanic flux of CH_3I from the Southern Ocean into the marine boundary layer at 40°S-50°S is 3.1 (1.9-5.2) $\mu g\ m^{-2}\ day^{-1}$ during the summer. For comparison, the global annual oceanic flux estimate reported by Moore and Groszko (1999) corresponds to 1.0 to 2.7 $\mu g\ m^{-2}\ day^{-1}$, and the open ocean range given in Butler et al. (2006) is 0.6 to 5.7 $\mu g\ m^{-2}\ day^{-1}$.

2.2.3.1 Bromine

Both Butler et al. (2006) and Quack et al. (2004) show the highest open ocean fluxes of $CHBr_3$ in areas of upwelling, such as near the equator and at ocean fronts, and their combined data suggest that tropical fluxes are highest in the Pacific, where equatorial upwelling is most intense. Quack and Wallace (2003) noted that subtropical coastal and shelf oceans of both hemispheres contribute significantly to global emissions, with 180 (72-270) Gg Br ($CHBr_3$) yr^{-1} emitted from their "shore" regime and 380 (240-940) Gg Br ($CHBr_3$) yr^{-1} emitted from their "shelf" regime, representing 23 and 48% of the entire oceanic $CHBr_3$ flux, respectively. Extrapolating Atlantic open ocean fluxes to the global ocean yielded 240 (32-800) Gg Br ($CHBr_3$) yr^{-1}, representing about one-third of the global oceanic $CHBr_3$ emission of ~800 (240-1800) Gg Br ($CHBr_3$) yr^{-1}. These estimates are similar to the 160 and 890 Gg Br yr^{-1} reported by Butler et al. (2006) for open ocean and global sources respectively. Quack and Wallace (2003) attribute much of the source to $CHBr_3$ production by phytoplankton, which they calculated to be ~240 Gg Br yr^{-1}.

The large differences between estimated open ocean fluxes and global fluxes underscore the importance of coastal waters as a substantial source of $CHBr_3$. High fluxes of many polyhalogenated VSLS are attributed mainly to attached macroalgae (e.g., Laturnus et al., 1996; Carpenter et al., 2000), and numerous investigators have reported very high mixing ratios in and above coastal waters (e.g., Carpenter and Liss, 2000). There have been, however, no systematic investigations of these gases in tropical coastal regions until recently, when Yokouchi et al. (2005b) measured atmospheric concentrations of $CHBr_3$, CH_2Br_2, and $CHBr_2Cl$ over several areas, including both Arctic and tropical coastal waters, and the open ocean, finding by far the highest amounts of these gases in association with tropical coasts. Their global estimate of the oceanic $CHBr_3$ source was 820 (± 310) Gg Br yr^{-1}, which is consistent with the independent estimates of Quack and Wallace (2003) and Butler et al. (2006).

Although coastal macroalgae are undoubtedly an important global source, Quack et al. (2004) and Butler et al. (2006) also provide evidence that the sources of $CHBr_3$ and CH_2Br_2 throughout the tropical open ocean are associated with the deep chlorophyll maximum near the thermocline. Transport of these gases to the ocean surface in association with upwelling and mixing is consistent with the higher concentrations and fluxes observed at the equator and near ocean fronts (Chuck et al., 2005; Butler et al., 2006). This may be significant because equatorial upwelling, which carries these gases to the surface where they are emitted, is influenced by wind speed and direction, which in turn are affected by climate, weather, and El Niño-Southern Oscillation (ENSO) events. This suggests a link between climate, wind-driven upwelling, and the supply of bromine to the tropical upper troposphere, where it can be transported to the lower stratosphere (see Section 2.4).

Several studies indicate that $CHBr_3$ sources contribute more organic and reactive bromine to the lower atmosphere than other organobromines. Carpenter et al.

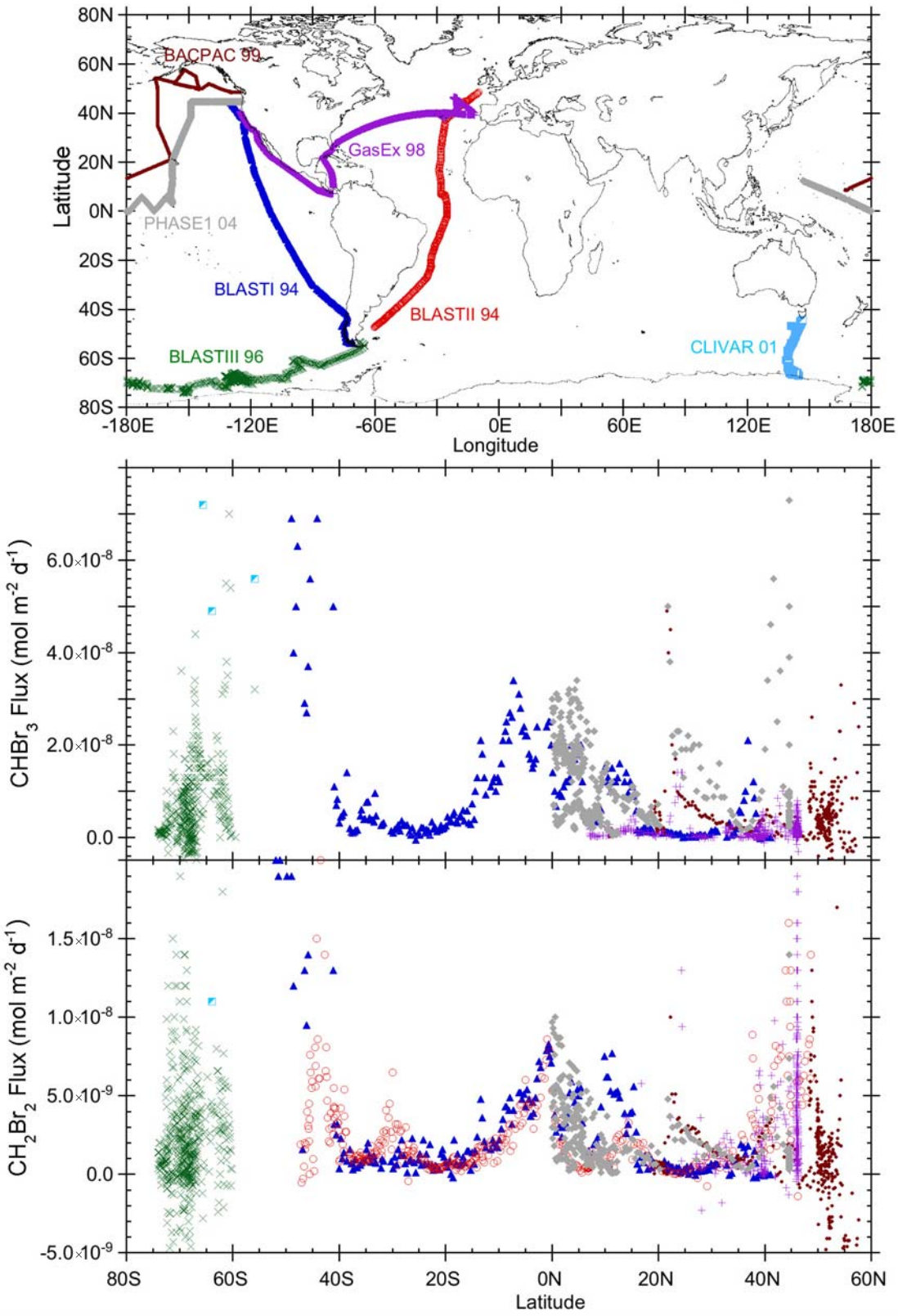

Figure 2-4. Plots of the oceanic fluxes of $CHBr_3$ and CH_2Br_2 into the marine boundary layer based upon data from seven research cruises between 1994 and 2004 (Butler et al., 2006). Cruise data are color-coded to match those in the map. All measurements are on the same calibration scale.

(2003) extrapolated their data to estimate molar source strengths of $CHBr_2Cl$ and CH_2Br_2, suggesting that the flux of $CHBr_2Cl$ is about 3-6% of that of $CHBr_3$, and that CH_2Br_2 emissions would be about 15-25% of the global $CHBr_3$ flux. Yokouchi et al. (2005b) suggest somewhat similar molar emission ratios, with $CHBr_2Cl$ amounting to ~7% and CH_2Br_2 to ~11% of the flux in coastal waters. Butler et al. (2006) noted that CH_2Br_2 fluxes were about 25-35% of $CHBr_3$ fluxes for data collected mostly in the open ocean. These values all fall within ranges estimated independently from concentration and lifetime data.

2.2.3.2 Iodine

Fluxes of iodinated VSLS are driven in part through photochemistry in the surface waters. Results of a study of the production of CH_3I in the tropical Atlantic Ocean support prior inferences that CH_3I is produced in the open ocean by a light-dependent production pathway that is not directly dependent on biological activity (Richter and Wallace, 2004). This assertion is supported by data from Smythe-Wright et al. (2005) and Chuck et al. (2005). Also, photo- or biodegradation of some polyhalogenated methanes can lead to the production of others. For example, Martino et al. (2005) carried out laboratory studies of aqueous degradation kinetics of the photolabile compounds CH_2I_2, CH_2BrI, and CH_2ClI in different types of natural and artificial seawater. Photolysis of CH_2I_2 in artificial and natural seawater generated CH_2ClI with a yield of 25-30%, suggesting that this reaction is an important source of marine CH_2ClI. Dark-incubations indicated that photolysis is the main abiotic degradation mechanism of CH_2I_2 in seawater and that CH_2I_2 originating at depth and transported to the surface would be photolyzed before escaping into the atmosphere. The longer aquatic photolytic lifetime of CH_2ClI allows this compound to vent to the atmosphere and indeed, although CH_2ClI has been detected at very low levels in the remote marine boundary layer, its sea-air fluxes appear to be of the same order as those of CH_3I (Carpenter et al., 2003; Chuck et al., 2005).

2.2.3.3 Chlorine

Although previous studies (e.g., Khalil et al., 1999) led Keene et al. (1999) to conclude that oceanic emissions of dichloromethane (CH_2Cl_2) could account for about 25% of the total emissions to the atmosphere, recent work by Moore (2004) suggests that the apparent supersaturation of this gas in higher latitude waters is an artifact of circulation and mixing. Moore (2004) interpreted the measurements of CH_2Cl_2 in waters of the North Atlantic and Labrador Sea to show that the compound at depth in the ocean is imprinted with an older atmospheric source, and appears to persist for years to decades in deeper waters. In this sense, the observed surface supersaturation of the gas would likely have resulted from the recent decline of this gas in the atmosphere (e.g., Simmonds et al., 2006; Thompson et al., 2004) with the ocean gradually re-equilibrating, and not necessarily the result of production in the ocean. Thus, the ocean "source" of 200 Gg Cl yr^{-1} would likewise be a matter of re-equilibration, not production.

2.2.4 Industrial and Other Anthropogenic Emissions

2.2.4.1 Bromine

Except for the chlorinated VSLS, anthropogenic emissions of most halogenated VSLS are presently dwarfed by natural emissions (Table 2-3). Emissions of $CHBr_3$ through water treatment, however, can be locally significant. Quack and Wallace (2003) reassessed the anthropogenic $CHBr_3$ source from water chlorination, including reactions on saltwater effluents, and suggested that it would amount to about 28 Gg Br yr^{-1} (0.20-110 Gg Br yr^{-1}), which is minor compared with natural sources (<5% of biogenic $CHBr_3$ emissions). Zhou et al. (2005) reported contributions from effluents from the chlorination of drinking, waste, and recreational waters of ~1-10% of the $CHBr_3$ emitted from the Great Bay area of New England, U.S. In the same region, they determined that the contribution from coastal power plant cooling effluents amounted to 15-50% of the $CHBr_3$ measured in the Great Bay, constituting most, if not all, of the anthropogenic source to the bay.

Because polar firn air provides a natural archive of "old" (typically from early 20th century) air, long-term trends of various gaseous species can, with some caveats, be reasonably reconstructed. Significant 20th century trends are often indicative of increasing anthropogenic emissions. For example, Worton et al. (2006) reported firn air measurements of the brominated trihalomethanes (THMs: $CHBr_3$, $CHCl_2Br$, $CHClBr_2$) and dihalomethanes (DHMs: CH_2Br_2 and CH_2ClBr) in Greenland. The brominated DHMs showed no annual trend over time, suggesting that their sources are almost entirely natural. The THMs, however, appeared to increase by 20% from 1950-1990. This translates to increases of ~16 ± 9, 0.7 ± 0.4, and 0.8 ± 0.3 Gg Br yr^{-1} for $CHBr_3$, $CHBr_2Cl$, and $CHBrCl_2$, respectively. Worton et al. (2006) noted that similarities in the trends in the deepest sections of the firn (oldest air) indicate that the three THMs may have similar sources. The authors further suggested that

chlorination of seawater for cooling coastal power plants may be the largest anthropogenic source of the brominated THMs. Emissions of THMs from water chlorination could potentially increase in the future in response to increasing demand for water treatment (potable and waste water) and power generation.

2.2.4.2 CHLORINE

Antarctic firn air measurements from Trudinger et al. (2004) show $CHCl_3$ and CH_2Cl_2 increasing in atmospheric mixing ratios from 3.9 ppt to 6.35 ppt and 1.4 ppt to 8.9 ppt, respectively, between 1940 and 1990. They noted that records of anthropogenic emissions of CH_2Cl_2 were consistent with their results. Northern Hemisphere firn air measurements from Worton et al. (2006) also support an anthropogenic contribution to $CHCl_3$. Their model calculations suggest anthropogenic emissions were ~14-20% of total $CHCl_3$ emissions (270-335 Gg Cl yr^{-1}) in 1950, and increased to 41-50% of the total (417-506 Gg Cl yr^{-1}) at the peak in global mixing ratio in about 1990. Anthropogenic emissions subsequently decreased to ~19% of total emissions (310 Gg Cl yr^{-1}) in 2001. This anthropogenic component was attributed mostly to paper and pulp manufacture, and the declining emissions since ~1990 to changes in working practices in this industry.

Recent ambient atmospheric data also suggest that emissions of these two gases are declining. Prinn et al. (2000) report data for $CHCl_3$ from 1983-1998 with a trend ranging from −0.1 to −0.4 ppt yr^{-1}. Simmonds et al. (2006) noted that measurements from Mace Head, Ireland, and from the National Oceanic and Atmospheric Administration (NOAA) U.S. global monitoring sites (Thompson et al., 2004) show a decrease in CH_2Cl_2 mixing ratios from 1995-2004 with trends of −0.7 ppt yr^{-1} (1995-2004) and −0.3 ppt yr^{-1} (1998-2004), while an increase of 0.05 ppt yr^{-1} was observed at Cape Grim, Australia.

Emissions of some chlorinated gases such as tetrachloroethene (C_2Cl_4) have been targeted for reduction owing to public health concerns. Levels of tropospheric C_2Cl_4, for which sources were estimated in WMO (2003) to be 95% anthropogenic, declined substantially between 1989 and 2002 (Simpson et al., 2004). During this period, annual mean C_2Cl_4 mixing ratios for the extratropical Northern Hemisphere dropped from 13.9 ± 0.5 ppt to less than half this value (6.5 ± 0.2 ppt), and global averages declined from 6.3 ± 0.6 ppt to 3.5 ± 0.2 ppt (Simpson et al., 2004). These values suggest that the global C_2Cl_4 burden decreased by roughly 820 Gg Cl between 1989-2002, and is consistent with decreasing anthropogenic Northern Hemispheric emissions. Simmonds et al. (2006) showed continued declines in C_2Cl_4 from 2000-2004. They report means (trends in parentheses) for Mace Head, Ireland, and Cape Grim, Australia, of 4.9 ppt (−0.18 ppt yr^{-1}) and 0.75 ppt (−0.01 ppt yr^{-1}), respectively.

High regional variability in emissions of anthropogenic VSLS is underscored by the study of Barnes et al. (2003) who, in contrast to the above, found no uniform trend of C_2Cl_4 between 1996 and 1999 at Harvard Forest, Massachusetts, U.S., but suggested that urban and industrial emissions of C_2Cl_4 for the New York City-Washington, D.C. corridor were increasing. Similarly, estimates from an aircraft study over Sagami Bay, Japan, suggest high emission rates of CH_2Cl_2 (61.8 Gg Cl yr^{-1}) and C_2Cl_4 (28.0 Gg Cl yr^{-1}) (Yokouchi et al., 2005a). These estimates, as well as those for $CHCl_3$ (6.2 Gg Cl yr^{-1}) and trichloroethene C_2HCl_3 (39.8 Gg Cl yr^{-1}), are consistent with the Japanese Pollutant Release and Transfer Register for 2002 (PRTR, 2004).

2.2.4.3 NEW VSL GASES

Future emissions of VSLS in the upper troposphere are potentially problematic. Trifluoroiodomethane (CF_3I) is being considered as a direct replacement for halon use in aircraft, and as a replacement for the potent greenhouse gas, hexafluoroethane (C_2F_6), currently used in the plasma etching industry. No information on its emission is currently available, although its use on aircraft could potentially lead to emission at altitude. This species is rapidly photolyzed (Table 2-1), but emission at altitude could provide a pathway for future injection of iodine to the stratosphere (Li et al., 2006). A new product, "PhostrEx" (PBr_3), has recently won approval from the U.S. Environmental Protection Agency for in-flight aircraft engine fire protection, and has passed all Federal Aviation Administration certification fire testing; future widespread use is possible. Although this compound is highly soluble and consequently has a very short lifetime (<0.1 s at 50% humidity), its release during flight in the upper troposphere could be of concern because of the low humidity and hence slower removal rates of the gas and its degradation products at these altitudes.

2.2.5 Sources and Distributions of Inorganic Halogens of Marine Origin

Any substance present in the upper troposphere can potentially be exported to the stratosphere; therefore inorganic halogens in the upper troposphere have to be considered to quantify the total import of halogens into the stratosphere. In the tropics, rapid convective transport means that VSLS may also be transported from the

boundary layer into the tropical upper troposphere (see Section 2.4.1).

BrO has been observed directly in the midlatitude marine boundary layer (Leser et al., 2003; Saiz-Lopez et al., 2004a). The presence of inorganic bromine generally in the marine boundary layer has also been inferred from the routinely observed large bromide deficit in sea salt aerosol (e.g., Sander et al., 2003). These occurrences are almost certainly due to halogen activation from sea salt by heterogeneous reaction chemistry.

Combinations of space-, ground-, and balloon-based measurements indicate that BrO is widely present in the free troposphere, with mixing ratios of 0.2-2 ppt (Harder et al., 1998; Wagner and Platt, 1998; Pundt et al., 2000; McElroy et al., 1999; Fitzenberger et al., 2000; Wagner et al., 2001; Van Roozendael et al., 2002; Richter et al., 2002; Schofield et al., 2004). The study by Yang et al. (2005), incorporating a detailed bromine chemistry scheme of gas-phase and heterogeneous reactions, showed that monthly mean mixing ratios of 0.1-1.0 ppt of BrO in the free troposphere can be explained by a combination of bromine release from sea salt aerosol and the breakdown of bromomethanes. Other bromine sources were not considered in this study, but might contribute (e.g., volcanic BrO, as noted above, and tropospheric decomposition of other organic bromine gases). They suggest that sea salt might contribute as much as 10% of the total Br in the upper troposphere.

In contrast to bromine, there is limited evidence for the presence of inorganic chlorine radicals in the free troposphere.

McFiggans et al. (2004) and Saiz-Lopez et al. (2006) reported direct coastal boundary layer observations of molecular iodine, ultrafine particle production, and iodocarbons. They demonstrated for the first time that ultrafine iodine-containing particles are produced by intertidal macroalgae exposed to ambient levels of ozone. However, the lifetime of inorganic iodine species released in the boundary layer is short, and they are generally unlikely to be transported to the stratosphere.

2.3 ATMOSPHERIC CHEMISTRY OF VSLS

The halogenated source compounds considered here are listed in Table 2-1. The Table gives the estimated local lifetimes (τ_{local}) for these compounds, defined as $(\tau_{local})^{-1} = (\tau_{OH})^{-1} + (\tau_J)^{-1}$ where (τ_{OH}) is the lifetime due to reactions with hydroxyl radical (OH), and (τ_J) is the lifetime due to ultraviolet (UV) photolysis. It is worth noting that even within these halogenated VSLS there is a wide range of local lifetimes, with values ranging from a few minutes to 150 days. The atmospheric loss processes for the source gases (organic halogens) occurs primarily in the gas phase via reaction with OH and UV photolysis. Multiphase processing of source gases is not a significant loss process and is not considered in this chapter.

The removal of inorganic halogenated reservoir species (e.g., hydrogen chloride, HCl) by wet and dry deposition is the main atmospheric loss process for inorganic halogens. Heterogeneous processes that recycle inorganic bromine and (most probably) iodine to insoluble reactive forms, may significantly increase the effective lifetime of Br_x and I_x (see boxed text in Section 2.1 for definition of Br_x; I_x is analogously defined) in the troposphere and the lower stratosphere and, as a result, enhance the efficiency of halogen transport via the PG pathway into the lower stratosphere, as discussed in Section 2.5.

Processing of both organic and inorganic halogenated degradation products on atmospheric aerosol and cloud particles is currently not well represented in atmospheric models, although the knowledge of these processes continues to improve. For example, a clearer picture is evolving regarding the partitioning of trace gases onto ice surfaces in cirrus clouds (Abbatt, 2003), and the mechanisms of halogen reactions on ice surfaces under tropospheric conditions (Fernandez et al., 2005). In this section, we assess the data needed to represent the atmospheric processing in both the gas and condensed phases of halogenated VSLS in atmospheric models.

2.3.1 Removal of Halogen Source Gases

The halogenated VSL SGs listed in Table 2-1, with the exception of CF_3I, C_2H_5Br, 1,2-dibromoethane (CH_2BrCH_2Br), and PBr_3 were evaluated in WMO (2003). The kinetic and photochemical parameters for the previously assessed VSL source gases have been updated in the recent evaluations of the International Union of Pure and Applied Chemistry (IUPAC, Atkinson et al., 2005; http://www.iupac-kinetic.ch.cam.ac.uk), and the National Aeronautics and Space Administration, (NASA) Jet Propulsion Laboratory (JPL), U.S. (Sander et al., 2006; http://jpldataeval.jpl.nasa.gov), with only minor revisions.

The atmospheric loss of the VSL SGs can be summarized as follows: chlorinated VSL compounds have long photolysis lifetimes and are predominantly removed in the troposphere through reaction with OH; the brominated VSLS are removed by a combination of UV photolysis and OH reaction depending on the degree of halogen substitution (for example, increased importance of photolysis with higher bromine substitution); and iodine-containing VSLS are removed almost exclusively by photolysis. Bayes et al. (2003) reported bromine atom quantum yields for the photolysis of $CHBr_3$ at several wavelengths be-

Table 2-4. OH rate coefficient and photochemical parameters for bromoethanes added since the WMO (2003) Assessment. Temperatures (*T*) in Kelvin.

Compound	k(OH) (cm^3 $molec^{-1}$ s^{-1})	k_{300}(OH) (cm^3 $molec^{-1}$ s^{-1})	Photolysis Rate Constant, J [a] (s^{-1})	References
Bromoethane (C_2H_5Br)	$2.9 \times 10^{-12}\exp(-640/T)$	3.43×10^{-13}	$<1 \times 10^{-9}$	Sander et al. (2006)
1,2-dibromoethane (CH_2BrCH_2Br)	$1.44 \times 10^{-11}\exp(-1270/T)$	2.1×10^{-13}	$<1 \times 10^{-9}$	Qiu et al. (1992); Sander et al. (2006)

[a] Atmospheric photolysis rate constants are globally and seasonally averaged estimates for 5 km altitude (because different models were used, the values should be considered approximate).

tween 303 and 324 nanometers (nm). Their results imply that the UV absorption cross section data currently recommended for use in the determination of the atmospheric photolysis rate of $CHBr_3$ may be systematically high by as much as 20% over this wavelength region.

The OH rate coefficients and atmospheric photolysis rates for C_2H_5Br and CH_2BrCH_2Br are given in Table 2-4. The photolysis lifetimes are significantly longer than their respective OH reaction lifetimes, and therefore photolysis is not an important atmospheric loss process for these compounds.

2.3.2 Tropospheric Lifetimes of Halocarbons

The lifetimes given in Tables 2-1 and 2-3 provide only an approximate estimate of the global mean lifetimes, because of significant regional variations in the OH radical concentration, solar flux, and the spatial and seasonal distributions of the halogen source gases. The geographic distribution of VSL SG surface fluxes with respect to these regional variations in the corresponding sinks is an important factor in determining the global mean atmospheric lifetimes of the VSL SGs. Warwick et al. (2006) have provided an estimate of the importance of the geographic flux distribution on the atmospheric lifetime of $CHBr_3$ by using a global atmospheric three-dimensional (3-D) model to calculate the $CHBr_3$ global atmospheric lifetime for a set of prescribed oceanic $CHBr_3$ emission data. In their calculations, the $CHBr_3$ atmospheric lifetime, defined as the global burden divided by the annual global loss, varied from 37 days in a scenario containing emissions distributed over the entire open ocean, to 15 days in a scenario in which $CHBr_3$ was emitted from tropical coastline regions only (see Table 2-5). The shorter lifetime in the tropical emission scenario is due to higher OH concentrations and UV levels in this region. This represents an uncertainty of approximately ±40% in the $CHBr_3$ atmospheric lifetime that is solely due to changes in the emission distribution. For halogen source gases with longer atmospheric lifetimes and better constrained flux distributions, this uncertainty will be reduced.

The different $CHBr_3$ emission scenarios in the Warwick et al. (2006) study also showed a significant variation in the amount of $CHBr_3$ reaching the tropical upper troposphere. A scenario based on a uniform ocean emission distribution of 210 Gg $CHBr_3$ yr^{-1} (Kurylo and Rodríguez et al., 1999; Carpenter and Liss, 2000) showed $CHBr_3$ peak mixing ratios of 0.2 ppt at 110 hPa, whereas a scenario with larger emissions (587 Gg $CHBr_3$ yr^{-1}) predominantly situated in the oceanic tropics, which showed better agreement to tropospheric observations, contained peak $CHBr_3$ mixing ratios of ~1 ppt at the same altitude.

Table 2-5. Bromoform emission scenarios used by Warwick et al. (2006).

Global Flux (Gg $CHBr_3$ yr^{-1})	Geographic Distribution of Emissions	Modeled Atmospheric Lifetime (days)
210	uniform ocean [a]	30
235	open ocean [b]	37
587	global coastlines [b]	26
400	tropical ocean [c]	21
587	tropical coastlines [c]	15
595	tropical ocean and tropical coastlines [c]	18

[a] Kurylo and Rodríguez et al. (1999).
[b] Quack and Wallace (2003).
[c] Warwick et al. (2006).

2.3.3 Production and Gas-Phase Removal of VSL Organic Product Gases

The first generation of stable reaction products formed following the gas-phase degradation of the halogenated VSL SGs was reviewed in WMO (2003). In general, the stable products consist of a variety of organic carbonyl (RC(O)R′) and peroxide (ROOR′) compounds, and inorganic halogen species. Since the last Assessment, little new evidence for the atmospheric reactivity and photolysis of these compounds has been reported. The recent IUPAC and JPL evaluations include the updates for these compounds where available. Detailed degradation mechanisms for halomethanes in general, and n-propyl bromide (n-C_3H_7Br) specifically, were given in WMO (2003). A major uncertainty in the evaluation of the impact of the degradation products is a lack of experimental data for their reactivity and photolysis.

The atmospheric degradation mechanisms for the VSL SGs are reasonably well understood, although quantification of the various possible reaction channels and degradation products is lacking in some cases. In general, the atmospheric degradation of the halogenated VSL source gases leads to the formation of compounds with atmospheric lifetimes shorter than the lifetime of the source gas. A notable exception is the formation of phosgene, $COCl_2$, which is a product formed in the degradation of the VSLS chloroform ($CHCl_3$) and tetrachloroethene (C_2Cl_4). Phosgene is also formed in the degradation of longer lived chlorinated compounds such as carbon tetrachloride (CCl_4) and methyl chloroform (CH_3CCl_3). In the stratosphere, $COCl_2$ is removed mainly by photolysis, since the rate constant for reaction with OH is relatively small ($<5 \times 10^{-15}$ centimeters cubed per molecule per second). On the basis of recently published cross sections (Atkinson et al., 2005; Sander et al., 2006), the local photolysis lifetime of $COCl_2$ is estimated to be similar to that of CFC-11 (trichlorofluoromethane; CCl_3F), and about twice that of CCl_4, at altitudes above 18 km at 30°N; thus significant stratospheric loss of $COCl_2$ is to be expected. Kindler et al. (1995), using a one-dimensional (1-D) model, reported a stratospheric lifetime for $COCl_2$ of ~2 years (for $COCl_2$ produced in the stratosphere); less than lifetimes calculated for long-lived SGs such as CCl_4. Kindler et al. calculated a much longer stratospheric lifetime (>8 years) for $COCl_2$ produced in the troposphere, which they explain as being due to the requirement for $COCl_2$ produced in the troposphere to be transported to higher stratospheric altitudes, where photolysis rates are greater. In the troposphere, removal of $COCl_2$ is dominated by aerosol washout (total wet removal lifetime of ~60 days from Kindler et al. (1995) and ~70 days from WMO, 2003). Therefore, wet removal of $COCl_2$ may further reduce the contribution of chlorinated source gases (both long-lived and VSLS) to stratospheric chlorine (see Section 2.3.4.1).

When loss of $CHBr_3$ is initiated by reaction with OH, the final organic decomposition product is likely to be carbonyl dibromide ($COBr_2$). When loss is initiated by photolysis, then formyl bromide (COHBr) is thought to be produced (Ko and Poulet et al., 2003). Present kinetics (Sander et al., 2006) indicate about two-thirds of the loss of $CHBr_3$ occurs by photolysis. There are few kinetic studies of $COBr_2$ and COHBr and no atmospheric observations of these species. Measurements of the UV cross sections (Libuda, 1992) indicate, however, that these compounds have a shorter lifetime due to photolysis loss than does $CHBr_3$. Many other organic intermediates are involved with the decomposition of other VSL SGs (e.g., Ko and Poulet et al., 2003).

2.3.4 Multiphase Processes Involving Inorganic Bromine and Iodine Compounds

Models used to predict tropospheric amounts of halocarbons and their degradation products currently use very simplified algorithms for heterogeneous processes and physical removal. Although the multiphase chemistry for inorganic bromine, and especially iodine compounds, is still poorly known, there are significant new data and understanding since the last Assessment, which are summarized below. This opens the possibility for a more realistic treatment of multiphase chemistry and more quantitative representation of the heterogeneous recycling of reactive halogens, the potential importance of which was highlighted in WMO (2003). In future model studies, the partitioning of gases on ice should be described using the suggested Langmuir description. Uptake on aqueous particles should, especially for very soluble species (see Yin et al., 2001), be calculated kinetically, i.e., not assuming instant equilibrium between gas and aqueous phase. The relevant Henry's law coefficients are provided in this section.

2.3.4.1 Wet Deposition Processes

The parameters needed to evaluate the rates of the processes leading to wet deposition are the partition coefficients for gas-phase degradation products into liquid water (the effective Henry's constants, H_{eff}), and on to ice surfaces (the Langmuir equilibrium constants, K_{eq}). Henry's constants were given for HOX and $XONO_2$ (X = Br and I) in the last Assessment. Subsequently, an exten-

sive database that covers these and other compounds including HCl, HBr, HI, $ClONO_2$, HOCl, BrCl, Br_2, I_2, ICl, and IBr is available from the National Institute of Standards and Technology (NIST) webbook (http://webbook.nist.gov/chemistry/). H_{eff} values for these species and for the organic chlorine reservoir $COCl_2$ are given in Table 2-6. The tropospheric removal of this and similar halogenated carbonyls was considered in depth in WMO (1995), and the conclusion that these compounds are relatively rapidly removed by precipitation remains valid.

A substantial amount of new data for trace gas-ice interaction at temperatures of the upper troposphere/lower stratosphere (UTLS; 200-230 K) has been reported from laboratory and field studies (Abbatt, 2003; Popp et al., 2004). Partitioning of HX (X = Cl or nitrate, NO_3) to the ice phase occurs by Langmuir-type adsorption, in which the amount of material adsorbed is normally limited to sub-monolayer surface coverage, depending on the partial pressure of the gas and the Langmuir equilibrium constant, K_{eq} (= $k_{adsorption}/k_{desorption}$). The surface coverage, θ (molec cm^{-2}), is given in terms of N_s (the maximum coverage in

Table 2-6. Henry's Law constants (*H*, in units of moles per liter per atmosphere) and uptake coefficients (γ_{het}) for heterogeneous processing of inorganic halogens.

	H_{298} ($M\ atm^{-1}$)	γ_{het}				
		$H_2O_{(l)}$	H_2O ice	H_2O ice HCl/HBr doped	Sulfuric acid, $H_2SO_{4\ (aq)}$	$H_2SO_{4\ (aq)}$ HCl/HBr doped (X = Cl, Br)
HOCl	260	–	$\gamma_0 > 0.2$ saturates [a]	0.3	time dependent	0.02-0.2 [a] dependent on H_{HOX} and H_{HX}
HOBr	93-1900	>0.01	0.3	0.004-0.3	>0.01 [b]	0.1-1
HOI	>45	–	–	0.05	0.015-0.07 [b]	>0.02
$ClONO_2$	hydrolysis	0.024 [c]	–	0.3-0.6	dependent on $[H_2SO_4]$, H, and T	dependent on H_{HX} [a]
$BrONO_2$	hydrolysis	0.06 [c]	>0.3	>0.2 [b]	>0.2 [c]	0.9 ($H_2SO_{4(s)}$)
$IONO_2$	hydrolysis	>0.1 [c]	–	>0.05 [b]	>0.3 [c]	–
Cl_2	0.093	–	>0.2 ($+HBr_{(g)}$)	–	–	–
Br_2	0.76	–	–	–	–	–
I_2	3.3	5×10^{-4}	–	0.02 (HI doped)	–	–
BrCl	0.94	<0.03	–	–	–	–
ICl	110	–	0.02	0.3	–	–
IBr	24	–	0.03	0.3	–	–
HCl	1.1* ($K_a = 10^7$ [d])	physical uptake only				
HBr	0.71* ($K_a = 10^9$ [d])	physical uptake only				
HI	2.5* [e] ($K_a = 3.2 \times 10^9$ [d])	physical uptake only				
$COCl_2$	0.07 [f]					

* $H_{eff} = H_{298} \times \exp(-\Delta H_s/R \times (1/T - 1/298)) \times (1 + K_a/[H^+])$ (K_a = acidity constant)

[a] http://www.iupac-kinetic.ch.cam.ac.uk/

[b] Protonation followed by reaction to form dihalogens.

[c] Reaction leading to hydrolysis to form HOX, where X = Br, I.

[d] The dissociation constants are from Arnaud (1966), or see Schweitzer et al. (2000).

[e] The physical constant is from Marsh and McElroy (1985).

[f] Slow hydrolysis occurs; see WMO (1995).

molec cm^{-2} at saturation), K_{eq}, and the gas partial pressure of the gas (P_{HX}):

$$\theta + N_s \frac{K_{eq} P_{HX}}{1 + K_{eq} P_{HX}}$$

For uptake on ice, the value of N_s is approximately 3×10^{14} molec cm^{-2} (Abbatt, 2003). At UTLS temperatures, nitric acid (HNO_3) and HX (X = Cl, Br, I) are strongly adsorbed and the process is important. Weak acids and organic species are generally weakly adsorbed and do not partition efficiently to ice. When formation of long-lived compounds (e.g., nitric acid trihydrate: NAT) is thermodynamically favored, there is a greater capacity for partitioning, since adsorption is not confined to the surface layer.

2.3.4.2 Heterogeneous Halogen Activation

Conversion of stable inorganic halogen reservoirs, which are removed by deposition, into reactive halogen radicals potentially lengthens the lifetime of inorganic halogen because the reactive products remain in the gaseous phase. The key heterogeneous reactions (where X and Y are atoms of Br, Cl, or I) leading to release of reactive halogens are:

$$HOX + Y^- + H^+ \rightarrow XY + H_2O$$

$$XONO_2 + Y^- + H^+ \rightarrow XY + HNO_3$$

$$XONO_2 + H_2O_{(aq)} \rightarrow HOX + HNO_{3\,(aq)}$$

These reactions can occur in aqueous aerosols (water, sulfuric acid, sea salt) or on ice or solid aerosol, and XY is partitioned into the gas phase where it is photolyzed.

Heterogeneous reaction kinetics are expressed in terms of dimensionless reactive uptake coefficients, γ_{het}, which allow the rate to be evaluated on a per-collision basis for a prescribed surface area of the condensed phase. Table 2-6 provides a summary, extended since the last Assessment, of representative γ_{het} values for surfaces relevant for the troposphere and the stratosphere. These are based on the updated IUPAC and JPL evaluations, and other recent literature sources.

The large uptake coefficients of halogen nitrates ($XONO_2$, where X = Cl or Br) into aqueous droplets (Deiber et al., 2004) means that uptake in liquid water clouds will be efficient, and since concentrations of bromide and iodide in precipitating clouds are likely to be very small, wet deposition will predominate over activation. Evaporating cloud droplets, however, will lead to reactive halogen recycling. Model calculations have suggested that uptake into cloud droplets can extend reactive halogen lifetime and lead to a vertical redistribution of inorganic bromine compounds (von Glasow et al., 2002). In their global model runs, von Glasow et al. (2004) showed that heterogeneous reactions can extend the lifetime of Br_y from about 6-9 days to about 9-15 days below 500 hPa, with smaller changes in the free troposphere. A laboratory study showed the release of labile dibromine monoxide (Br_2O) and molecular bromine (Br_2) from sulfuric acid solutions following exposure to the soluble species hypobromous acid (HOBr) and hydrogen bromide (HBr) (Iraci et al., 2005). These observations suggest that the PGI of Br_y species should be evaluated for various aerosol and cloud washout lifetimes.

Activation of halogens can also occur on ice surfaces, such as those in cirrus clouds. Laboratory studies have shown that Cl and Br activation by reaction of chlorine nitrate ($ClONO_2$) and HOBr with hydrogen chloride (HCl) on ice surfaces at UTLS temperatures scale linearly with the surface coverage of HCl (Mössinger et al., 2002; Fernandez et al., 2005). At typical tropospheric HCl concentrations, the rate of activation of bromine on ice clouds is probably fast, but chlorine activation is less efficient. Nevertheless recent field observations (Thornton et al., 2003) suggest that Cl activation is occurring on cirrus clouds, leading to the local production of ClO.

2.3.5 Iodine Chemistry

All iodine source gases with significant emissions fall into the category of halogenated VSLS. However, ozone destruction in the lower stratosphere due to catalytic cycles involving iodine remains poorly understood. New information on the chemistry of iodine species relevant for the atmosphere has been obtained since the WMO (2003) Assessment. The new chemical kinetics information may have significance for the efficiency of transport of iodine species to the UTLS and the ozone destruction efficiency factor for stratospheric I_y. Relevant multiphase iodine chemistry is presented in Section 2.3.4 above.

The IUPAC and JPL kinetics evaluations have critically reviewed all but the most recent kinetic and photochemical studies. Rate coefficients for the reactions of atomic iodine (I), IO, and nitric oxide (NO) with OIO (Joseph et al., 2005; Plane et al., 2006), and IO with methyl peroxy radicals (CH_3O_2) (Bale et al., 2005) have since been reported (in units of cm^3 $molec^{-1}$ s^{-1}) to be 1.1×10^{-10}, 1.2×10^{-10}, 7.6×10^{-13} exp(607/T), and 6.0×10^{-11}, respectively (rates are for room temperature only, except where noted). New photolysis quantum yield studies for OIO have also been reported (Joseph et al., 2005; Tucceri et al.,

2006). The OIO quantum yield (Φ) measurements indicate $\Phi(O(^3P)) < 0.007$ at 532 nm and between 558 and 578 nm, and $\Phi(I) < 0.24$ at 532 nm and <0.05 between 560 and 580 nm. Photolysis quantum yields at longer wavelengths have not yet been reported.

Reactions between halogen monoxide radicals have several product channels. The efficiency of ozone (O_3) loss depends on the halogen species and the product yields. For example, the IO self-reaction produces OIO (~40%) and iodine oxide dimer IOIO (~55%) at 1000 hPa (Bloss et al., 2001). The IOIO product is unstable (Misra and Marshall, 1998) and most likely rapidly thermally decomposes to yield OIO. Therefore, the effective OIO yield from the IO self-reaction is high. The efficiency of O_3 loss is reduced by photolysis of the halogen dioxides formed in the IO + IO and IO + BrO reactions, if an oxygen atom is produced.

OIO has a series of strong diffuse absorption bands in the region between 470 and 610 nm, but only the I atom-producing channel is energetically possible:

$$OIO + h\nu \rightarrow I + O_2$$

The alternate channel producing IO + O leading to no net O_3 loss requires wavelengths <470 nm. Recent laboratory studies (Joseph et al., 2005) show that OIO absorption at 562 nm leads to internal conversion from the excited state (OIO^*) to the vibrationally excited ground state ($OIO^\#$), rather than dissociation:

$$OIO + h\nu \rightarrow OIO^* \rightarrow OIO^\#$$

$$OIO^\# + M \rightarrow OIO + M$$

Nevertheless, a small probability of photolysis, integrated over the entire OIO absorption band, could still lead to significant photochemical conversion of OIO to I and consequent ozone loss.

Studies have shown that higher iodine oxides can nucleate to form new particles (Hoffmann et al., 2001; O'Dowd and Hoffmann, 2005). The formation of OIO in the gas phase appears to initiate this process. In the atmosphere, the oxidation of OIO by reaction with IO or OIO may lead to the formation of higher oxides (e.g., I_2O_3 and I_2O_4) that are of low volatility and may condense on pre-existing particles, providing a sink for reactive iodine. This is different from the oxidation mechanisms of chlorine and bromine oxides that do not lead to the formation of unreactive low-volatility oxides. This mechanism provides a possible explanation for the absence of detectable IO concentrations in the UTLS from degradation of iodocarbons, while the BrO radical derived from the oxidation of bromine source gases is clearly present in this region (see Sections 2.2.5 and 2.5).

2.4 DYNAMICS AND TRANSPORT IN THE TROPOPAUSE REGION AND IMPLICATIONS FOR VSLS

The distribution of VSLS is governed by the distribution of surface sources, and by competition between vertical transport (boundary layer to free troposphere to stratosphere) and chemical destruction or removal via washout. The implication for VSLS-related stratospheric ozone loss therefore depends crucially on the strength and spatial distribution of transport processes, and of the chemical, microphysical, or moist processes that remove the degradation product gases (PGs). Note in particular (see following sections) that rapid vertical transport, which potentially takes VSL SGs and PGs from the boundary layer to the tropopause region, is usually associated with moist processes (warm conveyor belts, convective clouds) that can potentially remove soluble PGs through washout. Nevertheless, such processes are potentially effective in the vertical transport of total bromine (or other halogens), since the time scale for such transport in an individual convection event (hours) is short compared with the time scale for chemical breakdown of the VSLS.

Given that VSL SGs and PGs reach the upper troposphere through potentially rapid transport mechanisms, it is important to establish how rapidly they are subsequently transported into the stratosphere via the SGI and PGI pathways. A schematic depiction of transport processes in the upper troposphere and lower stratosphere relevant to VSLS is shown in Figure 2-1. There is net transport across the tropopause from troposphere to stratosphere in the tropics and net transport across the tropopause from stratosphere to troposphere in the extratropics, with this net transport controlled by global-scale processes as part of the Brewer-Dobson circulation (Holton et al., 1995). However, when considering VSLS, it is particularly important to note first, that transport across the tropopause is in fact two-way, especially at mid-latitudes, with both troposphere-to-stratosphere transport (TST) and stratosphere-to-troposphere transport (STT), and second, that the transition from tropospheric chemical characteristics to stratospheric chemical characteristics takes place not in a sharp jump across a uniquely defined tropopause, but across a finite tropopause transition layer, most notably in the tropics. In the tropics, it is now conventional to describe the transition layer as the "tropical tropopause layer" (TTL). It is now clear that in the extratropics there is a corresponding "extratropical tropopause

layer" (ExTL). In both the tropics and the extratropics, large-scale and small-scale processes together play important roles in determining the structure of the tropopause layers. Representing these processes correctly poses particular difficulties for global chemical models. In the following, the tropics, including the tropical tropopause layer, and both vertical and quasi-horizontal exchange to the stratosphere, are discussed in Section 2.4.1. The extratropics and the extratropical tropopause layer are discussed in Section 2.4.2, and the representation of relevant processes in global models is discussed in Section 2.4.3.

2.4.1 Tropical Convection, the TTL, and Tropical Troposphere-to-Stratosphere Transport

The lower part of the tropical troposphere is dominated by ascent in convective clouds. The outflow from these clouds is concentrated in two distinct layers, a lower layer from about 2 to 5 km (800-550 hPa), and an upper layer from about 10 to 15 km (300-150 hPa). The compensating descent in the regions surrounding the clouds is associated with evaporative cooling in the lower layer, and radiative cooling in the upper layer (e.g., Folkins and Martin, 2005). In the lower part of the troposphere, moist convection can efficiently transport chemical species vertically via strong convective updrafts, but at the same time, the scavenging associated with convective precipitation can efficiently remove the soluble species (Crutzen and Lawrence, 2000; Mari et al., 2000; Barth et al., 2001). Studies using explicit modeling of convection have shown that scavenging in warm clouds should be considered as a kinetic rather than an equilibrium process (Yin et al., 2001; Barth et al., 2001). Such treatment is not included in the vast majority of global chemical models.

So far, the observational data on soluble species in the entrainment and detrainment zones of isolated or organized convective systems in the tropics that might better constrain these model results are still very limited. In cold clouds, as liquid water freezes and riming occurs around ice, chemical species are also absorbed into ice crystals by various processes, such as bubble inclusions within crystals. A limited number of field laboratory and theoretical studies have proposed trapping coefficients of chemicals in ice (e.g., Stuart and Jacobson, 2003; Krämer et al., 2006; see also Section 2.3.4.1). The current experimental data are apparently inconsistent, poorly understood, and only available for a limited set of chemical species (e.g., HCl, HBr). Parameterization of scavenging by ice crystals is only now being implemented in global models (Kärcher and Basko, 2004). For example, it has been found that if the gas retention coefficient (the fraction of dissolved gas that is retained as a liquid droplet freezes) of a highly soluble gas is allowed to vary in a relatively narrow range (0.5-1.0), the corresponding bulk gas transport within the cloud varies, for maritime clouds, by as much as a factor of 4 (Yin et al., 2002). See also Section 2.3 for a discussion of washout and solublities of VSL SGs and PGs. In addition, the microphysical structure of convective clouds and ice clouds is highly sensitive to the boundary layer aerosol concentration and shows variations between, for example, maritime and continental clouds (Yin et al., 2002; Kärcher and Lohmann, 2003; Nober et al., 2003; Ekman et al., 2004). This has implications for the concentration of trace gases inside anvil ice crystals.

The part of the tropical atmosphere above the level of maximum convective outflow (at about 12 km altitude, 345K potential temperature), and below the cold point tropopause (at about 17 km altitude, 380K potential temperature), is now commonly described as the TTL (see, for example, WMO, 2003; Gettelman and Forster, 2002). This definition of the TTL, equivalent to the "sub-stratosphere" of Thuburn and Craig (2002), has it as the region of the troposphere in which there is a transition between radiative-convective domination and radiative domination of the thermal balance. The TTL acts as a source region both for the stratospheric overworld and for the extratropical lowermost stratosphere (see Figure 2-1). Net exchange from the TTL to the stratospheric overworld in the tropics, say across the 100 hPa level as an approximation to the cold point tropopause, is regarded as dominated by large-scale ascent in the Brewer-Dobson circulation, with the strength of this circulation controlled by large-scale dynamical processes (e.g., Holton et al., 1995).

The overall picture of TTL processes is somewhat updated from WMO (2003), though estimates of transport time scales between the boundary layer and the lower part of the TTL are largely unchanged. A useful recent description of the relevant processes is given, for example, in Folkins and Martin (2005). In the "lower TTL" (12-15 km, 345-360K), convective penetration is sufficiently frequent so that most of the air detraining from convection descends to the lower troposphere. The upward mass flux in convective clouds, the magnitude of the radiative cooling outside the clouds, and hence the magnitude of the implied descent decays with height. Küpper et al. (2004) give estimates of the upward cumulus mass flux as a function of height from various modeling and data studies, but note that there are significant difficulties in estimating this flux. At a level z_0 (the level of zero radiative heating) of about 15 km or 360K, there is a transition from clear-sky radiative cooling to clear-sky radiative

heating. Only above z_0 in the "upper TTL" (15-17 km, 360-380K), where the upward cumulus mass flux is comparable to or less than the large-scale upward mass flux in the Brewer-Dobson circulation, does most air detraining from clouds ascend into the stratosphere.

Note at this stage that the TTL has been defined by some authors (e.g., Folkins et al., 1999; Sherwood and Dessler, 2001; Füeglistaler et al., 2004; Sinnhuber and Folkins, 2006) to be only this "upper TTL," i.e., only as the region above z_0. This definition is based on sound reasoning, but for consistency with WMO (2003) it is not adopted here, and the terms "lower TTL" and "upper TTL" are used as introduced previously.

Gettelman et al. (2004) noted that clouds reach the typical level z_0 (in their case identified by cloud brightness temperature <200K) only in relatively localized geographical regions, implying that air that is likely to ascend into the stratosphere is drawn from the surface in similarly localized regions. An equivalent statement is that the transport time scale from the surface to the upper TTL is likely to be significantly less in these localized regions than on average over the tropics. Such regions include the Western Equatorial Pacific during October to March (with a continuing but lesser role in other months) and the Bay of Bengal, Southeast Asia, and Panama regions during April to September (e.g., see Gettelman et al., 2004; Figure 9).

Somewhat similar conclusions to the above follow from recent trajectory calculations based on European Centre for Medium-Range Weather Forecasts (ECMWF) three-dimensional wind fields. In particular, the trajectory calculations of Füeglistaler et al. (2004) show that air that ultimately ascends into the tropical lower stratosphere crosses the lower boundary of the TTL preferentially in the West Pacific region in Northern Hemisphere winter and in a region centered on southeast Asia, but extending toward India and into the West Pacific, in Northern Hemisphere summer. The longitudinal variation of transport across the lower boundary of the TTL, according to the Füeglistaler et al. (2004) calculations, is shown in Figure 2-5. It should be noted that the wind datasets on which such trajectory calculations are based do not resolve individual convective cells and, therefore, that any results need cautious interpretation. Nonetheless, the overall behavior of the calculated trajectories is broadly as expected from the schematic picture of the TTL outlined previously. For example, the probability of ascent of forward trajectories into the stratosphere rapidly increases with the height of trajectory initialization.

The Füeglistaler et al. (2004) trajectory calculations predict a residence time (the time for forward trajectories to move up or down by 10K in terms of potential temperature) that is maximum (about 12 days) for trajectories starting at 360K (corresponding to z_0) and decreases to about 9 days for a layer centered at 370K. This implies a residence time for the 360K-380K layer of about 20 days. This is expected to be an underestimate, since it is expected that such transport calculations, through their use of vertical winds from meteorological datasets, overestimate vertical transport rates (both net transport and dispersion). On the other hand, the time scale of about 80 days to cross the 360-380K layer that has been inferred from a one-dimensional tropical-mean model (Folkins and Martin, 2005) is almost certainly an overestimate, since it neglects the dispersive effects of geographical variation in vertical velocity. On the evidence currently available, therefore, the residence time for air parcels in the 360K-380K layer is likely to be somewhat greater than 20 days. New calculations based on improved meteorological datasets, or using radiative transfer codes to calculate vertical velocities, are likely to refine this estimate of residence time in the near future. Transport time scales for the upper TTL (20 to 80 days on the basis of the Füeglistaler et al. (2004) and Folkins and Martin (2005) results mentioned above) are expected to be significantly longer than those for the lower TTL, i.e., about 10 days on the basis of typical cumulus mass fluxes estimated by Küpper et al. (2004). It is therefore inappropriate to assign a single transport time scale to the whole TTL extending from the maximum in convective outflow to the cold point. This point was noted in WMO (2003), but was confused by also giving estimates for a single turnover or replacement time of 10 to 13 days for the 250 hPa-100 hPa layer (i.e., the whole TTL by the more common definition).

The consequence of the longer timescale in the upper TTL for injection of VSLS is not yet clear; there might be more time for conversion from SG to PG, but the net effect of this on total halogen entering the stratosphere is likely to be small. A more important issue is whether there is significant scavenging of PGs in the upper TTL associated with uptake on cirrus clouds (see Section 2.3.4), thus limiting the transport of halogen into the stratosphere via the PGI pathway.

As noted previously, upward transport out of the TTL into the stratosphere is understood to be primarily controlled by large-scale dynamical processes, and there has been no reason to revise significantly net flux estimates over those given previously (e.g., Rosenlof, 1995). However, there have been recent changes in temperatures of the tropical lower stratosphere (e.g., Randel et al., 2004), with a significant reduction in temperatures more recently, i.e., 2000-2004 appears to be 1K cooler than the period 1995-1999. Implications for stratospheric water vapor are discussed in Chapter 5 of this Assessment. Simple dynamical arguments imply that this may be

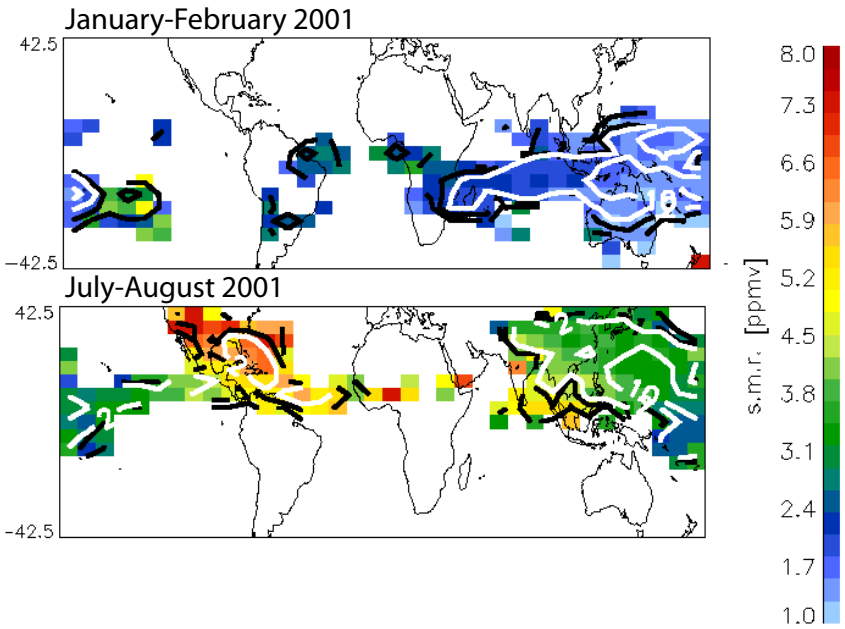

Figure 2-5. Results of 2-month backward trajectory calculations, using three-dimensional winds from ECMWF operational analysis data, reported by Füeglistaler et al. (2004). The backward trajectories were to points distributed evenly over the 400K surface in the tropics. The contour lines indicate the density of intersections of the backward trajectories with the 340K surface (corresponding roughly to the lower boundary of the TTL), relative to the density of such intersections if spread uniformly over the globe. The upper and lower panels show the density calculated from trajectories followed over the periods January-February 2001 (Northern Hemisphere (NH) winter) and July-August 2001 (NH summer), respectively. The conclusion is that air parcels reaching the tropical lower stratosphere are in NH winter drawn preferentially from the lower troposphere in the Western Pacific and, to a lesser extent, the Indian Ocean region. In the NH summer, the corresponding regions include the West Pacific, but extending significantly over Southeast Asia. (The color scale indicates the average mixing ratio of water vapor determined by the minimum saturation mixing ratio along each trajectory and assigned to the point of intersection of that trajectory with the 340K surface. See Chapter 5, Sections 5.2.5 and 5.3.5 for further discussion of water vapor and its implications for ozone.)

explained by a 10% increase in the upward mass flux out of the TTL, and that this is driven by changes in large-scale dynamical processes (Randel et al., 2006). It is, however, impossible to predict how long the current anomalously large upward mass flux will persist.

Exchange between the TTL and the extratropical lowermost stratosphere is achieved through quasi-horizontal transport associated with synoptic-scale eddies. This has been apparent for some time on the basis of observations of subtropical filaments in midlatitudes (e.g., Vaughan and Timmis, 1998; O'Connor et al., 1999), water vapor observations (e.g., Dessler et al., 1995) and, more recently, chemical observations in the extratropics (see Section 2.4.2). Trajectory and similar transport calculations based on meteorological data also show the possibility of such transport, particularly above the level of the subtropical jet (Chen, 1995; Haynes and Shuckburgh, 2000). Both direct observations of the chemical composition of the extratropical lowermost stratosphere (e.g., Randel et al., 2001; Prados et al., 2003) and transport calculations imply that transport from the TTL to the lowermost stratosphere is, at least in the Northern Hemisphere, highly seasonal, with much greater transport in summer than in winter. The air in the extratropical lowermost stratosphere may be regarded as a mixture of air that has been transported from the TTL, and air that has descended from the stratospheric overworld. The fraction of air from the TTL has been estimated by Hoor et al. (2005), on the basis of observed concentrations of carbon monoxide (CO) and of the carbon dioxide (CO_2) seasonal cycle, to be about one-third in winter, perhaps increasing to about one-half in summer. Similar conclusions have been obtained from other datasets.

Recent trajectory calculations of Levine et al. (2006) for Northern Hemisphere winter show that more than 75% of the air that enters the TTL, and subsequently reaches the stratosphere, does so through quasi-horizontal transport into the extratropical stratosphere. It is likely that this fraction will be larger in summer than in winter. It is interesting that, according to the Levine et al. (2006) calculations, the distribution of the entry locations of such air through the base of the TTL is spread relatively uniformly in longitude, in contrast to the corresponding contribution for air that subsequently reaches the tropical lower stratosphere. Note also that while the strength of this quasi-horizontal exchange with the extratropics is not

uniform with height, there is little reason to believe that convective penetration to the level z_0 has the same significance for such exchange as it does for exchange with the stratospheric overworld, since the quasi-horizontal exchange transport is not strongly affected by the direction of slow vertical motion.

A final issue concerns the spatial structure of chemical fields within the TTL. There is no reason to expect chemical fields to be homogeneous. Recent in situ observations have shown complex spatial structure in this region in chemical species with a whole range of lifetimes (e.g., Tuck et al., 2004) apparently resulting from several different mechanisms including different surface source regions, and transport out of the extratropical stratosphere. The spatial structure of VSL SGs and PGs are expected to be correspondingly variable.

2.4.2 Stratosphere-Troposphere Exchange in the Extratropics

Transport from the tropical upper troposphere to the extratropical lower stratosphere has been discussed in the previous section. There is also significant transport directly from the extratropical troposphere to the extratropical lower stratosphere, particularly in summer (e.g., Hintsa et al., 1998; Pan et al., 1997). However, the high static stability in the lower stratosphere, and the fact that the average circulation is downward, limit the vertical penetration of tropospheric air. The result is a finite transition layer (the ExTL) in which chemical characteristics vary continuously between the extratropical upper troposphere and lower stratosphere (see Figure 2-1). In principle, this transition layer is a region in which concentrations of VSL SGs and PGs may be relatively high, and in which substantial in situ ozone loss due to VSLS may take place. However, typical ozone mixing ratios in the ExTL are 300 parts per billion (ppb) or less, which limits the possible impacts on the ozone column.

Chemical measurements in the ExTL have increased significantly since WMO (2003). The location of the ExTL can be deduced, for example, from ozone, carbon monoxide (CO), total reactive nitrogen (NO_y), and water vapor (H_2O) data collected as part of the Stratosphere-Troposphere Experiments by Aircraft Measurements (STREAM) and the German Spurenstofftransport in der Tropopausenregion (SPURT) programs (Hoor et al., 2002; Fischer et al., 2000; Hoor et al., 2004; Krebsbach et al., 2006; Engel et al., 2006), which also show that the layer is deeper in summer, with a stronger tropospheric influence, than in winter. Note that CO has a short chemical lifetime of 2 to 3 months, making it a useful proxy for VSLS transport into the lower stratosphere. The upper limit of the ExTL has been estimated from enhanced CO and H_2O mixing ratios to be about 25K in potential temperature above the local tropopause defined by the 2 PVU (potential vorticity unit) surface, corresponding to about 2 km in height. Pan et al. (2004) identified the transition layer using aircraft data and characterized it as centered on the thermal tropopause, and about 2-3 km thick. Note that the thermal tropopause is usually above the tropopause defined by the 2 PVU surface.

Alongside the new observations of chemical species in the extratropical tropopause region, many recent studies have used trajectory calculations based on winds from large-scale meteorological datasets to investigate vertical transport processes, such as in the large body of work coordinated in the STACCATO (Influence of Stratosphere-Troposphere Exchange in a Changing Climate on Atmospheric Transport and Oxidation Capacity) project as summarized in Stohl et al. (2003). An important conclusion relevant to VSLS has been that warm conveyor belts associated with synoptic-scale baroclinic eddies, and associated frontal zones, play an important role in rapid transport from the boundary layer to the tropopause region. One consequence is that rapid upward transport tends to originate from the boundary layer in preferential longitudinal regions, such as the midlatitude storm track regions east of Japan and east of the U.S. (e.g., Sprenger and Wernli, 2003; see Figure 2-6 for further details). Surface emissions (e.g., anthropogenic or coastal VSLS) in these regions may therefore be more likely to contribute to the chemical composition of the extratropical tropopause region. The importance of warm conveyor belt transport, and the usefulness of trajectory calculations for studying such transport, have been confirmed in various case studies. For example, Nedelec et al. (2005) showed very high CO concentrations arising from Siberian fires observed by MOZAIC (Measurement of Ozone, Water Vapor, Carbon Monoxide and Nitrogen Oxides by In-service Airbus Aircraft) aircraft in the lower stratosphere.

Trajectory studies have confirmed that many air parcels moving from the boundary layer to the tropopause region remain in that region for several days (e.g., Wernli and Bourqui, 2002; Sprenger and Wernli, 2003), thus implying that VSL SGs or PGs transported into the very low stratosphere could have an impact on ozone loss. Since stretching rates of material surfaces in the extratropical tropopause region (which give an indication of the rate at which an anomalous air mass is stirred with, and eventually mixed with, its environment) are of the order of a few days (e.g., Stohl, 2001), it seems very unlikely that air masses arriving in the tropopause region

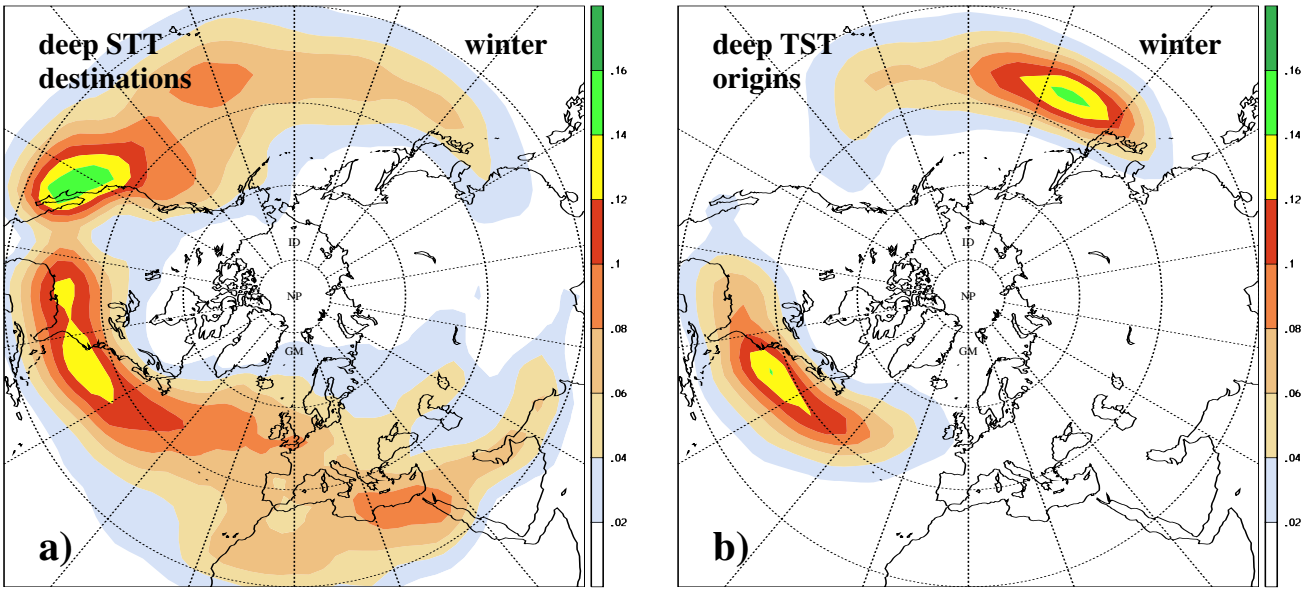

Figure 2-6. Geographical distribution of the (a) low tropospheric "destinations" of deep STT and (b) low tropospheric "origins" of deep TST events during winter. Values are in % and correspond to the probability that a low tropospheric air parcel (pressure > 700 hPa) was transported downward from the lowermost stratosphere during the previous four days (deep STT) or will be transported upwards into the lowermost stratosphere during the next four days (deep TST). The implication of (b) is that the probability of rapid transport from the surface to the tropopause region is strongly dependent on geographical location (at the surface). From Sprenger and Wernli (2003).

are predisposed to descend rapidly, but instead are likely to mix into the background.

Trajectory studies for the SPURT dataset (Hoor et al., 2004) imply that the composition of the ExTL is influenced by recent transport from the troposphere on time scales of days to a few weeks. While trajectory studies might be expected to capture the effects of warm conveyor belts, they almost certainly miss the effect of smaller-scale processes such as deep convection or convection embedded in frontal systems. The quantitative effect of deep convective injection of tropospheric chemical species into the extratropical lower stratosphere remains relatively uncertain. There are some in situ chemical measurements that point very clearly to such injection (e.g., Poulida et al., 1996; Fischer et al., 2003), while other measurements have given no direct evidence of penetration of extratropical convection into the stratosphere (Ridley et al., 2004). There are also studies that combine chemical measurements with meteorological or trajectory studies that argue for such penetration (e.g., Hegglin et al., 2004). Dessler and Sherwood (2004) argue that convective penetration to the 380K surface in midlatitudes, while much less frequent than in the tropics, is frequent enough to have a significant effect on water vapor at these altitudes, though not on ozone since the relative difference in ozone concentrations between troposphere and stratosphere is much smaller than the relative difference in water vapor concentrations.

Convection might contribute to troposphere to stratosphere transport (TST) directly by overshooting the tropopause at the anvil outflow (Mullendore et al., 2005), or indirectly by exciting gravity waves that break significantly above the convective clouds (Wang, 2003). Further, recent evidence for convective transport of low-altitude air into the lowermost stratosphere in the extratropics is provided by in situ observations in the stratosphere that show clear evidence of biomass burning products such as CO and aerosols, apparently arising from forest fires over Canada (e.g., Ray et al., 2004). Fromm and Servranckx (2003) have suggested that enhanced convective cells associated with the fires themselves may be very likely to penetrate the lower stratosphere; terms such as "pyro-convection" or "pyro-cumulonimbus" are becoming widely used to describe this phenomenon (e.g., Fromm et al., 2005). While the occasional penetration of pyro-convection events into the lower stratosphere has been observed, it is not clear at present that the pyro-convection has a significant effect on the overall chemical balance of the extratropical lowermost stratosphere.

2.4.3 Predictive Modeling of the Tropopause Region

Predictive modeling of the impact of VSLS on ozone depends on model representation of the processes discussed in Sections 2.4.1 and 2.4.2. In the tropics, the greatest challenge for models is representing convective processes, although in the TTL the subtle interplay between different processes, and the fact that significant changes in dynamical and chemical characteristics take place over 2-3 km, also present a challenge. In the extratropics, the transport characteristics of synoptic-scale eddies, and their interplay with smaller-scale processes, must be captured. These smaller-scale processes include gravity wave breaking, turbulence in the vicinity of jet streams, and radiative processes associated with upper level clouds. From the chemistry point of view, the representation of soluble species, as well as aerosols and microphysical processes, is still poor in global models. Scaling up the heterogeneous reactions on ice and aerosols to realistic parameterizations is still a major challenge for prediction of the tropopause region. Uncertainties in surface and lightning emissions may cause significant biases in simulating the chemical composition of the upper troposphere.

The parameterization of tropical convective processes in global-scale models remains a conceptual challenge, with different theoretical approaches possible. Basic thermodynamics are not well characterized, while transport and scavenging processes are even less well understood. One widely used method for parameterizing convective transport processes is based on the mass-flux formulation (Arakawa and Schubert, 1974), in which transport processes are represented by an ensemble of vertical mass fluxes at subgrid scales. This formulation however was originally developed for representing the subgrid-scale thermodynamic effects (phase changes and fluxes of heat and moisture) of convection, and its generalization to chemical transport processes is not straightforward (Donner et al., 2001). Lawrence and Rasch (2005) have shown that, for a single convection parameterization, differences in the implementation of detrainment and entrainment fluxes can result in significant differences in the upper tropospheric mixing ratios of short-lived tracers (lifetimes of a few days or less). In particular, the bulk formulation of convection, widely used in global models, in which entrainment and detrainment are each assumed to occur at a single level, may lead to underestimation of up to 30% in zonal and monthly mean concentrations of such tracers, relative to, for example, a more sophisticated formulation in which a distribution of entrainment and detrainment levels is assumed. One implication of the above is that VSLS could play an even more important role in the upper troposphere than previously thought.

Detailed evaluation of cumulus parameterizations, in comparison with observations and cloud resolving models, have recently taken place both with respect to thermodynamics (Yano et al., 2004) and with respect to tracers (Bell et al., 2002; Collins et al., 2002). More accurate estimates of mass fluxes, based on high-resolution data from either observations or modeling, could lead to improved parameterizations of these convective transports. Evaluation of the mass flux formulation against high-resolution spatial data obtained from explicit numerical models reveals that, in its standard form, it substantially underestimates vertical transport of heat, moisture, and momentum by deep convection (Yano et al., 2004), with improvement possible through nonlinear averaging of the large-scale variables. Similar issues will almost certainly arise in the convective transport of chemical tracers.

Notwithstanding these recent results on convective transport and scavenging effects (see Section 2.4.1), current global models necessarily make significant simplifications in their representation of convective transport and scavenging processes. In some models the two are linked (e.g., Considine et al., 2005), whereas in others the two are completely separate. Lack of relevant observations and model simulations means that there has been no systematic validation of model representation of convective processes acting on halogenated VSLS against observations. Historically, model representations of such processes have been validated against observations of radon and lead mixing ratios. Lead-210 (^{210}Pb) is produced in the atmosphere by radioactive decay of radon-222 (^{222}Rn), which has a radioactive half-life of 3.8 days. Lead-210, which has a radioactive half-life of about 22 years and can therefore be considered radioactively stable for this purpose, is removed by attachment to aerosols and washout. Most recently, building on the large amount of previous work on this subject, Considine et al. (2005) have presented an intercomparison of ^{222}Rn and ^{210}Pb calculated by the NASA Goddard GMI (Global Modeling Initiative) model using meteorological fields from three different general circulation models (GCMs)/data assimilation systems, and comparison with observations. The three different simulations show some common discrepancies relative to observations and the authors deduce, in particular, that midlatitude convective transport may represent detrainment at too great an altitude, and that cloud scavenging frequency in midlatitudes may be too great. Convective transport is confirmed to play a very important role in setting upper troposphere and lower stratosphere concentrations that are in good agreement with observations, though part of this role may

be indirect, for example, in bringing species from the boundary layer to the upper troposphere, from which they can be transported effectively by the larger-scale circulations. These findings are all potentially relevant to model simulations of halogenated VSLS, though it is difficult to extrapolate results directly to model skill for predicting VSLS, since the chemical properties and the location and time of emissions of the VSLS will be different from these radioactive tracers.

In the extratropics, the role of convection is not as great as in the tropics, and the fact that many of the relevant processes are relatively large scale might seem to make this region more accessible to global chemical transport models and global chemistry-climate models. The success of trajectory studies based on meteorological wind fields in reproducing chemical distributions observed in field experiments is encouraging in this regard. However, "operational" resolutions used for global chemical models are still relatively coarse. Comparison between global models and chemical data (e.g., Brunner et al., 2003) has revealed the limitations of such models that, for example, overestimate the two-way transport in the tropopause region, resulting in excessive ozone in the upper troposphere and excessive CO in the lower stratosphere. This is an indication that, for current models, useful quantitative prediction of the effect of halogens from VSLS penetrating the lower stratosphere in the extratropics remains difficult.

2.5 CONTRIBUTION OF HALOGENATED VSLS TO STRATOSPHERIC HALOGEN LOADING

2.5.1 Source Gas Injection (SGI) and Product Gas Injection (PGI)

The concept of source gas injection (SGI) and product gas injection (PGI) into the stratosphere was described in Chapter 2 of the last Assessment (Ko and Poulet et al., 2003) as well as the introduction to this chapter. For SGI, the VSL source gas (SG) is transported to the stratosphere and then reacts to release halogen atoms. Supply to the stratosphere depends on emission location and time, as well as details of the tropospheric transport (e.g., convection) and troposphere-to-stratosphere exchange. For PGI, either intermediate (i.e., organic) products or final (i.e., inorganic) products are produced in the troposphere, and these species are transported to the stratosphere. The details of PGI depend on the same factors as SGI, plus factors such as the photochemistry of the source species, intermediate products, and final products. The gas-phase partitioning between radical and longer lived inorganic reservoirs, as well as the solubility and heterogeneous reactivity of all species, are critical for assessing the efficiency of PGI (see Section 2.3). Indeed, differences in the efficiency of stratospheric supply of chlorine, bromine, and iodine from VSL organics might be due to differences in the photochemical properties of the respective inorganic products. Another important consequence of PGI is that measurements of the organic VSL SGs alone are not sufficient to determine the efficiency of stratospheric injection.

Injection of tropospheric particles into the stratosphere is another mechanism for cross-tropopause transport of halogens, depending on the chemical composition of the particles. The substantial organic content of many aerosol particles just above the tropopause suggests injection of tropospheric particles into the stratosphere, and the presence of Br on these particles suggests that cross-tropopause transport of bromine, in both directions, can occur by aerosols (Murphy et al., 1998; Murphy and Thomson, 2000). However, observations of this process are limited and, as a consequence, quantification of cross-tropopause halogen transport by aerosols is a considerable gap in our present state of knowledge. Most model simulations do not include cross-tropopause transport of halogens by aerosols in their estimates of PGI.

2.5.1.1 Observational Evidence for SGI

Bromine

Bromoform ($CHBr_3$) is thought to be the most abundant bromine-bearing VSL compound near the surface (Table 2-2). As noted previously in this chapter, $CHBr_3$ levels can reach or exceed 40 ppt near sea level (Yokouchi et al., 2005b). Observations reveal between ~0.2 ppt (Schauffler et al., 1998) and 1 ppt (Sturges et al., 2000) of $CHBr_3$ in the tropical free troposphere (see also Table 2-2). Measurements in the upper troposphere and tropopause region by Sturges et al. (2000) indicated $CHBr_3$ abundances of 0.5 ± 0.2 ppt for data collected during three flights (June and August 1998 and March 1999). Schauffler et al. (1998) measured 0.1 ppt of $CHBr_3$ at the tropical tropopause during February 1996. However, $CHBr_3$ was only detected at the tropical tropopause for one of three flight series that sampled this region. Bromoform exhibits similar variability near the midlatitude tropopause, ranging from near zero to a maximum abundance of ~0.7 ppt (Schauffler et al., 1999). The cross-tropopause transport of $CHBr_3$ is difficult to quantify from observations because of atmospheric variability and limited sampling. However, there are indications that, on

occasions, values of $CHBr_3$ are high enough near the tropical tropopause for SGI of $CHBr_3$ to be important for the bromine budget of the lowermost stratosphere. Specifically, if the approximately 0.5 ppt of $CHBr_3$ measured near the tropical tropopause by Sturges et al. (2000) turns out to be representative of the average mixing ratio in the TTL, it would provide an SGI flux that could maintain an additional 1.5 ppt of Br_y.

The VSL species CH_2Br_2 and CH_2BrCl are less abundant near the surface than $CHBr_3$, but are longer lived and therefore more likely to enter the stratosphere via SGI (Tables 2-1 and 2-3). Wamsley et al. (1998) showed that CH_2Br_2 and CH_2BrCl cross the tropopause, supplying ~2.3 ppt of Br_y by the SGI pathway. The total bromine content of the VSL species CH_2Br_2, CH_2ClBr, $CHCl_2Br$, $CHClBr_2$, and $CHBr_3$ was measured to be 2.2 ppt at the tropical tropopause during February 1996 (Schauffler et al., 1998) (see also the compilation in Table 2-2, which concludes a higher value of 3.5 ppt of bromine from these species). Plots of CH_2BrCl versus CFC-11, and CH_2Br_2 versus CFC-11, in the Wamsley study show that bromine from these compounds is released in the lowermost stratosphere (LMS), prior to the release of the majority of bromine from CH_3Br and halons. Bromine release in the LMS has important consequences for the photochemistry of this region. Significant supply of inorganic bromine (Br_y) leads to much faster ozone loss by two catalytic cycles represented by the rate-limiting steps defined by the BrO plus ClO, and BrO plus hydroperoxy radical (HO_2) reactions, compared with calculations that consider supply of bromine only from CH_3Br plus halons (Salawitch et al., 2005). A significant role for SGI injection of CH_2BrCl and CH_2Br_2 at all times, and lack thereof for $CHBr_3$ under some conditions, is consistent with their lifetimes for photochemical removal in the troposphere of 150, 120, and 26 days, respectively (Table 2-1).

Chlorine

Contributions to stratospheric inorganic chlorine (Cl_y) from VSL SGs are dominated by the species $CHCl_3$, CH_2ClCH_2Cl, CH_2Cl_2, C_2H_5Cl, and C_2Cl_4 and can potentially supply about 55 ppt of chlorine to the stratosphere (Table 2-2). These gases have natural and anthropogenic sources, as described in Section 2.2. The tropospheric lifetimes of these gases (30 to 150 days) are comparable to those for some of the brominated VSL SGs (see Table 2-1), so if SGI is important for bromine, it may also play a role for chlorine. Although the overall perturbation of Cl_y by VSLS is small (because the chlorine content of longer lived gases is much larger than that of the VSLS), this perturbation could be significant for the LMS, where the VSL SGs are more likely to release their chlorine content. This could lead to significantly higher levels of ClO in the LMS than would be present in models that only consider supply of Cl_y from long-lived gases.

Iodine

The supply of stratospheric iodine presently appears to be dominated by methyl iodide (CH_3I) (e.g., Davis et al., 1996; Table 2-2). Abundances of CH_3I range from ~0.8 ppt in the marine boundary layer to ~0.08 ppt in the tropical upper troposphere (Table 2-2). Higher values of CH_3I, occasionally reaching ~1.0 ppt, were reported in the subtropical upper troposphere (Davis et al., 1996). The much shorter lifetimes of iodinated VSLS compared with most brominated VSLS (Table 2-1) suggests, in general, less efficient SGI of iodine to the stratosphere.

2.5.1.2 Observational Evidence for PGI

Bromine

PGI refers to cross-tropopause transport of degradation products of VSL source gases, as well as final inorganic products. For bromine, the discussion of observational evidence for PGI begins with the suggestion of a global, ubiquitous background abundance of 1 to 2 ppt of bromine monoxide (BrO) distributed throughout the troposphere (Harder et al., 1998; Müller et al., 2002; Richter et al., 2002; Van Roozendael et al., 2002). Model simulations indicate that Br_y levels of 4 to 8 ppt are needed in the middle troposphere to sustain this much BrO (Yang et al., 2005). If 4 to 8 ppt of Br_y is present in the global troposphere, then cross-tropopause transport of these species could dominate the bromine budget of the LMS (Ko et al., 1997; Pfeilsticker et al., 2000). As explained below, it is unclear whether BrO is present at this level in the whole troposphere. There is no evidence of enough inorganic chlorine or iodine in the global troposphere to perturb stratospheric Cl_y or I_y in a manner comparable to the potential perturbation to stratospheric Br_y by tropospheric, inorganic bromine.

The presence of 1 to 2 ppt of BrO in the troposphere was first suggested based on comparison of total column BrO from the Global Ozone Monitoring Experiment (GOME) to stratospheric columns inferred from balloon measurements of BrO profiles (Harder et al., 1998). Observations of the solar zenith angle (SZA) variation of differential slant column density of GOME BrO also indicated that much of the column measured by GOME lies below the tropopause, perhaps due to the presence of 2 to 3 ppt of BrO between the tropopause and the surface

(Müller et al., 2002; Van Roozendael et al., 2002). Measurements of BrO and O_4 (the O_2-dimer) columns over the Pacific suggest 0.5 to 2.0 ppt of BrO uniformly distributed throughout the troposphere (Richter et al., 2002). A global, ubiquitous distribution of 2 to 3 ppt of BrO would account nearly completely for the "additional" stratospheric bromine reported by GOME (Van Roozendael et al., 2002; Salawitch et al., 2005). The fact that excess BrO is seen year round by GOME, at all latitudes (e.g., Chance, 1998; Hegels et al., 1998), argues against the springtime release of bromine from sea-ice and frost flowers (the so-called bromine explosion; see, for example McElroy et al., 1999) being the primary source of tropospheric background BrO.

Other observations, however, contradict the notion of a global, background level of BrO at an abundance of 2 to 3 ppt. Ground-based observations of direct and scattered sunlight reveal mean abundances of BrO in the troposphere over Lauder, New Zealand (45°S), of ~0.2 ppt and an upper limit of 0.9 ppt over this site (Schofield et al., 2004). Low values of tropospheric BrO are also observed over Arrival Heights, Antarctica (78°S), except for bromine explosion events (Schofield et al., 2006). Balloon profiles of tropospheric BrO indicate levels that peak at ~2.3 ppt, but more commonly lie between ~0.4 and 0.6 ppt (Fitzenberger et al., 2000). If BrO levels in the global free troposphere are less than 1 ppt, then the GOME observations of total BrO columns imply larger stratospheric BrO columns than can be accounted for by that supplied by CH_3Br and halons (Salawitch et al., 2005).

The role of VSLS in maintaining the global tropospheric background levels of BrO and total Br_y is a subject of active research. Von Glasow et al. (2004) showed that the stratosphere-to-troposphere flux of inorganic bromine combined with the tropospheric decomposition of CH_3Br was insufficient to maintain tropospheric levels of BrO approaching ~2 ppt. They examined the sensitivity of tropospheric BrO to various latitudinal distributions of surface emissions of VSL SGs. Although the resulting distributions of BrO and Br_y differed, the available data were too sparse and uncertain to place strong constraints on the geographic distribution of surface emissions. Yang et al. (2005) presented model results indicating that sea salt sources dominate the supply of bromine to the lower troposphere, and that VSL SGs are responsible for the majority of bromine in the upper troposphere. Warwick et al. (2006) suggested, based on a comparison of modeled and measured $CHBr_3$, that a large portion of $CHBr_3$ emissions occurs in the tropics. They also showed that emissions of VSL SGs (i.e., $CHBr_3$, CH_2Br_2, CH_2BrCl, $CHBrCl_2$), together with CH_3Br, could maintain ~2 ppt of Br_y in the tropical free troposphere, and between 0 and 2 ppt of Br_y in the rest of the troposphere. Levels of Br_y were lower in the rest of the troposphere in this simulation, which involved only VSL SGs, because of aerosol washout of product gas and the co-location of surface emissions and convection in the tropics.

There have been no atmospheric observations of organic degradation products of VSL SG decomposition to date, such as $COBr_2$ and COHBr from decomposition of $CHBr_3$ (Section 2.3). Most modeling studies have assumed direct conversion to inorganic bromine upon the decomposition of $CHBr_3$ and other VSL SGs. Field observations to assess the accuracy of this assumption represent another gap in our present knowledge.

Chlorine

In contrast to the situation for bromine and iodine, the tropospheric abundance of Cl_y is likely dominated by hydrogen chloride (HCl). The reason for the different behavior of the halogen families is that production of HCl from Cl plus methane (CH_4) is exothermic, while production of hydrogen bromide and hydrogen iodide (HBr and HI) by reactions involving CH_4 is endothermic. As a result, PGI for chlorine should be defined by the troposphere-to-stratosphere transport of HCl. Efficient scavenging of HCl by clouds and aerosols is generally considered to lead to negligible PGI of inorganic chlorine species. Measurements of HCl in the subtropical upper troposphere reveal abundances between 0 and 80 ppt, but simultaneous observations of other species indicate these levels of HCl are maintained by stratosphere-to-troposphere transport of Cl_y, rather than tropospheric degradation of VSL SGs (Marcy et al., 2004).

There are many organic decomposition products of chlorinated VSLS, most of which have not been measured in the atmosphere to date. An important exception is phosgene ($COCl_2$), produced by the decomposition of chlorinated organic gases (see Section 2.3.3). $COCl_2$ has a significant abundance in the upper tropical troposphere (on average 22.5 ppt, or 45 ppt as chlorine, Table 2-2), and a longer photochemical lifetime than some of its VSLS parent compounds (Section 2.3.3). There are no known surface sources of $COCl_2$. If $COCl_2$ were present in the TTL, where its removal processes are inefficient, it could potentially play a role in the PGI of chlorinated VSLS.

In this Assessment we have not, however, included phosgene in our evaluation of the contribution of VSLS to stratospheric Cl_y. One reason for $COCl_2$ not being included is that tropospheric $COCl_2$ is evidently produced by the decomposition of both long-lived and VSL source gases (Section 2.3.3). In the case of degradation of long-

lived gases that decompose primarily in the stratosphere, the majority of the tropospheric $COCl_2$ contribution is transported from the stratosphere (Kindler et al., 1995). Consequently, upper tropospheric measurements of $COCl_2$ do not necessarily define the contribution from degradation of VSL source gases alone to its abundance. The possibility exists for some degree of "double-counting" of Cl_y if $COCl_2$ is included in a summation of chlorine derived from the tropospheric abundances of all source gases. In addition, Kindler et al. (1995), based on a 1-D model, stated that only about 0.4% of $COCl_2$ produced in the troposphere is transported to, and decomposes in, the stratosphere. Measured stratospheric profiles of $COCl_2$ presented by Toon et al. (2001), however, appear to contradict this conclusion, since they show a much larger decline in mixing ratio with altitude than the model profiles of Kindler et al. (1995), and are instead consistent with the expected stratospheric loss of this compound discussed in Section 2.3.3. More detailed modeling and measurement studies of $COCl_2$ are needed to quantify whether or not it represents a significant route for PGI of stratospheric chlorine from VSL source gases. For the present we conclude that the contribution of $COCl_2$ to "additional" stratospheric Cl_y may range from a negligible amount (based on Kindler et al., 1995) to an upper limit of 40-50 ppt based on observed upper tropospheric abundances (Table 2-2 and Section 2.2.1).

Iodine

Both I_2 and IO have been observed in the marine boundary layer (Section 2.2.1). The tropospheric photochemical lifetimes of I_2 and IO are very short (Saiz-Lopez and Plane, 2004), and iodine oxides may self-nucleate, leading to efficient atmospheric removal by aerosols (Hoffmann et al., 2001). As a result, ozone depletion models do not typically consider transfer of inorganic iodine species across the tropopause, even though these species are abundant in parts of the boundary layer.

Product gas injection of decomposition products of CH_3I could be important, particularly if rapid convection lofts air parcels containing CH_3I into the TTL, where aerosol and cloud washout may be inefficient. In the future, decomposition products of CF_3I may also have to be considered (Section 2.2.4.3). However, no field observations of CH_3I and CF_3I decomposition products are available. The present state of knowledge for iodine is focused on defining stratospheric levels of I_y, rather than quantification of PGI sources.

2.5.1.3 Model Estimates of SGI and PGI

The SGI and PGI fluxes can be calculated from global model simulations of a single source gas and their products by tagging and keeping separate the degradation products produced in the stratosphere from those produced in the troposphere. The lack of atmospheric observations of the organic intermediate species, combined with limited knowledge of the kinetics of these intermediates and the recycling of inorganic halogen compounds, means estimates of PGI injection presently rely on parameterizations of these processes that are untested against observations. The studies described below, updating progress since the last Assessment, consider SGI and PGI of bromine.

Prior to this Assessment, calculations involving two-dimensional (2-D) (Dvortsov et al., 1999) and 3-D (Nielsen and Douglass, 2001) models showed that oceanic release of $CHBr_3$ could maintain about 1 ppt of bromine to the stratosphere. These calculations assumed a 10-day lifetime due to "washout" by aerosols and clouds for the inorganic products produced following the decomposition of $CHBr_3$.

Sinnhuber and Folkins (2006) used a one-dimensional mechanistic model of the tropical troposphere to quantify stratospheric supply of Br_y from $CHBr_3$ as a function of aerosol and cloud washout lifetime. In the model, Br_y reaching the stratosphere is determined by the detrainment from convection of $CHBr_3$ above the level of zero radiative heating (z_0, see Section 2.4.1). Convective mass fluxes are constrained by observed temperature and humidity. Rapid washout of Br_y in the convective cloud was assumed, resulting in no detrainment of Br_y (i.e., product gas). Product gas is therefore formed from degradation of source gas following detrainment. A first order, uniform washout lifetime for Br_y in the clear-sky atmosphere below 17 km was treated as an adjustable parameter. By assuming rapid washout for Br_y in a particular simulation, they showed that injection of Br_y from the SGI pathway maintains about 0.5 ppt of Br_y per ppt of surface $CHBr_3$, generally consistent with the results of Dvortsov et al. (1999) and Nielsen and Douglass (2001). They also examined the sensitivity of PGI to washout lifetime. The PGI of Br_y was 0.3 ppt, 0.8 ppt, and 1.6 ppt, per ppt of surface $CHBr_3$, for lifetimes of 10, 30, and 100 days, respectively (Figure 2-7). They discussed how the washout of soluble species from the TTL depends on details of ice microphysics and could, in principle, be inefficient if air detraining from deep convection is dry.

The delivery of total Br_y via both SGI and PGI routes varied from 0.8 to 2.1 ppt, per ppt of surface $CHBr_3$, as the washout lifetime increased from 10 to 100 days.

It is also useful to use model results to diagnose the SGI and PGI flux as a percentage of the flux of VSLS emitted at the surface, as opposed to relating it to mixing ratios as in the above study. Warwick et al. (2006) conducted a 3-D model simulation considering surface fluxes of $CHBr_3$ and other VSL SGs. Convection in this model was parameterized using the mass flux scheme of Tiedtke (1989) and included convective updrafts and large-scale subsidence associated with deep and shallow convection. An average tropospheric lifetime of 10 days relative to rainout was assumed for inorganic bromine. Among the scenarios were two cases where the $CHBr_3$ emission flux was either uniform in the open ocean or was limited to the tropical coastlines. As discussed in Section 2.3.2, the calculated lifetimes for the open ocean case are 30-37 days, compared with 15 days for the tropical coastline case. The SGI fluxes in the two simulations were practically the same at about 0.7% of the total surface emission flux. The PGI fluxes were 4% and 5% respectively. The Warwick et al. study also showed that $CHBr_3$, together with the VSLS CH_2Br_2, CH_2BrCl, $CHBr_2Cl$, and $CHBrCl_2$, could together maintain 3 to 4 ppt Br_y in the tropical lower stratosphere.

The Atmospheric and Environmental Research, Inc. (AER) 2-D model (Rinsland et al., 2003) was also used to simulate $CHBr_3$. The model used the convection parameterization from Dvortsov et al. (1998). Washout in the model was parameterized by a first-order removal rate that was constant in time. For a fixed uniform surface mixing ratio boundary condition, the SGI flux was 0.3% of the surface emission flux and the residence time of SGI Br_y in the stratosphere was 1.4 years. Assuming the same residence time, the PGI flux was 0.6%, about twice the SGI value. Note that in the Dvortsov et al. (1999) and the Nielsen and Douglass (2001) studies, the PGI flux was three times and twice the SGI flux, respectively. These studies confirm the suggestion that the sum of the two (PGI + SGI fluxes) could be as large as a few percent of surface emissions. As discussed in Section 2.4.3, the calculated mixing ratio of the product gas in the stratosphere is related to the SGI and PGI fluxes through the residence time in the model stratosphere. It is important to note that the larger fluxes calculated in Warwick et al. (2006) (a few percent versus less than 1%) were accompanied by smaller residence times for the stratosphere (0.2 years versus about 1.4 years). This may be related to whether diagnosed fluxes represent the net fluxes across the tropopause.

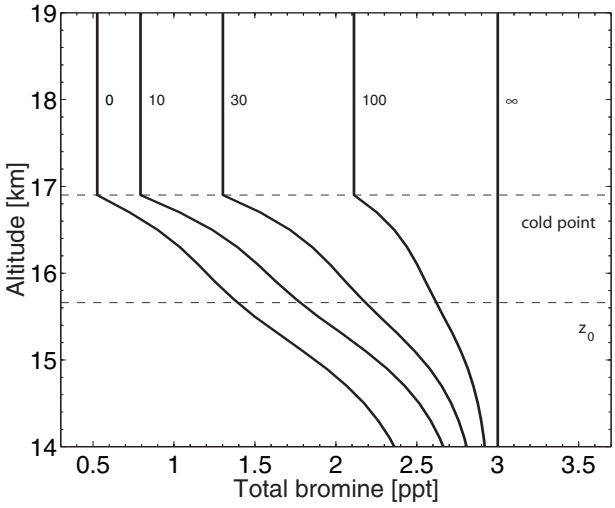

Figure 2-7. Calculated profile of total bromine from bromoform present as both product gas (Br_y) and source gas ($CHBr_3$), defined as $Br_y + 3 \cdot CHBr_3$, for different values of the lifetime of Br_y in days (numbers given in graph), based on a one-dimensional model of the tropical atmosphere. The calculations assume 1 ppt of $CHBr_3$ in the boundary layer and that no Br_y is detrained from convection (i.e., model assumes efficient uptake and removal of Br_y in clouds). Locations of the level of zero radiative heating and the cold point tropopause in the model are indicated. From Sinnhuber and Folkins (2006).

Finally it should be noted that the aforementioned model studies do not include possible heterogeneous reactions (Platt and Hönninger, 2003) that liberate inorganic bromine back to the gas phase (Section 2.3.4), which might result in more efficient PGI of Br_y from $CHBr_3$ than was considered in past Assessments.

2.5.2 Estimates of VSLS Contributions to Stratospheric Halogens Based on Measurements of Inorganic Species

This section focuses on the contributions of VSL halocarbons to the stratospheric budgets of bromine, chlorine, and iodine, based on measurements of inorganic species. For chlorine and bromine, the material is focused mainly on studies that compare the total halogen content of inorganic species with the halogen content of organics. Typically the difference between the inorganic and organic budgets is computed for an organic budget containing just long-lived SGs. The resulting difference is then interpreted as being the contribution to the stratospheric

halogen loading by VSLS. This method is unable to distinguish between SGI and PGI, and would also include contributions from product gases that do not originate from VSLS. For bromine the long-lived SG budget is defined by the total bromine content of CH_3Br and the three or four halons that are commonly used to define baseline halogen scenarios for this and previous Assessments. For chlorine species the long-lived SG budget is defined by the 12 species (CFC-11, CFC-12, CFC-113, CFC-114, CFC-115, CCl_4, CH_3CCl_3, HCFC-22, HCFC-141b, HCFC-142b, halon-1211, and CH_3Cl; see Chapter 1) used to define the baseline halogen loading scenarios in this and prior Assessments. As defined in the introduction, the terms Br_y^{VSLS} and Cl_y^{VSLS} refer to the component of stratospheric Br_y and Cl_y, respectively, due to SGI and PGI of sources other than these long-lived SGs. For iodine, the discussion is focused on quantification of total stratospheric inorganic iodine (I_y) based on measurements of IO, since supply is thought to be exclusively from VSL SGs. These approaches represent the present state of knowledge regarding quantification of the contribution of VSLS on the stratospheric halogen loadings.

2.5.2.1 BROMINE

Prior to this Assessment, balloonborne observations of BrO in the middle stratosphere at midlatitudes were shown to be consistent with stratospheric Br_y of 21.5 ± 3 ppt (Pfeilsticker et al., 2000). The total amount of organic bromine in the upper troposphere reported in this study was 18.4 (+1.8 / −1.5) ppt, based on measurements of CH_3Br, four halons, and a variety of VSL SGs. The higher levels of Br_y inferred from BrO, compared with Br_y inferred from the suite of organics, suggested either direct transport of VSL PGs or inorganic bromine across the tropopause, or perhaps larger abundances of VSL SGs in the tropics compared with midlatitudes where the balloon observations were obtained. Ground-based observations of column BrO from many stations were shown to be consistent with a total stratospheric bromine abundance of 20 ± 4 ppt, reflecting a ~5 ppt contribution from VSLS (Sinnhuber et al., 2002). Also in the last Assessment, a time series of Br_y inferred from BrO measurements in the middle stratosphere over several years was shown to exceed Br_y from CH_3Br + halons by an amount consistent with supply of 4 to 5 ppt of Br_y from VSLS (Figure 1-8, WMO, 2003). However, the interpretation of these data in the last Assessment was tentative, with the possibility of "calibration errors either in the measurements of BrO or the organic source gases" being noted as a possible explanation of the observations.

Since the last Assessment, there have been many studies, described below, that quantify Br_y^{VSLS}. Most of these studies, based on measurements of BrO by many techniques, conclude that stratospheric Br_y exceeds the amount of bromine that can be supplied solely by CH_3Br and halons. Therefore, since the last Assessment, we have gained greater confidence that the stratospheric bromine budget is affected by cross-tropopause transport of brominated VSLS, by either the SGI and/or PGI routes, and that the difference noted in the last Assessment is not due to "calibration errors."

Figure 2-3 updates the time series of stratospheric and tropospheric bromine shown in the last Assessment (Figure 1-8, WMO, 2003). Observations of BrO using balloonborne differential optical absorption spectroscopy (DOAS) have been used to estimate stratospheric Br_y (Dorf, 2005; Dorf et al., 2006a). The most accurate analysis is based on estimating the mixing ratio of BrO for the middle stratosphere from the slope of BrO slant column versus air column above the balloon float altitude (the "Langley" method) and then using a photochemical model to deduce Br_y from measured BrO. Results for five flights, from 1996 to 2005, are illustrated (points labeled "DOAS BrO Langley obs.") in Figure 2-3. Numerical values are also given in Table 2-7. Estimates of Br_y^{VSLS} are based on the difference between Br_y inferred from BrO and the bromine content of CH_3Br and halons ($Br_y^{CH3Br+Halons}$). The estimate of $Br_y^{CH3Br+Halons}$ considers age of air, inferred from measured tracers, and neglects tropospheric gradients (i.e., it assumes that the sum of bromine from source and associated product gases at the tropical tropopause, notably in the case of CH_3Br, is represented by the mean of observed global surface mixing ratios). The difference between Br_y inferred from BrO and $Br_y^{CH3Br+Halons}$ yields the estimated value for Br_y^{VSLS} (bottom row, Table 2-7). The mean and standard deviation for Br_y^{VSLS}, considering all five flights, is 4.1 ± 1 ppt. The overall uncertainty of this estimate, which is dominated by the accuracy of the BrO measurements and by the kinetics used to estimate Br_y from BrO, is ±2.5 ppt (see Table 2-7 for discussion of uncertainties). Values of Br_y^{VSLS} are illustrated in Figure 2-3 by the difference between the time series of Br_y inferred from BrO and $Br_y^{CH3Br+Halons}$.

Other DOAS-based estimates of Br_y are also shown in Figure 2-3. These estimates, labeled "DOAS BrO profiles," are derived from model interpretation of BrO profiles in the lower stratosphere. The DOAS BrO profile estimate is considered to be a less reliable method for inferring Br_y^{VSLS} compared with the Langley method (Dorf, 2005). It is reassuring that the two methods give good agreement, since this shows an overall level of con-

Table 2-7. Contribution to stratospheric Br_y^{VSLS} based on DOAS balloon BrO profiles.

	Leon, Spain 1996	Kiruna, Sweden 1999	Aire sur l'Adour, France 2003	Kiruna, Sweden 2003	Teresina, Brazil 2005
Br_y from BrO (ppt)[a]	17.8	19.9	20.1	20.4	21.5
Age (yrs)	5	6	5	5	5
CH_3Br (ppt)[b]	9.2	9.3	9.6	9.5	8.8
Halons (ppt)[b]	5.2	5.8	7.2	7.2	7.5
Br_y^{VSLS} (ppt)[c]	3.4	4.8	3.3	3.7	5.2

[a] The 1σ precision of Br_y estimated using the Langley method is about 0.7 ppt. The total uncertainty is 2.5 ppt, which represents the precision as well as uncertainties in the BrO cross section (±8%) and the photochemical correction used to convert BrO to Br_y (±8%).

[b] Estimates of $Br_y^{CH3Br+Halons}$ are obtained from Montzka et al. (2003), assuming no tropospheric gradient of CH_3Br.

[c] The mean and standard deviation of the 5 estimates of Br_y^{VSLS} are 4.1 ± 1 ppt. The standard deviation is consistent with the estimated precision in Br_y. Considering the overall uncertainty in Br_y from BrO, and assuming that $Br_y^{CH3Br+Halons}$ is well known, leads to a range for Br_y^{VSLS} of 4.1 ± 2.5 ppt, which is the value for DOAS given in Table 2-8. From Dorf (2005).

sistency between the two methods that sample different parts of the atmosphere. DOAS BrO profile estimates are also available for more fights than the estimates based on the Langley method, resulting in a more complete time series for stratospheric Br_y. The fact that values of Br_y in the lower and middle stratosphere are similar lends credence to the notion that VSLS contribute significantly to stratospheric Br_y.

The values of Br_y inferred from the balloon observations of BrO shown in Figure 2-3 imply, by an amount that is larger than the overall uncertainty, a significant contribution to stratospheric Br_y from VSLS. In addition, the values of Br_y observed during the past few years indicate a "leveling off" that appears to be consistent with the behavior of $Br_y^{CH3Br+Halons}$ (Dorf et al., 2006b). This suggests that Br_y^{VSLS} has not changed dramatically between 1996 and 2005, the time period of the stratospheric observations, and that changes in the surface emissions of CH_3Br and halons are being reflected in the stratospheric abundance of Br_y.

As noted above, Figure 2-3 neglects tropospheric gradients of CH_3Br that may, at least partly, result from its tropospheric degradation. The mixing ratios of CH_3Br in the TTL may be about 7% smaller than the globally averaged surface value (Schauffler et al., 1999; Montzka et al., 2003). If the bromine compounds resulting from tropospheric decomposition of CH_3Br do not reach the stratosphere, then estimates of Br_y^{VSLS} that rely on surface mixing ratios of CH_3Br may consequently be too low by up to 0.6 ppt.

Salawitch et al. (2005) examined GOME column BrO as well as measurements of BrO from aircraft and balloons. Their study suggested Br_y^{VSLS} between 4 and 10 ppt; best agreement with aircraft data was achieved for a value of 6.9 ppt, while a balloon profile of BrO in the summer tropics (Pundt et al., 2002) suggested a value closer to 10 ppt. Sinnhuber et al. (2002, 2005) showed that the gas-phase reaction of bromine nitrate ($BrONO_2$) with oxygen atom triplet ($O(^3P)$) proceeds quickly enough (Soller et al., 2001) to affect the partitioning of Br_y species. Nearly all of the studies presented here consider this reaction, even though it is not included in any of the past JPL or IUPAC evaluations. The exception is the study of Salawitch et al. (2005), who relied solely on JPL kinetics. Had they included this reaction, their values of Br_y^{VSLS} from the aircraft and balloon data would have been ~6 ppt and ~8 ppt, respectively. The Salawitch et al. (2005) values of Br_y^{VSLS} are a little higher than those derived from the DOAS measurements, but are generally consistent with the picture presented in Figure 2-3.

Since the last Assessment, attention has also focused on the interpretation of satellite observations of BrO. As noted previously, observations of column BrO from GOME reveal abundances of total column BrO, throughout the global atmosphere, that are much larger than expected based on simulations that assume supply of atmospheric bromine from only CH_3Br and halons (Figure 2-8, top panel). Measurements of column BrO from the Scanning Imaging Absorption Spectrometer for Atmospheric Cartography (SCIAMACHY) satellite instrument confirm the accuracy of the GOME observations of column BrO (Sinnhuber et al., 2005; Sioris et al., 2006). Recent scientific studies have focused on quantifying whether the much higher than expected levels of BrO reported by GOME reside in the stratosphere, the troposphere, or perhaps in both layers at levels important for the photochemical environment. Evidence for and against a global, background tropospheric level of BrO large

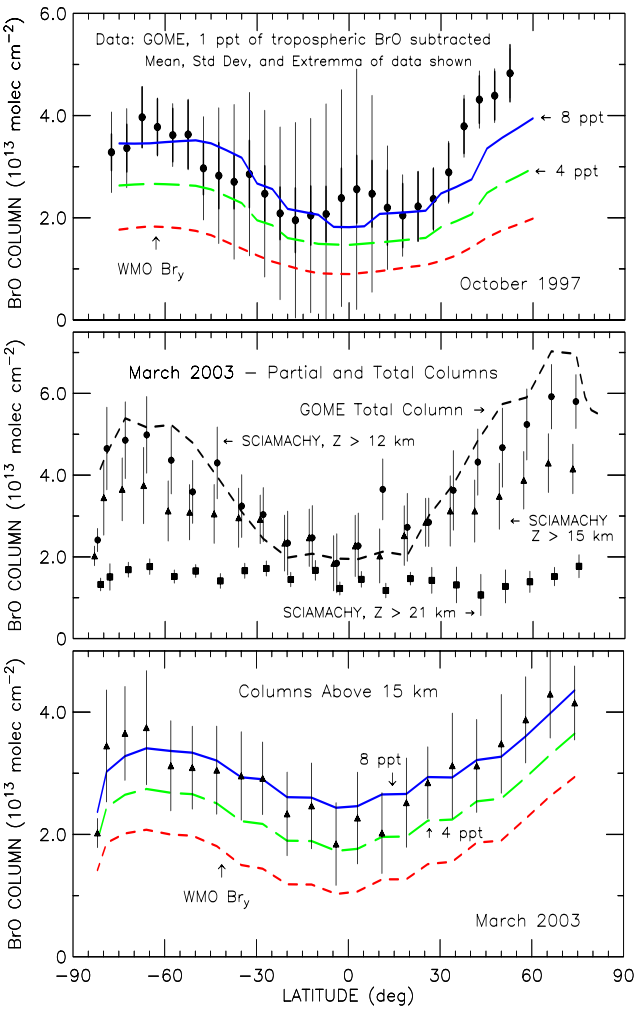

Figure 2-8. Top panel: Comparison of estimated stratospheric column BrO from GOME, October 1997, assuming a uniform 1 ppt distribution of BrO in the troposphere (close to the upper limit of 0.9 reported by Schofield et al., 2004) with stratospheric column BrO from the AER 2-D model, for the WMO (2003) "best guess" scenario Ab (labeled WMO Br_y) and for simulations assuming Br_y^{VSLS} of 4 and 8 ppt, respectively. Plotted points show mean, standard deviation (thick error bars) and extreme values (thin error bars) of GOME data in 5°-wide latitude bins. The reasonably good agreement between the 8 ppt curve and the data suggest the BrO signal measured by GOME may be due to the presence of higher amounts of BrO in both the stratosphere and troposphere than is assumed in most models. After Chance (1998) and Salawitch et al. (2005). Middle panel: Comparison of total column BrO measured by GOME (March, 2003) vs. latitude and partial column BrO above various altitudes, based on BrO profiles from SCIAMACHY limb radiances. The comparison suggests a large component of the GOME total column resides between ~12 and 21 km. Bottom panel: Comparison of total column BrO above 15 km from SCIAMACHY with BrO partial columns from the AER 2-D model, found for the WMO Br_y and for model simulations assuming Br_y^{VSLS} of 4 and 8 ppt. Model simulations from Salawitch et al. (2005); SCIAMACHY BrO from Sioris et al. (2006).

enough to account for excess BrO revealed by GOME and SCIAMACHY are described in Section 2.5.1.2. Clearly, a better definition of tropospheric BrO would clarify the stratospheric implications of the column BrO measurements, from both satellite and ground-based instruments.

Measurements of BrO profiles from SCIAMACHY provide new insight on the global stratospheric distribution of BrO. However, retrievals of BrO have been conducted by two groups and the scientific interpretations differ considerably. Retrievals by Sioris et al. (2006) show large abundances in the tropical tropopause layer and lowermost stratosphere, consistent with large abundances of stratospheric Br_y, ~24 to 25 ppt, and $Br_y^{VSLS} = 8.4 \pm 2$ ppt (Sioris et al., 2006) (Figure 2-8, middle and bottom panels). Retrievals of SCIAMACHY BrO by Sinnhuber et al. (2005) suggest stratospheric $Br_y = 18 \pm 3$ ppt, implying a smaller value for Br_y^{VSLS} of 3 ± 3 ppt (Figure 2-9). The BrO retrievals of Sinnhuber et al. (2005) show a deficit in the tropical lower stratosphere compared with calculations, particularly for model simulations that include Br_y from VSLS (Figure 2-9, panel labeled "18.5 km"). This deficit is contrary to the expectation of a significant perturbation to stratospheric Br_y from VSLS. Conversely, partial BrO columns retrieved by Sioris et al. (2006) show large abundances in the tropical LMS, consistent with supply of Br_y from VSLS (Figure 2-8, middle).

The retrievals of BrO in these two studies also offer different views on tropospheric BrO. Comparison of the Sinnhuber et al. (2005) stratospheric BrO profiles (based on limb radiances) and total column BrO measurements (based on nadir radiances) suggests the presence of 1 ± 0.5 ppt of tropospheric BrO (Figure 2-9, bottom). On the other hand, the consistency of BrO columns integrated above 12 km (limb) from SCIAMACHY and total column BrO from GOME (nadir) shown by Sioris et al. (2006) suggests a much smaller level of global tropospheric BrO (Figure 2-8, middle). The reason for these alternate interpretations of SCIAMACHY radiances is due to differences in the BrO retrievals computed by the two groups and does not appear to be related to either the methods used to infer

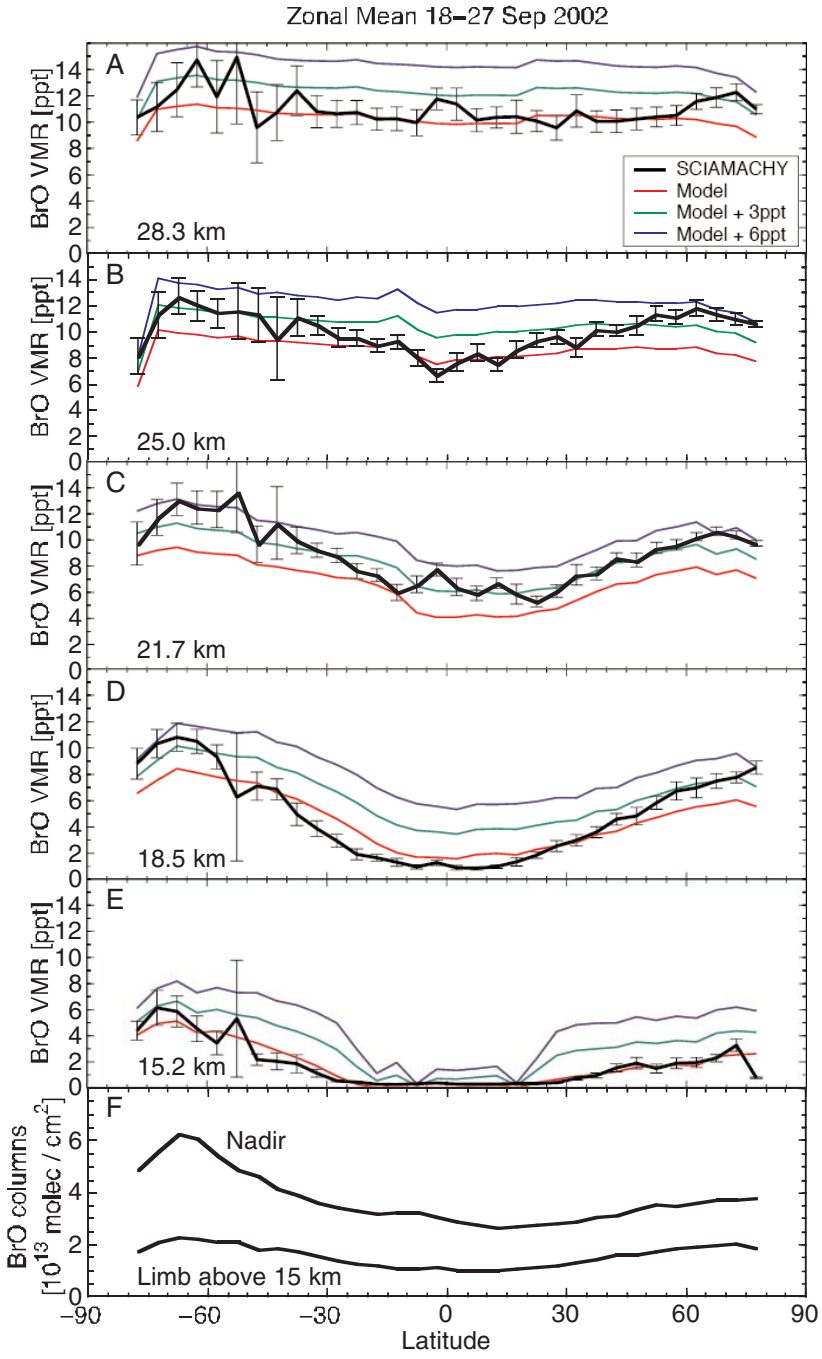

Figure 2-9. SCIAMACHY BrO observations. Panels A-E: Comparison between BrO volume mixing ratios (VMR) retrieved from SCIAMACHY limb radiances and model calculations for different altitudes. SCIAMACHY error bars are derived from the standard deviation of BrO measurements within each latitude bin. The modeled BrO was calculated from an estimate of Br_y derived from Michelson Interferometer for Passive Atmospheric Sounding (MIPAS) measurements of CFC-11 and the Wamsley et al. (1998) relation between Br_y and CFC-11 (scaled to the time of observation) and a photochemical model estimate of BrO/Br_y. Three model runs are shown: Br_y from only CH_3Br and halons (i.e., WMO Br_y) (red line), and using Br_y^{VSLS} of 3 ppt of Br_y (green line) and 6 ppt (blue line). Panel F: Total BrO column from SCIAMACHY nadir measurements compared with the integrated vertical BrO column above 15 km from SCIAMACHY limb observations. The difference between the integrated limb and the nadir column implies the presence of a significant amount of BrO below 15 km, corresponding to an average BrO mixing ratio of about 1.0 ± 0.5 ppt between the surface and 15 km. Adapted from Sinnhuber et al. (2005).

Br_y from BrO, or to assumptions regarding $Br_y^{CH3Br+Halons}$. The SCIAMACHY BrO retrievals are sensitive to the determination of the tangent height of the limb radiances and methods used to account for spectral residuals (Sioris et al., 2006). Efforts are underway to compare balloon profiles of BrO with the SCIAMACHY retrievals (Dorf et al., 2006a). However, much work remains to understand the differences between the various retrievals of BrO and to reduce the uncertainty in the global distribution of BrO retrieved from SCIAMACHY radiances, which is perhaps best reflected by the contrasting results of Sinnhuber et al. (2005) and Sioris et al. (2006).

Measurements of BrO from the Microwave Limb Sounder (MLS) have also been used to quantify Br_y^{VSLS} (Livesey et al., 2006). These observations, shown in Figure 2-10, imply a value for Br_y of 18.6 ± 5.5 ppt for the upper stratosphere (~30 to 42 km), between 55°S and 55°N, from September 2004 to August 2005. The uncertainty reflects the accuracy of the MLS measurements of BrO and possible errors in kinetic parameters used to infer Br_y from BrO. Livesey et al. (2006) inferred Br_y from BrO using two modeling approaches, but place greater confidence in the approach that uses a model constrained by MLS measurements of O_3 and nitrous oxide (N_2O) (PSS results in Figure 2-10). Their value of Br_y^{VSLS} is 3.0 ± 5.5 ppt.

Observations of BrO in the polar vortices provide an opportunity to examine the bromine budget in an environment where all of the organic precursors have decomposed, and where the low levels of reactive nitrogen oxides ($NO + NO_2 = NO_x$) imply that nearly all of Br_y is contained in the two species BrO and bromine chloride (BrCl). These observations, discussed in Chapter 4, also support a significant, non-zero value for Br_y^{VSLS}. As discussed in Chapter 4, the 6 to 8 ppt enhancement of BrO_x (BrO+BrCl) in the Arctic vortex (Frieler et al., 2006), presumably from VSLS, relative to standard models (see Figure 4-16 in Chapter 4) may account for the discrepancy between measured and modeled chemical loss rates for Arctic ozone that was noted in the last Assessment.

Table 2-8 shows estimates of Br_y^{VSLS} from nine studies. The central value from each study is given, as well as a range. For most studies, the uncertainty of Br_y^{VSLS} was explicitly calculated while, for a few, it has been estimated by this Assessment based on information in each paper (see Table 2-8). The range was estimated using different methods by the various studies; the original papers should be consulted for details. Estimates of Br_y^{VSLS} from ground-based studies are included. The Sinnhuber et al. (2002) study, discussed in the last Assessment, has been described above. Schofield et al. (2004, 2006) examined direct and scattered sunlight to

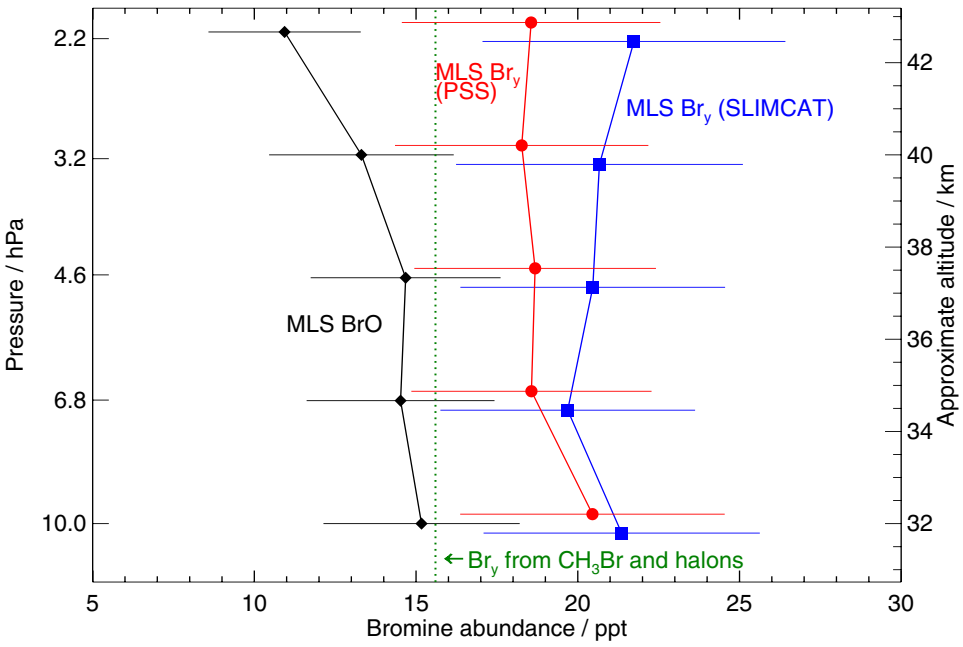

Figure 2-10. Measurement of BrO from Aura MLS versus pressure, for limb scans covering 55°S to 55°N, September 2004 to August 2005, and values of Br_y inferred from MLS BrO using estimates of BrO/Br_y from the SLIMCAT model (blue) and from a photochemical steady state (PSS) model (red) constrained by MLS BrO, O_3, and H_2O, and values of NO_y and CH_4 derived from MLS N_2O. The value of Br_y due to CH_3Br and halons during the time of measurement is shown by the dotted line. Error bars reflect the accuracy of MLS BrO and uncertainties in the model estimate of Br_y. The analysis using the PSS simulation was considered to be a more reliable estimate for stratospheric Br_y because this model is constrained by measured O_3 and exhibits a profile for NO_2 that agrees well with Halogen Occultation Experiment (HALOE) satellite measurements. The stratospheric bromine loading is estimated to be 18.6 ± 5.5 ppt, implying Br_y^{VSLS} = 3.0 ± 5.5 ppt. From Livesey et al. (2006).

retrieve BrO profiles over Lauder, New Zealand (45°S), and Arrival Heights, Antarctica (78°S). They concluded that stratospheric column BrO was consistent with Br_y^{VSLS} of 6 ± 3 ppt at both locations.

Estimates of the Br_y^{VSLS} given in Table 2-8 range from lows of 3.0 ± 5.5 ppt (MLS data: Livesey et al., 2006) and 3 ± 3 ppt (SCIAMACHY retrievals: Sinnhuber et al., 2005) to highs of 4 to 10 ppt (aircraft and balloon data: Salawitch et al., 2005) and 8.4 ± 2 ppt (SCIAMACHY retrievals: Sioris et al., 2006). Dorf (2005) report a value of 4.1 ± 2.5 ppt from many years of balloon observations. Sheode et al. (2006) report a value of 3.5 ± 4 ppt, based on analysis of two years of SCIAMACHY data. This study is an update to Sinnhuber et al. (2005), who considered SCIAMACHY data over a 10-day period; the slightly larger uncertainty given by Sheode et al. (2006) is due to increased atmospheric variability over the longer time period.

The mean of the central values of Br_y^{VSLS} given in Table 2-8 is 5 ppt. This is the "ensemble" value reported at the bottom of the table. It is difficult to ascribe a true uncertainty to this ensemble value, given that uncertainties in Br_y^{VSLS} were determined using different methods, and in some cases were estimated by this Assessment. As a result, we place greater confidence in the range of central values in the Table (3 to 8 ppt) as an estimate of the uncertainty in Br_y^{VSLS}. While three of the studies could not rule out a zero contribution from VSLS, the majority of studies pointed to a positive value for Br_y^{VSLS} large enough to affect ozone photochemistry in the LMS (Section 2.6).

2.5.2.2 CHLORINE

Measurements of HCl in the subtropics typically exceed 50 ppt (Marcy et al., 2004). As noted above, these

Table 2-8. Contribution to stratospheric Br_y^{VSLS}.

Data Source	Br_y^{VSLS} Central Value (ppt)	Br_y^{VSLS} Range (ppt)	Reference
Ground-based BrO 11 sites, 78°S-79°N	5	1-9 [a]	Sinnhuber et al. (2002)
Ground-based BrO Lauder, New Zealand, 45°S	6	3-9	Schofield et al. (2004)
Ground-based BrO Arrival Heights, Antarctica, 78°S	6	3-9	Schofield et al. (2006)
DOAS Balloon BrO Profiles 5°S-68°N, 0-35 km	4.1	1.6-6.6	Dorf, 2005
Aircraft & Balloon BrO Profiles, 22°S-35°N, 17-32 km and GOME Satellite Column BrO, 60°S-60°N	7	4-10 [a]	Salawitch et al. (2005)
SCIAMACHY Satellite BrO Profiles 80°S-80°N, 15-28 km	8.4	6.4-10.4	Sioris et al. (2006)
SCIAMACHY Satellite BrO Profiles 80°S-80°N, 15-28 km	3	0-6	Sinnhuber et al. (2005)
SCIAMACHY Satellite BrO Profiles 80°S-80°N, 15-28 km	3.5	0-7.5	Sheode et al. (2006)
MLS Satellite BrO Profiles 55°S-55°N, 30-42 km	3.0	0-8.5	Livesey et al. (2006)
Ensemble	**5 (3-8)** [b]		

DOAS, Differential Optical Absorption Spectroscopy; GOME, Global Ozone Monitoring Experiment; SCIAMACHY, Scanning Imaging Absorption Spectrometer for Atmospheric Cartography; MLS, Microwave Limb Sounder.

[a] Range estimated by this Assessment, based on the uncertainty in stratospheric Br_y inferred from BrO that was stated in the reference.

[b] Average and range of the central values of the 8 estimates of Br_y^{VSLS}.

data have been interpreted as being evidence for supply of HCl from the stratosphere, rather than being due to the decomposition of VSL SGs. There have been no studies, since the last Assessment, quantifying the influence of VSL SGs on measured HCl in the tropical TTL or LMS. Such a study would require accurate and precise measurement of HCl and a suite of organic chlorine species, including long-lived SGs and VSL SGs, plus either detailed model analysis and/or observations of dynamical tracers to be able to isolate the effects on chlorine of transport from above (where the longer lived SGs decompose) and from below (where VSL SGs potentially contribute).

Another avenue for assessing the role of VSL compounds on stratospheric chlorine, which has received some attention since the last Assessment, is quantification of stratospheric chlorine either by measurements of a suite of compounds in the middle stratosphere or by measurement of HCl in the upper stratosphere. Nassar et al. (2006) quantified total stratospheric chlorine ($Cl_{TOT,}$ the sum of simultaneous measurements of organic and inorganic species; see Figure 1-12 of Chapter 1) based primarily on data from the Atmospheric Chemistry Experiment Fourier Transform Spectrometer (ACE-FTS). They report a value of Cl_{TOT} of 3.65 ppb over the period February 2004 to January 2005, for both Southern and Northern Hemisphere midlatitudes. The 1σ precision of Cl_{TOT} is 0.09 ppb and the estimated accuracy is 0.13 ppb. The estimated contribution of just long-lived species to Cl_y during this time period is 3.41 ppb (this estimate is based on a mean age for stratospheric air of 5 years and an age of air spectrum width of 3 years, applied to the WMO 2002 baseline scenario Ab (see Chapters 1 and 3 of this Assessment) for the 12 long-lived chlorine species). The fact that the ACE-FTS value of Cl_{TOT} exceeds this value of Cl_y could be indicative of a contribution from VSLS. On the other hand, the combined uncertainty of the ACE-FTS value of Cl_{TOT} (accuracy + precision) nearly overlaps with the expected value of Cl_y from just long-lived species.

Time series of HCl near 55 km from the ATMOS (Atmospheric Trace Molecule Spectroscopy experiment), HALOE (Halogen Occultation Experiment), MLS, and ACE-FTS instruments are shown in Figure 1-12 of Chapter 1, where it is discussed in terms of trends of Cl_y in the stratosphere. In the Figure these measurements are compared with modeled stratospheric abundances of HCl due to long-lived chlorinated gases alone (dashed line), and enhanced by the addition of 100 ppt of chlorine to represent a possible contribution from VSLS and phosgene (solid lines). Because of the level of uncertainty in the respective satellite measurements (note the error bars in Figure 1-12, which represent 2-sigma uncertainty), it is difficult to discriminate between the model runs with and without enhanced chlorine. The model run based on long-lived source gases alone appears closer to the HALOE measurements of HCl, which are lower than those obtained by the other instruments (although within their reported error limits). The MLS, ATMOS, and ACE-FTS measurements are suggestive of a contribution of chlorine from VSLS. The contribution of VSLS to stratospheric Cl_y cannot be quantified definitively given the current level of accuracy of the satellite HCl measurements.

2.5.2.3 IODINE

Solomon et al. (1994) suggested that if stratospheric inorganic iodine (I_y) levels were close to 1.0 ppt, catalytic cycles involving IO + BrO and IO + ClO could be responsible for a significant component of midlatitude ozone trends. That suggestion has led to considerable effort to better understand the photochemistry of inorganic iodine species (e.g., Bösch et al., 2003, and references therein) and to define the stratospheric iodine budget.

Wennberg et al. (1997), based on analysis of ground-based spectra, reported an upper limit for I_y of 0.2 ppt. Pundt et al. (1998) reported a similar upper limit, based on analysis of balloonborne spectra. Both studies were summarized in the last Assessment. Since the last Assessment, several additional studies of the I_y budget have appeared. Bösch et al. (2003), based on balloonborne solar occultation spectra in the UV/visible region from flights at middle and high latitudes, report an upper limit for I_y of 0.1 ppt. Recent measurements of IO in the tropics, using the same technique, also show very low levels of IO (Butz, 2006) (Figure 2-11). These observations suggest that either much less iodine enters the stratosphere than expected based on levels of CH_3I near the surface, or that stratospheric iodine resides either in gaseous species besides IO or perhaps in particulate form (see Section 2.3.5). As noted above, the tropospheric lifetime of the dominant iodine VSL SGs is much smaller (i.e., ~5 days) than the tropospheric lifetime of many brominated VSLS (>100 days). This could account for SGI of bromine and little or no SGI of iodine. Furthermore, observations of self-nucleation of iodine oxides (Hoffmann et al., 2001) and iodine uptake on tropospheric aerosols (Murphy and Thomson, 2000) could account for inefficient transfer of I_y to the stratosphere via PGI.

The only evidence of significant levels of stratospheric iodine is provided by ground-based observations of spectra recorded at 79°N that show, on some days, signs of elevated column IO (Wittrock et al., 2000). The SZA variation of slant column density of IO was used to suggest that the elevated IO lies in the stratosphere, with an

abundance of I_y as high as 0.8 ppt. The considerable variation in I_y for different days is difficult to reconcile in terms of a large stratospheric contribution, particularly for high-latitude air masses that should lack any residual CH_3I. Higher levels of IO were seen in February 1997 compared with March 1997, associated with lower levels of NO_x in February. Similar observations of the SZA variation of slant column IO in the Antarctic have been used to argue for a burden located primarily in the troposphere (Frieß et al., 2001). The observation of highly elevated IO on some days by Wittrock et al. (2000) is presently the only piece of observational evidence supporting a large source of I_y from VSLS. It should be recalled, however, that the ozone destruction efficiency of iodine is large compared with that of both bromine and chlorine, and IO abundances in the stratosphere of several tenths of 1 ppt could be potentially significant (Figure 2-2).

2.6 POTENTIAL IMPACT OF VSLS ON OZONE

In WMO (2003) the focus of this topic was on (1) the theoretical basis for estimating the change in column ozone from emissions of organic VSL SGs, and (2) the theoretical basis for estimating Ozone Depletion Potentials (ODPs), including the differences (Wuebbles and Ko, 1999; Wuebbles et al., 2001) from the standard ODP definition, and initial analyses of location-dependent ODPs for one VSL SG, n-propyl bromide. WMO (2003) gave a comprehensive evaluation of the theoretical basis and procedures for estimating ozone column effects and ODPs of VSL SGs; the discussion here is intended to update that evaluation.

2.6.1 Effects of Halogenated VSLS on Column Ozone

Halogens supplied by the decomposition of VSLS have the potential to significantly alter the photochemistry of ozone in the upper troposphere (UT) and lowermost stratosphere (LMS). Within models that consider supply of bromine solely from CH_3Br plus halons, pure odd-hydrogen radical (HO_x) photochemistry is the dominant loss process for odd oxygen in the LMS (Salawitch et al., 2005; see Figure 2-2). As discussed in Section 2.5, Br_y^{VSLS} in the LMS, maintained by the SGI and PGI pathways, can potentially cause significant local perturbation to the Br_y budget. Inorganic tropospheric bromine may also be transported in the LMS and contribute to additional Br_y^{VSLS} (as discussed in Section 2.5). Enhanced levels of bromine lead to greater efficiency for ozone loss by the BrO + ClO catalytic cycle, particularly during times of high aerosol loading following major volcanic eruptions (Salawitch et al., 2005; Sinnhuber et al., 2006). Because of this cycle, Br_y^{VSLS} enhances ozone depletion due to CFCs and other chlorocarbons. If Br_y^{VSLS} is 5 ppt, as suggested by the assessment presented in Section 2.5, and if the majority of this bromine is present in the LMS, then ozone loss by the BrO + HO_2 cycle becomes greatly enhanced (Salawitch et al., 2005). Indeed, at Br_y^{VSLS} between 4 to 8 ppt, ozone loss by bromine cycles through-

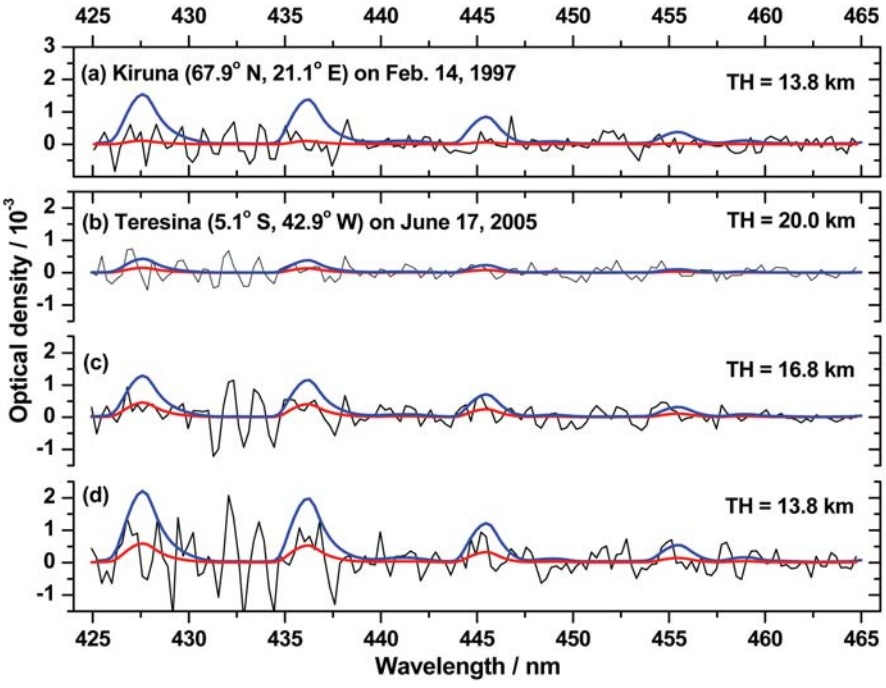

Figure 2-11. Comparison of measured and expected IO absorption by balloonborne UV/visible solar occultation spectroscopy at high and low latitudes (black line: measured IO + residual absorption; red line: inferred IO absorption: blue line: the expected IO absorption assuming [IO] = 0.5 ppt for the 0 to 20 km altitude range). Panels (a) and (b) are for observations within the lowermost stratosphere, and panels (c) and (d) for observations within the tropical tropopause layer. TH = tangent height. Panel (a) is adopted from Bösch et al. (2003), and panels (b) to (d) are from Butz (2006).

out the lowermost stratosphere can approach ozone loss by HO_x cycles alone (Figure 2-2).

In the last Assessment, a value of 45 was given for the relative effectiveness of stratospheric ozone depletion by bromine; the so-called α parameter (Section 1.4.4, WMO, 2003). This value has been reassessed in Chapter 8 of this Assessment (Section 8.2.2), and the recommendation made that the value of α be increased to 60 (65 for the Antarctic stratosphere). As a consequence, the semi-empirically determined values of ODPs for all brominated source gases have now increased. Some models that also include VSLS in their calculations suggest even larger values for α. For example, Sinnhuber et al. (2006), using the University of Bremen two-dimensional model (Chipperfield and Feng, 2003), derive values for α of 66 without Br_y^{VSLS} and 69 including Br_y^{VSLS}, suggesting an impact on α from halogenated VSLS. Updated versions of the Atmospheric and Environmental Research, Inc., (AER) (U.S.) and University of Illinois at Urbana-Champaign (UIUC) (U.S.) models that include Br_y^{VSLS} from gases discussed earlier in this chapter (i.e., CH_2Cl_2, $CHCl_3$, C_2HCl_3, C_2Cl_4, CH_2BrCl, CH_2Br_2, $CHBr_2Cl$, $CHBrCl_2$, and $CHBr_3$) both derive an α of 61. More work is needed to assess the importance of Br_y^{VSLS} on α.

There was no attempt in WMO (2003) to quantify the effects of halogenated VSLS on past trends, or on future changes in stratospheric ozone or ozone columns. Since then, there has been increasing awareness that VSLS have a potentially important effect on chlorine and bromine in the lower stratosphere. As discussed in Section 2.5 of this report, halogenated VSLS appear to add about 5 ppt, on average, of reactive bromine (Br_y) to the lower stratosphere. Although significant uncertainties remain, analyses with the AER 2-D chemical transport model in Salawitch et al. (2005) suggest that this constant amount of Br_y added to the lower stratosphere has a noticeable impact on past trends in column ozone, as shown in Figure 2-12. Similar results were found using the University of Bremen 2-D model (Sinnhuber et al., 2006). Indeed, the inclusion of additional Br_y^{VSLS} may lead to better agreement between modeled and observed stratospheric ozone trends, particularly during times of perturbed aerosol loading, especially in the Northern Hemisphere (Salawitch et al., 2005; Sinnhuber et al., 2006). (Similar findings are discussed in Chapter 3, Section 3.4.3.2, and shown in Figure 3-25.) Both of these simulations assumed that Br_y^{VSLS} was constant over time, due to primarily natural sources. Increased ozone depletion due to Br_y^{VSLS} was caused by the ability of bromine to enhance ozone loss by ClO derived from CFCs, as outlined above (Chapter 3 also discusses impacts of Br_y^{VSLS} on ozone trends). The effect of anthropogenic emissions of Br_y^{VSLS} or possible long-term changes in Br_y^{VSLS} due to climate change or natural variability, have yet to be studied (see Section 2.7).

Several recent studies (e.g., von Glasow et al., 2004; Yang et al., 2005) suggest that inorganic bromine from halogenated VSLS could lead to reductions in tropospheric ozone. The effect on tropospheric ozone should largely be regional in nature, but may have implications on global-scale ozone concentrations. Reductions in ozone occur due to a direct effect (increased loss by the BrO + HO_2 cycle) and an indirect effect (reduced production due to decreased levels of NO) that is ultimately driven by increased efficiency of the $BrONO_2$ hydrolysis sink of NO_x (Lary, 2005). More accurate evaluations will be dependent on improved knowledge about the bromine budget in the troposphere. If anthropogenic production of brominated VSLS becomes important in the future, the effect of inorganic product gas on tropospheric ozone will have to be evaluated to quantify the impact of these compounds on total column ozone.

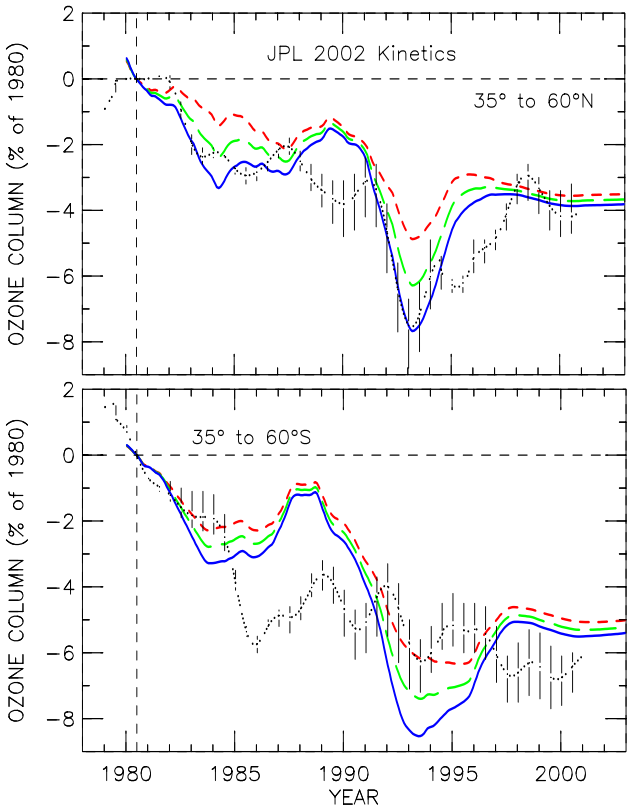

Figure 2-12. Calculated change in column ozone relative to 1980 levels using the AER 2-D model for stratospheric Br_y^{VSLS} of 0 (red), 4 (green), and 8 (blue) ppt for 35°N-60°N (top) and for 35°S-60°S (bottom), compared with observed trends in total ozone (black line). Based on Salawitch et al. (2005).

2.6.2 ODPs for Halogenated VSLS

There have been only a few new reported studies of the ODPs for VSL SGs since the last Assessment. The additional model estimates of SGI and PGI fluxes provide an opportunity to update the estimates for ODP using Equation 2.15 from Ko and Poulet et al. (2003). Using the results discussed in Section 2.5.1 as a guideline, it is reasonable to assume that for a source gas with a local tropospheric lifetime of about 25 days and uniform landmass emissions, 1% of the emitted flux enters the stratosphere via the SGI and PGI pathways. We make the additional assumption that the residence time of the Br_y introduced by either pathway is similar to that of the Br_y produced by long-lived SGs. The order of magnitude estimate for the ODP of a species with molecular weight comparable to that of CFC-11, and a local lifetime of about 25 days, can be determined to be c. 0.003 if it contains 1 chlorine atom, and c. 0.18 if it contains 1 bromine atom (assuming an alpha factor of 60 for bromine). A simple scaling for iodinated compounds is not possible because of their shorter lifetimes and the uncertainty of the alpha factor for iodine. The resulting ODP for any given compound with the above characteristics would be linearly dependent on the number of chlorine or bromine atoms.

Using the UIUC zonally averaged 2-D model, Li et al. (2006) have re-evaluated the ODPs for surface emissions of trifluoroiodomethane (CF_3I), a compound that is proposed as a replacement for bromotrifluoromethane (halon-1301, $CBrF_3$) in firefighting and inhibition applications. The model used an updated representation of iodine chemistry relative to an earlier study of the ODP of CF_3I (Solomon et al., 1994). They found an ODP of 0.013 for emissions evenly distributed over the Northern Hemisphere (compared with <0.008 from Solomon et al. (1994)), 0.011 for emissions distributed over 30°N to 60°N, and 0.018 for emissions distributed over 5°S to 30°N. Li et al. (2006) also consider the effects of potentially using CF_3I in aircraft. The resulting ODPs depend heavily on the altitude and latitude of the emissions. For example, emissions peaking at 6-9 km were calculated to give an ODP of 0.084 for emissions occurring at 30°N-40°N and 0.25 for emissions occurring at 0-10°N. Another proposed replacement for halon-1301 in aircraft engine fire applications, phosphorus tribromide (PBr_3), has not been evaluated, but should also have non-zero ODPs.

The ODP of n-propyl bromide was considered at length in WMO (2003), but there have been no new evaluations since that date.

2.7 POTENTIAL FUTURE CONSIDERATIONS

The impact of halogenated VSLS on stratospheric halogen loading and ozone depletion is, as discussed in Sections 2.5.1 and 2.6.1, currently thought to be relatively small (but significant) compared with that from the long-lived halocarbons. The present-day impact arises principally from the brominated VSLS, whereas the contributions from chlorinated and iodinated gases (for instance, to EESC) are small.

This situation could potentially change in the future. Small anthropogenic emissions of halogenated VSLS already exist (e.g., n-C_3H_7Br, $CHCl_3$, CH_2Cl_2, C_2Cl_4, etc.; see Section 2.2.4). These could increase in the future (although several of these have evidently decreased in the last decade, as previously discussed), or new products could enter commercial use (e.g., CF_3I; Sections 2.2.4.3 and 2.6.2). However, as noted previously, the majority of halogenated VSLS have partly or wholly natural origins, and therefore contribute to the natural background halogen loading of the stratosphere. This is set against a future trend of declining concentrations of long-lived anthropogenic halogenated gases, and hence a potentially larger relative impact from halogenated VSLS.

The exact sources and intensities of natural VSLS emissions are largely linked to biogenic activity in both the marine and terrestrial biospheres (there is also evidence of some abiotic marine emissions; see Section 2.2.3.2). It is conceivable that biogenic emissions could change in response to, for example, changing global temperatures, atmospheric CO_2, rainfall, land use, vegetative cover, and oceanic productivity. Evidence for this is presently sparse (Section 2.2). In one study (Butler et al., 2006), positive correlations between open ocean flux rates of $CHBr_3$ and CH_3I with sea surface temperature (SST) were reported. The authors noted, however, that SST might simply be a proxy for some other driver (e.g., incident radiation, latitude, etc.). They further noted that while SST (and also wind speed) largely dictate sea-air flux rates, other significant parameters, such as nutrient supply and stratification of surface waters, are also affected by SST and wind speed, and may have important modifying effects (both positive and negative) on overall emission rates. Another study, reported in Section 2.2.2, showed that measurements of organo-halogen emissions from rice paddies indicate an apparent positive correlation between temperature and CH_3I emissions (Redeker and Cicerone, 2004). On the other hand, firn records of the atmospheric abundance of several halogenated VSLS suggest minimal

long-term changes throughout the second half of the 20th century, other than small changes in the Northern Hemisphere atmosphere for a few gases with evident anthropogenic sources (Worton et al., 2006; Sturges et al., 2001).

It is noted that inorganic VSLS in the boundary layer, notably BrO from halogen activation reactions (Sections 2.2.5 and 2.5.1.2), might be sensitive to climatic changes. Hollwedel et al. (2004), for instance, suggest a link between observed increases in springtime BrO column density with increased annual sea ice coverage, but we do not consider it likely that boundary layer VSLS from high latitudes will be transported to the stratosphere. There might, however, be a potential link between inorganic halogen released from sea salt in the free troposphere and wind speed-dependent generation of marine aerosol (see also Section 2.2.5).

It is significant that several of the limited studies to date point toward maximum flux rates of halogenated VSLS in the tropics (Section 2.2). This coincides with the region where strong convection can most effectively and quickly transport VSLS to the tropopause region (Section 2.4). Changes in circulation and meteorology in the tropics might also exert a powerful modifying influence on the contribution of VSLS to stratospheric halogen loading. These effects could be either positive or negative. For example, a stronger future Brewer-Dobson circulation (as suggested by Butchart et al., 2006) could increase the rate of vertical transport of VSLS from the TTL into the stratosphere, whereas enhanced precipitation could decrease the efficiency of the PGI route (Section 2.3.4.1). Changes in the latitudes of the subtropical jets, or equivalently the extent of the tropospheric Hadley circulation (Fu et al., 2006), might be associated with changes in quasi-horizontal transport of VSLS from the TTL into the lowermost stratosphere.

Future changes in the chemical processing of VSLS and their product gases could also influence their atmospheric concentrations (Section 2.3), for example, through changes in OH abundance.

Our understanding of these many processes is presently too poor to allow any quantitative prediction of possible future halogenated VSLS trends.

REFERENCES

Abbatt, J.P.D., Interactions of atmospheric trace gases with ice surfaces: Adsorption and reaction, *Chem. Rev., 103* (12), 4783-4800, 2003.

Afe, O.T., A. Richter, B. Sierk, F. Wittrock, and J.P. Burrows, BrO emission from volcanoes: A survey using GOME and SCIAMACHY measurements, *Geophys. Res. Lett., 31*, L24113, doi: 10.1029/2004GL020944, 2004.

Arakawa, A., and W.H. Schubert, Interaction of a cumulus cloud ensemble with large-scale environment, Part 1, *J. Atmos. Sci., 31* (3), 674-701, 1974.

Arnaud, P., Cours de chimie organique, 3rd ed., Gauthier-Villars, Paris, 1966.

Atkinson, R., D.L. Baulch, R.A. Cox, J.N. Crowley, R.F. Hampson, R.G. Hynes, M.E. Jenkin, J.A. Kerr, M.J. Rossi, and J. Troe, *Summary of Evaluated Kinetic and Photochemical Data for Atmospheric Chemistry*, Available: http://www.iupac-kinetic.ch.cam.ac.uk, 2005.

Bale, C.S.E., C.E. Canosa-Mas, D.E. Shallcross, and R.P. Wayne, A discharge-flow study of the kinetics of the reactions of IO with CH_3O_2 and CF_3O_2, Phys. *Chem. Chem. Phys., 7* (10), 2164-2172, 2005.

Barnes, D.H., S.C. Wofsy, B.P. Fehlau, E.W. Gottleib, J.W. Elkins, G.S. Dutton, and S.A. Montzka, Urban/industrial pollution for the New York City-Washington, D.C., corridor, 1996-1998: 1. Providing independent verification of CO and PCE emissions inventories, *J. Geophys. Res., 108* (D6), 4185, 2003.

Barth, M.C., A.L. Stuart, and W.C. Skamarock, Numerical simulations of the July 10, 1996, Stratospheric-Tropospheric Experiment: Radiation, Aerosols, and Ozone (STERAO)-deep convection experiment storm: Redistribution of soluble tracers, *J. Geophys. Res., 106* (D12), 12381-12400, 2001.

Bayes, K.D., R.R. Friedl, S.P. Sander, and D.W. Toohey, Measurements of quantum yields of bromine atoms in the photolysis of bromoform from 266 to 324 nm, *J. Geophys. Res., 108* (D3), 4095, 2003.

Bell, N., L. Hsu, D.J. Jacob, M.G. Schultz, D.R. Blake, J.H. Butler, D.B. King, J.M. Lobert, and E. Maier-Reimer, Methyl iodide: Atmospheric budget and use as a tracer of marine convection in global models, *J. Geophys. Res., 107* (D17), 4340, 2002.

Blake, D., Methane, nonmethane hydrocarbons, alkyl nitrates, and chlorinated carbon compounds including 3 chlorofluorocarbons (CFC-11, CFC-12, and CFC-113) in Whole-air Samples in *Trends: A compendium of data on global change*, Carbon Dioxide Information Analysis Center, Oak Ridge National Laboratory, U.S. Department of Energy, Oak Ridge, Tenn., U.S.A., Available: http://cdiac.esd.ornl.gov/trends/otheratg/blake/blake.html, 2005.

Blake, N.J., D.R. Blake, O.W. Wingenter, B.C. Sive, L.M. McKenzie, J.P. Lopez, I.J. Simpson, H.E. Fuelberg, G.W. Sachse, B.E. Anderson, G.L. Gregory, M.A. Carroll, G. Albercook, and F.S. Rowland, Influence

of southern hemispheric biomass burning on mid-tropospheric distributions of nonmethane hydrocarbons and selected halocarbons over the remote South Pacific, *J. Geophys. Res., 104* (D13), 16213-16232, doi: 10.1029/1999JD900067, 1999a.

Blake, N.J., D.R. Blake, O.W. Wingenter, B.C. Sive, C.H. Kang, D.C. Thornton, A.R. Bandy, E. Atlas, F. Flocke, J.M. Harris, and F.S. Rowland, Aircraft measurements of the latitudinal, vertical, and seasonal variations of NMHCs, methyl nitrate, methyl halides, and DMS during the First Aerosol Characterization Experiment (ACE 1), *J. Geophys. Res., 104* (D17), 21803-21818, doi: 10.1029/1999JD900238, 1999b.

Blake, N.J., D.R. Blake, I.J. Simpson, J.P. Lopez, N.A.C. Johnston, A.L. Swanson, A.S. Katzenstein, S. Meinardi, B.C. Sive, J.J. Colman, E. Atlas, F. Flocke, S.A. Vay, M.A. Avery, and F.S. Rowland, Large-scale latitudinal and vertical distributions of NMHCs and selected halocarbons in the troposphere over the Pacific Ocean during the March-April 1999 Pacific Exploratory Mission (PEM-Tropics B), *J. Geophys. Res., 106* (D23), 32627-32644, 2001.

Blake, N.J., D.R. Blake, I.J. Simpson, S. Meinardi, A.L. Swanson, J.P. Lopez, A.S. Katzenstein, B. Barletta, T. Shirai, E. Atlas, G. Sachse, M. Avery, S. Vay, H.E. Fuelberg, C.M. Kiley, K. Kita, F.S. Rowland, NMHCs and halocarbons in Asian continental outflow during TRACE-P: Comparison to PEM-West B, *J. Geophys. Res., 108* (D20), 8806, 2003a.

Blake, N.J., D.R. Blake, A.L. Swanson, E. Atlas, F. Flocke, and F.S. Rowland, Latitudinal, vertical, and seasonal variations of C1 -C4 alkyl nitrates in the troposphere over the Pacific Ocean during PEM-Tropics A and B: Oceanic and continental sources, *J. Geophys. Res., 108* (D2), 8242, doi: 10.1029/2001JD001444, 2003b.

Bloss, W.J., D.M. Rowley, R.A. Cox, and R.L. Jones, Kinetics and products of the IO self-reaction, *J. Phys. Chem. A, 105* (33), 7840-7854, 2001.

Bobrowski, N., G. Honninger, B. Galle, and U. Platt, Detection of bromine monoxide in a volcanic plume, *Nature, 423* (6937), 273-276, 2003.

Bösch, H., C. Camy-Peyret, M.P. Chipperfield, R. Fitzenberger, H. Harder, U. Platt, and K. Pfeilsticker, Upper limits of stratospheric IO and OIO inferred from center-to-limb-darkening-corrected balloon-borne solar occultation visible spectra: Implications for total gaseous iodine and stratospheric ozone, *J. Geophys. Res., 108* (D15), 4455, 2003.

Brunner, D., J. Staehelin, H.L. Rogers, M.O. Köhler, J.A. Pyle, D. Hauglustaine, L. Jourdain, T.K. Berntsen, M. Gauss, I.S.A. Isaksen, E. Meijer, P. van Velthoven, G. Pitari, E. Mancini, V. Grewe, and R. Sausen, An evaluation of the performance of chemistry transport models by comparison with research aircraft observations. Part 1: Concepts and overall model performance, *Atmos. Chem. Phys., 3*, 1609-1631, 2003.

Bureau, H., H. Keppler, and N. Métrich, Volcanic degassing of bromine and iodine: Experimental fluid/melt partitioning data and applications to stratospheric chemistry, *Earth Planet. Sci. Lett., 183* (1-2), 51-60, 2000.

Butchart, N., A.A. Scaife, M. Bourqui, J. de Grandpré, S.H.E. Hare, J. Kettleborough, U. Langematz, E. Manzini, F. Sassi, K. Shibata, D.Shindell, and M. Sigmond, Simulations of anthropogenic change in the strength of the Brewer-Dobson circulation, *Clim. Dyn., 27* (7-8), 727-741, 2006.

Butler, J.H., D.B. King, S.A. Montzka, J.M. Lobert, S.A. Yvon-Lewis, and N.J. Warwick, Oceanic fluxes of $CHBr_3$, CH_2Br_2, and CH_3I into the marine boundary layer, *Global Biogeochem. Cycles, 21*, doi: 10.1029/2006GB002732, in press, 2006.

Butz, A., *Case Studies of Stratospheric Nitrogen, Chlorine, and Iodine Photochemistry Based on Balloon borne UV/visible and IR Absorption Spectroscopy*, Ph.D. thesis, University of Heidelberg, Heidelberg, Germany, Available: http://www.ub.uni-heidelberg.de/archiv/6696, 2006.

Carpenter, L.J., Iodine in the Marine Boundary Layer, *Chem. Rev., 103* (12), 4953-4962, 2003.

Carpenter, L.J., and P.S. Liss, On temperate sources of bromoform and other reactive organic bromine gases, *J. Geophys. Res., 105* (D16), 20539-20548, 2000.

Carpenter, L.J., G. Malin, P.S. Liss, and F.S. Küpper, Novel biogenic iodine-containing trihalomethanes and other short-lived halocarbons in the coastal East Atlantic, *Global Biogeochem. Cycles, 14* (4), 1191-1204, 2000.

Carpenter, L.J., P.S. Liss, and S.A. Penkett, Marine organohalogens in the atmosphere over the Atlantic and Southern Oceans, *J. Geophys. Res., 108* (D9), 4256, 2003.

Carpenter, L.J., D.J. Wevill, S. O'Doherty, G. Spain, and P.G. Simmonds, Atmospheric bromoform at Mace Head, Ireland: seasonality and evidence for a peatland source, *Atmos. Chem. Phys., 5*, 2927-2934, 2005.

Chance, K., Analysis of BrO measurements from the Global Ozone Monitoring Experiment, *Geophys. Res. Lett., 25* (17), 3335-3338, 1998.

Chen, P., Isentropic cross-tropopause mass exchange in the extratropics, *J. Geophys. Res., 100* (D8), 16661-16674, 1995.

Chipperfield, M.P., and W. Feng, Comment on: Stratospheric Ozone Depletion at northern mid-latitudes in the 21st century: The importance of future concentrations of greenhouse gases nitrous oxide and methane, *Geophys. Res. Lett., 30* (7), 1389, doi: 10.1029/2002GL016353, 2003.

Choi, Y., S. Elliott, I.J. Simpson, D.R. Blake, J.J. Colman, M.K. Dubey, S. Meinardi, F.S. Rowland, T. Shirai, and F.A. Smith, Survey of whole air data from the second airborne Biomass Burning and Lightning Experiment using principal component analysis, *J. Geophys. Res., 108* (D5), 4163, doi: 10.1029/2002JD002841, 2003.

Chuck, A.L., S.M. Turner, and P.S. Liss, Oceanic distributions and air-sea fluxes of biogenic halocarbons in the open ocean, *J. Geophys. Res., 110*, C10022, doi: 10.1029/2004JC002741, 2005.

Cohan, D.S., G.A. Sturrock, A.P. Biazar, and P.J. Fraser, Atmospheric methyl iodide at Cape Grim, Tasmania, from AGAGE observations, *J. Atmos. Chem., 44* (2), 131-150, 2003.

Collins, W.J., R.G. Derwent, C.E. Johnson, and D.S. Stevenson, A comparison of two schemes for the convective transport of chemical species in a Lagrangian global chemistry model, *Quart. J. Roy. Meteorol. Soc., 128* (581), 991-1009, 2002.

Considine, D.B., D.J. Bergmann, and H. Liu, Sensitivity of Global Modeling Initiative chemistry and transport model simulations of radon-222 and lead-210 to input meteorological data, *Atmos. Chem. Phys., 5*, 3389-3406, 2005.

Cox, M.L., G.A. Sturrock, P.J. Fraser, S.T. Siems, and P.B. Krummel, Identification of regional sources of methyl bromide and methyl iodide from AGAGE observations at Cape Grim, Tasmania, *J. Atmos. Chem., 50* (1), 59-77, 2005.

Crutzen, P.J., and M.G. Lawrence, The impact of precipitation scavenging on the transport of trace gases: A 3-dimensional model sensitivity study, *J. Atmos. Chem., 37* (1), 81-112, 2000.

Davis, D., J. Crawford, S. Liu, S. McKeen, A. Bandy, D. Thornton, F. Rowland, and D. Blake, Potential impact of iodine on tropospheric levels of ozone and other critical oxidants, *J. Geophys. Res., 101* (D1), 2135-2147, 1996.

Deiber, G., C. George, S. Le Calvé, F. Schweitzer, and P. Mirabel, Uptake study of $ClONO_2$ and $BrONO_2$ by halide containing droplets, *Atmos. Chem. Phys., 4* (5), 1291-1299, 2004.

Dessler, A.E., and S.C. Sherwood, Effect of convection on the summertime extratropical lower stratosphere, *J. Geophys. Res., 109*, D23301, doi: 10.1029/2004JD005209, 2004.

Dessler, A.E., E.J. Hintsa, E.M. Weinstock, J.G. Anderson, and K.R. Chan, Mechanisms controlling water vapor in the lower stratosphere: "A tale of two stratospheres," *J. Geophys. Res., 100* (D11), 23167-23172, 1995.

Donner, L.J., C.J. Seman, R.S. Hemler, and S. Fan, A cumulus parameterization including mass fluxes, convective vertical velocities, and mesoscale effects: Thermodynamic and hydrological aspects in a general circulation model, *J. Clim., 14* (16), 3444-3463, 2001.

Dorf, M., *Investigation of Inorganic Stratospheric Bromine Using Balloon-borne DOAS Measurements and Model Simulations*, Ph.D. thesis, University of Heidelberg, Heidelberg, Germany, Available: http://www.ub.uni-heidelberg.de/archiv/6093, 2005.

Dorf, M., H. Bösch, A. Butz, C. Camy-Peyret, M.P. Chipperfield, A. Engel, F. Goutail, K. Grunow, F. Hendrick, S. Hrechanyy, B. Naujokat, J.-P. Pommereau, M. Van Roozendael, C. Sioris, F. Stroh, F. Weidner, and K. Pfeilsticker, Balloon-borne stratospheric BrO measurements: comparison with Envisat/SCIAMACHY BrO limb profiles, *Atmos. Chem. Phys., 6* (9), 2483-2501, 2006a.

Dorf, M., J.H. Butler, A. Butz, C. Camy-Peyret, M.P. Chipperfield, L. Kritten, S.A. Montzka, B. Simmes, F. Weidner, and K. Pfeilsticker, Long-term observations of stratospheric bromine reveal slow down in growth, *Geophys. Res. Lett., 33*, doi: 10.1029/2006GL027714, in press, 2006b.

Dvortsov, V.L., M.A. Geller, V.A. Yudin, and S.P. Smyshlyaev, Parameterization of the convective transport in a two-dimensional chemistry-transport model and its validation with radon 222 and other tracer simulations, *J. Geophys. Res., 103* (D17), 22047-22062, 1998.

Dvortsov, V.L., M.A. Geller, S. Solomon, S.M. Schauffler, E.L. Atlas, and D.R. Blake, Rethinking reactive halogen budgets in the midlatitude lower stratosphere, *Geophys. Res. Lett., 26* (12), 1699-1702, 1999.

Ekman, A.M.L., C. Wang, J. Wilson, and J. Ström, Explicit simulations of aerosol physics in a cloud-resolving model: a sensitivity study based on an observed convective cloud, *Atmos. Chem. Phys., 4*, 773-791, 2004.

Engel, A., H. Bönisch, D. Brunner, H. Fischer, H. Franke,

G. Günther, C. Gurk, M. Hegglin, P. Hoor, R. Königstedt, M. Krebsbach, R. Maser, U. Parchatka, T. Peter, D. Schell, C. Schiller, U. Schmidt, N. Spelten, T. Szabo, U. Weers, H. Wernli, T. Wetter, and V. Wirth, Highly resolved observations of trace gases in the lowermost stratosphere and upper troposphere from the Spurt project: An overview, *Atmos. Chem. Phys., 6*, 283-301, 2006.

Fernandez, M.A., R.A. Cox, and R.G. Hynes, Kinetics of ClONO2 reactive uptake on ice surfaces at temperatures of the upper troposphere, *J. Phys. Chem. A, 109* (44), 9986-9996, 2005.

Fischer, H., F.G. Wienhold, P. Hoor, O. Bujok, C. Schiller, P. Siegmund, M. Ambaum, H.A. Scheeren, and J. Lelieveld, Tracer correlations in the northern high latitude lowermost stratosphere: Influence of cross-tropopause mass exchange, *Geophys. Res. Lett., 27* (1), 97-100, 2000.

Fischer, H., M. de Reus, M. Traub, J. Williams, J. Lelieveld, J. de Gouw, C. Warneke, H. Schlager, A. Minikin, R. Scheele, and P. Siegmund, Deep convective injection of boundary layer air into the lowermost stratosphere at midlatitudes, *Atmos. Chem. Phys., 3*, 739-745, 2003.

Fitzenberger, R., H. Bösch, C. Camy-Peyret, M.P. Chipperfield, H. Harder, U. Platt, B.-M. Sinnhuber, T. Wagner, and K. Pfeilsticker, First profile measurements of tropospheric BrO, *Geophys. Res. Lett., 27* (18), 2921-2924, 2000.

Folkins, I., and R.V. Martin, The vertical structure of tropical convection and its impact on the budgets of water vapor and ozone, *J. Atmos. Sci., 62* (5), 1560-1573, 2005.

Folkins, I., M. Loewenstein, J. Podolske, S.J. Oltmans, and M. Proffitt, A barrier to vertical mixing at 14 km in the tropics: Evidence from ozonesondes and aircraft measurements, J. Geophys. Res., 104 *(D18), 22095-22102, 1999*.

Fraser, P.J., D.E. Oram, C.E. Reeves, S.A. Penkett, and A. McCulloch, Southern hemispheric halon trends (1978-1998) and global halon emissions, *J. Geophys. Res., 104* (D13), 15985-15999, 1999.

Frieler, K., M. Rex, R.J. Salawitch, T. Canty, M. Streibel, R.M. Stimpfle, K. Pfeilsticker, M. Dorf, D.K. Weisenstein, S. Godin-Beekmann, and P. von der Gathen, Toward a better quantitative understanding of polar stratospheric ozone loss, *Geophys. Res. Lett., 33*, L10812, doi: 10.1029/2005GL025466, 2006.

Frieß, U., T. Wagner, I. Pundt, K. Pfeilsticker, and U. Platt, Spectroscopic measurements of tropospheric iodine oxide at Neumayer Station, Antarctica, *Geophys. Res. Lett., 28* (10), 1941-1944, 2001.

Fromm, M.D., and R. Servranckx, Transport of forest fire smoke above the tropopause by supercell convection, *Geophys. Res. Lett., 30* (10), 1542, 2003.

Fromm, M., R. Bevilacqua, R. Servranckx, J. Rosen, J.P. Thayer, J. Herman, and D. Larko, Pyro-cumulonimbus injection of smoke to the stratosphere: Observations and impact of a super blowup in northwestern Canada on 3-4 August 1998, *J. Geophys. Res., 110*, D08205, doi: 10.1029/2004 JD005350, 2005.

Fu, Q., C.M. Johanson, J.M. Wallace, and T. Reichler, Enhanced mid-latitude tropospheric warming in satellite measurements, *Science, 312* (5777), 1179, 2006.

Füeglistaler, S., H. Wernli, and T. Peter, Tropical troposphere-to-stratosphere transport inferred from trajectory calculations, *J. Geophys. Res., 109*, D03108, doi: 10.1029/2003JD004069, 2004.

Gettelman, A., and P.M.F. Forster, A climatology of the tropical tropopause layer, *J. Meteorol. Soc. Japan, 80* (4B), 911-924, 2002.

Gettelman, A., P.M.F. Forster, M. Fujiwara, Q. Fu, H. Vömel, L.K. Gohar, C. Johanson, and M. Ammerman, Radiation balance of the tropical tropopause layer, *J. Geophys. Res., 109*, D07103, doi: 10.1029/2003JD004190, 2004.

Harder, H., C. Camy-Peyret, F. Ferlemann, R. Fitzenberger, T. Hawat, H. Osterkamp, M. Schneider, D. Perner, U. Platt, P. Vradelis, and K. Pfeilsticker, Stratospheric BrO profiles measured at different latitudes and seasons: Atmospheric observations, *Geophys. Res. Lett., 25* (20), 3843-3846, 1998.

Haynes, P., and E. Shuckburgh, Effective diffusivity as a diagnostic of atmospheric transport 2. Troposphere and lower stratosphere, *J. Geophys. Res., 105* (D18), 22795-22810, 2000.

Hegels, E., P.J. Crutzen, T. Klüpfel, D. Perner, and J.P. Burrows, Global distribution of atmospheric bromine-monoxide from GOME on earth observing satellite ERS-2, *Geophys. Res. Lett., 25* (16), 3127-3130, 1998.

Hegglin, M.I., D. Brunner, H. Wernli, C. Schwierz, O. Martius, P. Hoor, H. Fischer, U. Parchatka, N. Spelten, C. Schiller, M. Krebsbach, U. Weers, J. Staehelin, and T. Peter, Tracing troposphere-to-stratosphere transport above a mid-latitude deep convective system, *Atmos. Chem. Phys., 4*, 741-756, 2004.

Hintsa, E.J., K.A. Boering, E.M. Weinstock, J.G. Anderson, B.L. Gary, L. Pfister, B.C. Daube, S.C.

Wofsy, M. Loewenstein, J.R. Podolske, J.J. Margitan, and T.P. Bui, Troposphere-to-stratosphere transport in the lowermost stratosphere from measurements of H_2O, CO_2, N_2O and O_3, *Geophys. Res. Lett., 25* (14), 2655-2658, 1998.

Hoffmann, T., C.D. O'Dowd, and J.H. Seinfeld, Iodine oxide homogeneous nucleation: An explanation for coastal new particle production, *Geophys. Res. Lett., 28* (10), 1949-1952, 2001.

Hollwedel, J., M. Wenig, S. Beirle, S. Kraus, S. Kühl, W. Wilms-Grabe, U. Platt, and T. Wagner, Year-to-year variations of spring time polar tropospheric BrO as seen by GOME, *Adv. Space Res., 34* (4), 804-808, 2004.

Holton, J.R., P.H. Haynes, M.E. McIntyre, A.R. Douglass, R.B. Rood, and L. Pfister, Stratosphere-troposphere exchange, *Rev. Geophys., 33* (4), 403-439, 1995.

Hoor, P., H. Fischer, L. Lange, J. Lelieveld, and D. Brunner, Seasonal variations of a mixing layer in the lowermost stratosphere as identified by the CO-O_3 correlation from in situ measurements, *J. Geophys. Res., 107* (D5), 4044, 2002.

Hoor, P., C. Gurk, D. Brunner, M.I. Hegglin, H. Wernli, and H. Fischer, Seasonality and extent of extra-tropical TST derived from in-situ CO measurements during SPURT, *Atmos. Chem. Phys., 4*, 1427-1442, 2004.

Hoor, P., H. Fischer, and J. Lelieveld, Tropical and extra-tropical tropospheric air in the lowermost stratosphere over Europe: A CO-based budget, *Geophys. Res. Lett., 32*, L07802, doi: 10.1029/2004 GL022018, 2005.

Iraci, L.T., R.R. Michelsen, S.F.M. Ashbourn, T.A. Rammer, and D.M. Golden, Uptake of hypobromous acid (HOBr) by aqueous sulfuric acid solutions: Low-temperature solubility and reaction, *Atmos. Chem. Phys., 5*, 1577-1587, 2005.

Joseph, D.M., S.H. Ashworth, and J.M.C. Plane, The absorption cross-section and photochemistry of OIO, *J. Photochem. Photobiol. A, 176* (1-3 Spec. Iss.), 68-77, 2005.

Kärcher, B., and M.M. Basko, Trapping of trace gases in growing ice crystals, J. Geophys. Res., 109, D22204, doi: 10.1029/2004JD005254, 2004.

Kärcher, B., and U. Lohmann, A parameterization of cirrus cloud formation: Heterogeneous freezing, *J. Geophys. Res., 108* (D14), 4402, 2003.

Keene, W.C., M.A.K. Khalil, D.J. Erickson III, A. McCulloch, T.E. Graedel, J.M. Lobert, M.L. Aucott, S.L. Gong, D.B. Harper, G. Kleiman, P. Midgley, R.M. Moore, C. Seuzaret, W.T. Sturges, C.M. Benkovitz, V. Koropalov, L.A. Barrie, and Y.F. Li, Composite global emissions of reactive chlorine from anthropogenic and natural sources: Reactive Chlorine Emissions Inventory, *J. Geophys. Res., 104* (D7), 8429-8440, 1999.

Khalil, M.A.K., Reactive chlorine compounds in the atmosphere, Chapter 2 in *Reactive Halogen Compounds in the Atmosphere, Vol. 4, Part E of The Handbook of Environmental Chemistry*, edited by P. Fabian, and O.N. Singh, 45-79, Springer-Verlag, Heidelberg, Germany, 1999.

Khalil, M.A.K., and R.A. Rasmussen, Atmospheric chloroform, *Atmos. Environ., 33* (7), 1151-1158, 1999.

Khalil, M.A.K., R.M. Moore, D.B. Harper, J.M. Lobert, D.J. Erickson, V. Koropalov, W.T. Sturges, and W.C. Keene, Natural emissions of chlorine-containing gases: Reactive Chlorine Emissions Inventory, *J. Geophys. Res., 104* (D7), 8333-8346, 1999.

Kindler, T.P., W.L. Chameides, P.H. Wine, D.M. Cunnold, F.N. Alyea, and J.A. Franklin, The fate of atmospheric phosgene and the stratospheric chlorine loadings of its parent compounds: CCl_4, C_2Cl_4, C2HCl3, CH_3CCl_3, and $CHCl_3$, *J. Geophys. Res., 100* (D1), 1235-1252, 1995.

Knight, G.P., and J.N. Crowley, The reactions of IO with HO_2, NO and CH_3SCH_3: Flow tube studies of kinetics and product formation, *Phys. Chem. Chem. Phys., 3*, 393-401, 2001.

Ko, M.K.W., and G. Poulet (Lead Authors), D.R. Blake, O. Boucher, J.H. Burkholder, M. Chin, R.A. Cox, C. George, H.-F. Graf, J.R. Holton, D.J. Jacob, K.S. Law, M.G. Lawrence, P.M. Midgley, P.W. Seakins, D.E. Shallcross, S.E. Strahan, D.J. Wuebbles, and Y. Yokouchi, Very short-lived halogen and sulfur substances, Chapter 2 in *Scientific Assessment of Ozone Depletion: 2002, Global Ozone Research and Monitoring Project–Report No. 47*, World Meteorological Organization, Geneva, Switzerland, 2003.

Ko, M.K.W., N.D. Sze, C.J. Scott, and D.K. Weisenstein, On the relation between stratospheric chlorine/bromine loading and short-lived tropospheric source gases, *J. Geophys. Res., 102* (D21), 25507-25518, 1997.

Kondo, Y., M. Koike, K. Kita, H. Ikeda, N. Takegawa, S. Kawakami, D. Blake, S.C. Liu, M. Ko, Y. Miyazaki, H. Irie, Y. Higashi, B. Liley, N. Nishi, Y. Zhao, and T. Ogawa, Effects of biomass burning, lightning, and convection on O_3, CO, and NO_y over the tropical Pacific and Australia in August–October 1998 and 1999, *J. Geophys. Res., 108* (D3), 8402, doi: 10.1029/2001JD000820, 2002.

Krämer, M., C. Schiller, H. Ziereis, J. Ovarlez, and H.

Bunz, Nitric acid partitioning in cirrus clouds: The role of aerosol particles and relative humidity, *Tellus, 58B* (2), 141-147, 2006.

Krebsbach, M., C. Schiller, D. Brunner, G. Günther, M.I. Hegglin, D. Mottaghy, M. Riese, N. Spelten, and H. Wernli, Seasonal cycles and variability of O_3 and H_2O in the UT/LMS during SPURT, *Atmos. Chem. Phys., 6*, 109-125, 2006.

Küpper, C., J. Thuburn, G.C. Craig, and T. Birner, Mass and water transport into the tropical stratosphere: A cloud-resolving simulation, *J. Geophys. Res., 109*, D10111, doi: 10.1029/2004JD004541, 2004.

Kurylo, M.J., and J.M. Rodríguez (Lead Authors), M.O. Andreae, E.L. Atlas, D.R. Blake, J.H. Butler, S. Lal, D.J. Lary, P.M. Midgley, S.A. Montzka, P.C. Novelli, C.E. Reeves, P.G. Simmonds, L.P. Steele, W.T. Sturges, R.F. Weiss, and Y. Yokouchi, Short-lived ozone-related compounds, Chapter 2 in *Scientific Assessment of Ozone Depletion: 1998*, World Meteorological Organization, Geneva, Switzerland, 1999.

Lary, D.J., Halogens and the chemistry of the free troposphere, *Atmos. Chem. Phys., 5*, 277-237, 2005.

Laturnus, F., C. Wiencke, and H. Kloser, Antarctic macroalgae - Sources of volatile halogenated organic compounds, *Mar. Environ. Res., 41* (2), 169-181, 1996.

Lawrence, M.G., and P.J. Rasch, Tracer transport in deep convective updrafts: Plume ensemble versus bulk formulations, *J. Atmos. Sci., 62* (8), 2880-2894, 2005.

Lee-Taylor, J., and K.R. Redeker, Reevaluation of global emissions from rice paddies of methyl iodide and other species, *Geophys. Res. Lett., 32*, L15801, doi: 10.1029/2005GL022918, 2005.

Leser, H., G. Hönninger, and U. Platt, MAX-DOAS measurements of BrO and NO_2 in the marine boundary layer, *Geophys. Res. Lett., 30* (10), 1537, 2003.

Levine, J.G., P. Braesicke, N.R.P. Harris, N.H. Savage, and J.A. Pyle, Pathways and timescales for troposphere-to-stratosphere transport via the tropical tropopause layer and their relevance for very short lived substances, *J. Geophys. Res*., in press, 2006.

Li, Y., K.O. Patten, D. Youn, and D.J. Wuebbles, Potential impacts of CF_3I on ozone as a replacement for CF_3Br in aircraft applications, *Atmos. Chem. Phys.. 6*, 4559-4568, 2006.

Libuda, H.G., Spektroskopische und kinetische Untersuchungen an halogenierten Carbonylverbindungen von atmosphärischem Interesse, Ph.D. thesis, University of Wuppertal, Germany, 1992.

Liss, P.S., and P.G. Slater, Flux of gases across the air-sea interface, *Nature, 247* (5438), 181-184, 1974.

Livesey, N.J., L.J. Kovalenko, R.J. Salawitch, I.A. MacKenzie, M.P. Chipperfield, W.G. Read, R.F. Jarnot, and J.W. Waters, EOS Microwave Limb Sounder observations of upper stratospheric BrO: Implications for bromine, *Geophys. Res. Lett., 33*, L20817, doi: 10.1029/2006GL026930, 2006.

Lobert, J.M., W.C. Keene, J.A. Logan, and R. Yevich, Global chlorine emissions from biomass burning: Reactive Chlorine Emission Inventory, *J. Geophys. Res., 104* (D7), 8373-8390, 1999.

Low, J.C., N.Y. Wang, J. Williams, and R.J. Cicerone, Measurements of ambient atmospheric C2H5Cl and other ethyl and methyl halides at coastal California sites and over the Pacific Ocean, *J. Geophys. Res., 108* (19), 4608, 2003.

Marcy, T.P., D.W. Fahey, R.S. Gao, P.J. Popp, E.C. Richard, T.L. Thompson, K.H. Rosenlof, E.A. Ray, R.J. Salawitch, C.S. Atherton, D.J. Bergmann, B.A. Ridley, A.J. Weinheimer, M. Loewenstein, E.M. Weinstock, and M.J. Mahoney, Quantifying stratospheric ozone in the upper troposphere with in situ measurements of HCl, *Science, 304* (5668), 261-265, 2004.

Mari, C., D.J. Jacob, and P. Bechtold, Transport and scavenging of soluble gases in a deep convective cloud, *J. Geophys. Res., 105* (D17), 22255-22268, 2000.

Marsh, A.R.W., and W.J. McElroy, The dissociation constant and Henry's law constant of HCl in aqueous solution, *Atmos. Environ., 19* (7), 1075-1080, 1985.

Martino, M., P.S. Liss, and J.M.C. Plane, The photolysis of dihalomethanes in surface seawater, *Environ. Sci. Technol., 39* (18), 7097-7101, 2005.

McCulloch, A., Chloroform in the environment: Occurrence, sources, sinks and effects, Chemosphere, 50 (10), 1291-1308, 2003.

McCulloch, A., M.L. Aucott, T.E. Graedel, G. Kleiman, P.M. Midgley, and Y.-F. Li, Industrial emissions of trichloroethene, tetrachloroethene, and dichloromethane: Reactive Chlorine Emissions Inventory, *J. Geophys. Res., 104* (D7), 8417-8427, 1999.

McElroy, C.T., C.A. McLinden, and J.C. McConnell, Evidence for bromine monoxide in the free troposphere during the Arctic polar sunrise, *Nature, 397* (6717), 338-341, 1999.

McFiggans, G., H. Coe, R. Burgess, J. Allan, M. Cubison, M.R. Alfarra, R. Saunders, A. Saiz-Lopez, J.M.C. Plane, D. Wevill, L. Carpenter, A.R. Rickard, and P.S. Monks, Direct evidence for coastal iodine particles from Laminaria macroalgae - Linkage to emissions of molecular iodine, *Atmos. Chem. Phys., 4* (3), 701-713, 2004.

Misra, A., and P. Marshall, Computational investigations of iodine oxides, *J. Phys. Chem. A, 102* (45), 9056-9060, 1998.

Montzka, S.A., J.H. Butler, B.D. Hall, D.J. Mondeel, and J.W. Elkins, A decline in tropospheric organic bromine, *Geophys. Res. Lett., 30* (15), 1826, 2003.

Moore, R.M., Dichloromethane in North Atlantic waters, *J. Geophys. Res., 109*, C09004, doi: 10.1029/2004-JC002397, 2004.

Moore, R.M., and W. Groszko, Methyl iodide distribution in the ocean and fluxes to the atmosphere, *J. Geophys. Res., 104* (C5), 11163-11172, 1999.

Mössinger, J.C., R.G. Hynes, and R.A. Cox, Interaction of HOBr and HCl on ice surfaces in the temperature range 205-227 K, *J. Geophys. Res., 107* (D24), 4740, 2002.

Mullendore, G.L., D.R. Durran, and J.R. Holton, Cross-tropopause tracer transport in midlatitude convection, *J. Geophys. Res., 110*, D06113, doi: 10.1029/-2004JD005059, 2005.

Müller, R.W., H. Bovensmann, J.W. Kaiser, A. Richter, A. Rozanov, F. Wittrock, and J.P. Burrows, Consistent interpretation of ground based and GOME BrO slant column data, *Adv. Space Res., 29* (11), 1655-1660, 2002.

Muramatsu, Y., and S. Yoshida, Volatilization of methyl iodide from the soil-plant system, *Atmos. Environ., 29* (1), 21-25, 1995.

Murphy, D.M., and D.S. Thomson, Halogen ions and NO+ in the mass spectra of aerosols in the upper troposphere and lower stratosphere, *Geophys. Res. Lett., 27* (19), 3217-3220, 2000.

Murphy, D.M., D.S. Thomson, and T.J. Mahoney, In situ measurements of organics, meteoritic material, mercury, and other elements in aerosols at 5 to 19 kilometers, *Science, 282* (5394), 1664-1669, 1998.

Nassar, R., P.F. Bernath, C.D. Boone, C. Clerbaux, P.F. Coheur, G. Dufour, L. Froidevaux, E. Mahieu, J.C. McConnell, S.D. McLeod, D.P. Murtagh, C.P. Rinsland, K. Semeniuk, R. Skelton, K.A. Walker, and R. Zander, A global inventory of stratospheric chlorine in 2004, *J. Geophys. Res., 111*, D22312, doi: 10.1029/2006JD007073, 2006.

Nedelec, P., V. Thouret, J. Brioude, B. Sauvage, J.-P. Cammas, and A. Stohl, Extreme CO concentrations in the upper troposphere over northeast Asia in June 2003 from the in situ MOZAIC aircraft data, *Geophys. Res. Lett., 32*, L14807, 2005.

Nielsen, J.E., and A.R. Douglass, A simulation of bromoform's contribution to stratospheric bromine, *J. Geophys. Res., 106* (D8), 8089-8100, 2001.

Nober, F.J., H.F. Graf, and D. Rosenfeld, Sensitivity of the global circulation to the suppression of precipitation by anthropogenic aerosols, *Global Planet. Change, 37* (1), 57-80, 2003.

O'Connor, F.M., G. Vaughan, and H. De Backer, Observations of subtropical air in the European mid-latitude lower stratosphere, *Quart. J. Roy. Meteorol. Soc., 125* (560), 2965-2986, 1999.

O'Dowd, C.D., and T. Hoffmann, Coastal new particle formation: A review of the current state-of-the-art, *Environ. Chem., 2*, 245-255, 2005.

Pan, L., S. Solomon, W. Randel, J.F. Lamarque, P. Hess, J. Gille, E.W. Chiou, and M.P. McCormick, Hemispheric asymmetries and seasonal variations of the lowermost stratospheric water vapor and ozone derived from SAGE II data, *J. Geophys. Res., 102* (D23), 28177-28184, 1997.

Pan, L.L., W.J. Randel, B.L. Gary, M.J. Mahoney, and E.J. Hintsa, Definitions and sharpness of the extratropical tropopause: A trace gas perspective, *J. Geophys. Res., 109*, D23103, 2004.

Peters, C., S. Pechtl, J. Stutz, K. Hebestreit, G. Hönninger, K.G. Heumann, A. Schwarz, J. Winterlik, and U. Platt, Reactive and organic halogen species in three different European coastal environments, *Atmos. Chem. Phys., 5*, 3357-3375, 2005.

Pfeilsticker, K., W.T. Sturges, H. Bösch, C. Camy-Peyret, M.P. Chipperfield, A. Engel, R. Fitzenberger, M. Müller, S. Payan, and B.-M. Sinnhuber, Lower stratospheric organic and inorganic bromine budget for the Arctic winter 1998/99, *Geophys. Res. Lett., 27* (20), 3305-3308, 2000.

Plane, J.M.C., D.M. Joseph, B.J. Allan, S.H. Ashworth, and J.S. Francisco, An experimental and theoretical study of the reactions of OIO + NO and OIO + OH, *J. Phys. Chem. A, 110* (1), 93-100, 2006.

Platt, U., and G. Hönninger, The role of halogen species in the troposphere, *Chemosphere, 52* (2), 325-338, 2003.

Popp, P.J., R.S. Gao, T.P. Marcy, D.W. Fahey, P.K. Hudson, T.L. Thompson, B. Kärcher, B.A. Ridley, A.J. Weinheimer, D.J. Knapp, D.D. Montzka, D. Baumgardner, T.J. Garrett, E.M. Weinstock, J.B. Smith, D.S. Sayres, J.V. Pittman, S. Dhaniyala, T.P. Bui, and M.J. Mahoney, Nitric acid uptake on subtropical cirrus cloud particles, *J. Geophys. Res., 109*, D06302, 2004.

Poulida, O., R.R. Dickerson, and A. Heymsfield, Stratosphere-troposphere exchange in a midlatitude mesoscale convective complex. 1. Observations, *J. Geophys. Res., 101* (D3), 6823-6836, 1996.

Prados, A.I., G.E. Nedoluha, R.M. Bevilacqua, D.R. Allen, K.W. Hoppel, and A. Marenco, POAM III ozone in

the upper troposphere and lowermost stratosphere: Seasonal variability and comparisons to aircraft observations, *J. Geophys. Res., 108* (D7), 4218, 2003.

Prinn, R.G., R.F. Weiss, P.J. Fraser, P.G. Simmonds, D.M. Cunnold, F.N. Alyea, S. O'Doherty, P. Salameh, B.R. Miller, J. Huang, R.H.J. Wang, D.E. Hartley, C. Harth, L.P. Steele, G. Sturrock, P.M. Midgley, and A. McCulloch, A history of chemically and radiatively important gases in air deduced from ALE/GAGE/AGAGE, *J. Geophys. Res., 105* (D14), 17751-17792, 2000.

PRTR, *Pollutant Release and Transfer Register 2002-Japan*, PRTR Data, (in Japanese), 197 pp., Minist. Econ. Trade Ind., Tokyo, Available at: http://www.chem.unep.ch/prtr/, 2004.

Pundt, I., J.P. Pommereau, C. Phillips, and E. Lateltin, Upper limit of iodine oxide in the lower stratosphere, *J. Atmos. Chem., 30* (1), 173-185, 1998.

Pundt, I., M. Van Roozendael, T. Wagner, A. Richter, M. Chipperfield, J.P. Burrows, C. Fayt, F. Hendrick, K. Pfeilsticker, U. Platt, and J.-P. Pommereau, Simultaneous UV-vis measurements of BrO from balloon, satellite and ground: implications for tropospheric BrO, in *Stratospheric Ozone 1999, Proc. 5th European Symp., 27* September-1 October 1999, St. Jean de Luz, France, edited by N.R.P. Harris, M. Guirlet, and G.T. Amanatidis, *Air Pollution Research Rep. 73, EUR 19340*, 316-319. European Commission, Luxembourg, 2000.

Pundt, I., J.-P. Pommereau, M.P. Chipperfield, M. Van Roozendael, and F. Goutail, Climatology of the stratospheric BrO vertical distribution by balloon-borne UV-visible spectrometry, *J. Geophys. Res., 107* (D24), 4806, doi: 10.1029/2002JD002230, 2002.

Qiu, L.X., S.H. Shi, S.B. Xing, and X.G. Chen, Rate constants for the reactions of hydroxyl with five halogen-substituted ethanes from 292 to 366 K, *J. Phys. Chem., 96* (2), 685-689, 1992.

Quack, B., and D.W.R. Wallace, Air-sea flux of bromoform: Controls, rates, and implications, *Global Biogeochem. Cycles, 17* (1), 1023, 2003.

Quack, B., E. Atlas, G. Petrick, V. Stroud, S. Schauffler, and D.W.R. Wallace, Oceanic bromoform sources for the tropical atmosphere, *Geophys. Res. Lett., 31*, L23S05, 2004.

Randel, W.J., F. Wu , A. Gettelman, J.M. Russell III, J.M. Zawodny, S.J. Oltmans, Seasonal variation of water vapor in the lower stratosphere observed in Halogen Occultation Experiment data, *J. Geophys. Res., 106* (D13), 14313-14325, 2001.

Randel, W.J., F. Wu, S.J. Oltmans, K. Rosenlof, and G.E. Nedoluha, Interannual changes of stratospheric water vapor and correlations with tropical tropopause temperatures, *J. Atmos. Sci., 61* (17), 2133-2148, 2004.

Randel, W.J., F. Wu, H. Vömel, G.E. Nedoluha, and P. Forster, Decreases in stratospheric water vapor after 2001: Links to changes in the tropical tropopause and the Brewer-Dobson circulation, *J. Geophys. Res., 111*, D12312, doi: 10.1029/2005JD006744, 2006.

Ray, E.A., K.H. Rosenlof, E.C. Richard, P.K. Hudson, D.J. Cziczo, M. Loewenstein, H.-J. Jost, J. Lopez, B. Ridley, A. Weinheimer, D. Montzka, D. Knapp, S.C. Wofsy, B.C. Daube, C. Gerbig, I. Xueref, and R.L. Herman, Evidence of the effect of summertime mid-latitude convection on the subtropical lower stratosphere from CRYSTAL-FACE tracer measurements, *J. Geophys. Res., 109*, D18304, doi: 10.1029/2004JD004655, 2004.

Redeker, K.R., and R.J. Cicerone, Environmental controls over methyl halide emissions from rice paddies, Global Biogeochem. Cycles, 18, GB1027, 2004.

Redeker, K.R., N.-Y. Wang, J.C. Low, A. McMillan, S.C. Tyler, and R.J. Cicerone, Emissions of methyl halides and methane from rice paddies, *Science, 290* (5493), 966-969, 2000.

Redeker, K.R., S. Meinardi, D. Blake, and R. Sass, Gaseous emissions from flooded rice paddy agriculture, *J. Geophys. Res., 108* (D13), 4386, 2003.

Reeves, C.E., W.T. Sturges, G.A. Sturrock, K. Preston, D.E. Oram, J. Schwander, R. Mulvaney, J.-M. Barnola, and J. Chappellaz, Trends of halon gases in polar firn air: Implications for their emission distributions, *Atmos. Chem. Phys., 5* (8), 2055-2064, 2005.

Richter, A., F. Wittrock, A. Ladstätter-Weißenmayer, and J.P. Burrows, GOME measurements of stratospheric and tropospheric BrO, *Adv. Space Res., 29* (11), 1667-1672, 2002.

Richter, U., and D.W.R. Wallace, Production of methyl iodide in the tropical Atlantic Ocean, *Geophys. Res. Lett., 31*, L23S03, doi: 10.1029/2004GL020779, 2004.

Ridley, B., E. Atlas, H. Selkirk, L. Pfister, D. Montzka, J. Walega, S. Donnelly, V. Stroud, E. Richard, K. Kelly, A. Tuck, T. Thompson, J. Reeves, D. Baumgardner, W.T. Rawlins, M. Mahoney, R. Herman, R. Friedl, F. Moore, E. Ray, and J. Elkins, Convective transport of reactive constituents to the tropical and mid-latitude tropopause region: I. Observations, *Atmos. Environ., 38* (9), 1259-1274,

2004.

Rinsland, C.P., D.K. Weisenstein, M.K.W. Ko, C.J. Scott, L.S. Chiou, E. Mahieu, R. Zander, and P. Demoulin, Post-Mount Pinatubo eruption ground-based infrared stratospheric column measurements of HNO_3, NO, and NO_2 and their comparison with model calculations, *J. Geophys. Res., 108* (D15), 4437, 2003.

Rosenlof, K.H., Seasonal cycle of the residual mean meridional circulation in the stratosphere, *J. Geophys. Res., 100* (D3), 5173-5191, 1995.

Rowley, D.M., W.J. Bloss, R.A. Cox, and R.L. Jones, Kinetics and products of the IO + BrO reaction, *J. Phys. Chem. A, 105* (33), 7855-7864, 2001.

Saiz-Lopez, A., and J.M.C. Plane, Novel iodine chemistry in the marine boundary layer, *Geophys. Res. Lett., 31*, L04112, doi: 10.1029/2003GL019215, 2004.

Saiz-Lopez, A., J.M.C. Plane, and J.A. Shillito, Bromine oxide in the mid-latitude marine boundary layer, *Geophys. Res. Lett., 31*, L03111, 2004a.

Saiz-Lopez, A., R.W. Saunders, D.M. Joseph, S.H. Ashworth, and J.M.C. Plane, Absolute absorption cross-section and photolysis rate of I_2, *Atmos. Chem. Phys., 4* (5), 1443-1450, 2004b.

Saiz-Lopez, A., J.M.C. Plane, G. McFiggans, P.I. Williams, S.M. Ball, M. Bitter, R.L. Jones, C. Hongwei, and T. Hoffmann, Modelling molecular iodine emissions in a coastal marine environment: the link to new particle formation, *Atmos. Chem. Phys., 6* (4), 883-895, 2006.

Salawitch, R.J., D.K. Weisenstein, L.J. Kovalenko, C.E. Sioris, P.O. Wennberg, K. Chance, M.K.W. Ko, and C.A. McLinden, Sensitivity of ozone to bromine in the lower stratosphere, *Geophys. Res. Lett., 32* (5), 1-5, 2005.

Saltzman, E.S., M. Aydin, W.J. De Bruyn, D.B. King, and S.A. Yvon-Lewis, Methyl bromide in preindustrial air: Measurements from an Antarctic ice core, *J. Geophys. Res., 109* (5), D05301, 1-8, 2004.

Sander, R., W.C. Keene, A.A.P. Pszenny, R. Arimoto, G.P. Ayers, E. Baboukas, J.M. Cainey, P.J. Crutzen, R.A. Duce, G. Hönninger, B.J. Huebert, W. Maenhaut, N. Mihalopoulos, V.C. Turekian, and R. Van Dingenen, Inorganic bromine in the marine boundary layer: A critical review, *Atmos. Chem. Phys., 3* (5), 1301-1336, 2003.

Sander, S.P., R.R. Friedl, D.M. Golden, M.J. Kuyolo , G.K. Moortgat, H. Keller-Rudek, P.H. Wine, A.R. Ravishankara, C.E. Kolb, M.J. Molina, B.J. Finlayson-Pitts, R.E., Huie, and V.L. Orkin, *Chemical Kinetics and Photochemical Data for Use in Atmospheric Studies: Evaluation No. 15, JPL Publication 06-2*, Jet Propulsion Laboratory, Pasadena, Calif., 2006.

Schauffler, S.M., E.L. Atlas, F. Flocke, R.A. Lueb, V. Stroud, and W. Travnicek, Measurements of bromine containing organic compounds at the tropical tropopause, *Geophys. Res. Lett., 25* (3), 317-320, 1998.

Schauffler, S.M., E.L. Atlas, D.R. Blake, F. Flocke, R.A. Lueb, J.M. Lee-Taylor, V. Stroud, and W. Travnicek, Distributions of brominated organic compounds in the troposphere and lower stratosphere, *J. Geophys. Res., 104* (D17), 21513-21535, 1999.

Scheeren, H.A., J. Lelieveld, J.A. de Gouw, C. van der Veen, and H. Fischer, Methyl chloride and other chlorocarbons in polluted air during INDOEX, *J. Geophys. Res., 107* (D19), 8015, doi: 10.1029/2001JD001121, 2002.

Schofield, R., K. Kreher, B.J. Connor, P.V. Johnston, A. Thomas, D. Shooter, M.P. Chipperfield, C.D. Rodgers, and G.H. Mount, Retrieved tropospheric and stratospheric BrO columns over Lauder, New Zealand, *J. Geophys. Res., 109*, D14304, doi: 10.1029/2003JD004463, 2004.

Schofield, R., P.V. Johnston, A. Thomas, K. Kreher, B.J. Connor, S. Wood, D. Shooter, M.P. Chipperfield, A. Richter, R. von Glasow, and C.D. Rodgers, Tropospheric and stratospheric BrO columns over Arrival Heights, Antarctica, 2002, *J. Geophys. Res., 111*, D22310, doi: 10.1029/2005JD007022, 2006.

Schweitzer, F., P. Mirabel, and C. George, Uptake of hydrogen halides by water droplets, *J. Phys. Chem. A*, 104 (1), 72-76, 2000.

Sheode, N., B.-M. Sinnhuber, A. Rozanov, and J.P. Burrows, Towards a climatology of stratospheric bromine monoxide from SCIAMACHY limb observations, *Atmos. Chem. Phys. Discuss., 6*, 6431-6466, 2006.

Sherwood, S.C., and A.E. Dessler, A model for transport across the tropical tropopause, *J. Atmos. Sci., 58* (7), 765-779, 2001.

Simmonds, P.G., A.J. Manning, D.M. Cunnold, A. McCulloch, S. O'Doherty, R.G. Derwent, P.B. Krummel, P.J. Fraser, B. Dunse, L.W. Porter, R.H.J. Wang, B.R. Greally, B.R. Miller, P. Salameh, R.F. Weiss, and R.G. Prinn, Global trends, seasonal cycles, and European emissions of dichloromethane, trichloroethene, and tetrachloroethene from the AGAGE observations at Mace Head, Ireland, and Cape Grim, Tasmania, *J. Geophys. Res., 111*, D18304, doi: 10.1029/2006JD007082, 2006.

Simpson, I.J., O.W. Wingenter, D.J. Westberg, H.E. Fuelberg, C.M. Kiley, J.H. Crawford, S. Meinardi,

D.R. Blake, and F.S. Rowland, Airborne measurements of cirrus-activated C2Cl4 depletion in the upper troposphere with evidence against Cl reactions, *Geophys. Res. Lett., 30* (20), 2025, doi: 10.1029/2003GL017598, 2003.

Simpson, I.J., S. Meinardi, N.J. Blake, F.S. Rowland, and D.R. Blake, Long-term decrease in the global atmospheric burden of tetrachloroethene (C2Cl4), *Geophys. Res. Lett., 31*, L08108, doi: 10.1029/2003GL019351, 2004.

Singh, H.B., L.J. Salas, and R.E. Stiles, Methyl halides in and over the eastern Pacific (40°N-32°S), *J. Geophys. Res., 88* (C6), 3684-3690, 1983.

Sinnhuber, B.-M., and I. Folkins, Estimating the contribution of bromoform to stratospheric bromine and its relation to dehydration in the tropical tropopause layer, *Atmos. Chem. Phys., 6*, 4755-4761, 2006.

Sinnhuber, B.-M., D.W. Arlander, H. Bovensmann, J.P. Burrows, M.P. Chipperfield, C.-F. Enell, U. Frieß, F. Hendrick, P.V. Johnston, R.L. Jones, K. Kreher, N. Mohamed-Tahrin, R. Müller, K. Pfeilsticker, U. Platt, J.-P. Pommereau, I. Pundt, A. Richter, A.M. South, K.K. Tørnkvist, M. Van Roozendael, T. Wagner, and F. Wittrock, Comparison of measurements and model calculations of stratospheric bromine monoxide, *J. Geophys. Res., 107* (D19), 4398, doi: 10.1029/2001JD000940, 2002.

Sinnhuber, B.-M., A. Rozanov, N. Sheode, O.T. Afe, A. Richter, M. Sinnhuber, F. Wittrock, J.P. Burrows, G.P. Stiller, T. von Clarmann, and A. Linden, Global observations of stratospheric bromine monoxide from SCIAMACHY, *Geophys. Res. Lett., 32*, L20810, doi: 10.1029/2005GL023839, 2005.

Sinnhuber, B.-M., N. Sheode, M. Sinnhuber, M.P. Chipperfield, and W. Feng, The contribution of anthropogenic bromine emissions to past stratospheric ozone trends: A modelling study, *Atmos. Chem. Phys. Discuss., 6*, 6497-6524, 2006.

Sioris, C.E., L.J. Kovalenko, C.A. McLinden, R.J. Salawitch, M. Van Roozendael, F. Goutail, M. Dorf, K. Pfeilsticker, K. Chance, C. von Savigny, X. Liu, T.P. Kurosu, J.-P. Pommereau, H. Bösch, and J. Frerick, Latitudinal and vertical distribution of bromine monoxide in the lower stratosphere from Scanning Imaging Absorption Spectrometer for Atmospheric Chartography limb scattering measurements, *J. Geophys. Res., 111*, D14301, doi: 10.1029/2005JD006479, 2006.

Smythe-Wright, D., S.M. Boswell, C.H. Lucas, A.L. New, and M.S. Varney, Halocarbon and dimethyl sulphide studies around the Mascarene Plateau, *Phil. Trans. R. Soc. Lond. A*, 363 (1826), 169-185, 2005.

Soller, R., J.M. Nicovich, and P.H. Wine, Temperature-dependent rate coefficients for the reactions of $Br(^2P_{3/2})$, $Cl(^2P_{3/2})$, and $O(^3P_J)$ with $BrONO_2$, *J. Phys. Chem. A, 105* (9), 1416-1422, 2001.

Solomon, S., R.R. Garcia, and A.R. Ravishankara, On the role of iodine in ozone depletion, *J. Geophys. Res., 99* (D10), 20491-20499, 1994.

Sprenger, M., and H. Wernli, A northern hemispheric climatology of cross-tropopause exchange for the ERA15 time period (1979-1993), *J. Geophys. Res., 108* (D12), 8521, 2003.

Stohl, A., A 1-year Lagrangian "climatology" of airstreams in the Northern Hemisphere troposphere and lowermost stratosphere, *J. Geophys. Res., 106* (D7), 7263-7279, 2001.

Stohl, A., P. Bonasoni, P. Cristofanelli, W. Collins, J. Feichter, A. Frank, C. Forster, E. Gerasopoulos, H. Gäggeler, P. James, T. Kentarchos, H. Kromp-Kolb, B. Krüger, C. Land, J. Meloen, A. Papayannis, A. Priller, P. Seibert, M. Sprenger, G.J. Roelofs, H.E. Scheel, C. Schnabel, P. Siegmund, L. Tobler, T. Trickl, H. Wernli, V. Wirth, P. Zanis, and C. Zerefos, Stratosphere-troposphere exchange: A review, and what we have learned from STACCATO, *J. Geophys. Res., 108* (D12), 8516, 2003.

Stuart, A.L., and M.Z. Jacobson, A timescale investigation of volatile chemical retention during hydrometeor freezing: Nonrime freezing and dry growth riming without spreading, *J. Geophys. Res., 108* (D6), 4178, 2003.

Sturges, W.T., D.E. Oram, L.J. Carpenter, S.A. Penkett, and A. Engel, Bromoform as a source of stratospheric bromine, *Geophys. Res. Lett., 27* (14), 2081-2084, 2000.

Sturges, W.T., H.P. McIntyre, S.A. Penkett, J. Chappellaz, J.-M. Barnola, R. Mulvaney, E. Atlas, and V. Stroud, Methyl bromide, other brominated methanes and methyl iodide in polar firn air, *J. Geophys. Res., 106* (D2), 1595-1606, 2001.

Stutz, J., R. Ackermann, J.D. Fast, and L. Barrie, Atmospheric reactive chlorine and bromine at the Great Salt Lake, Utah, *Geophys. Res. Lett., 29* (10), 1380, doi: 10.1029/2002GL014812, 2002.

Thompson, T.M. (Ed.), J.H. Butler, B.C. Daube, G.S. Dutton, J.W. Elkins, B.D. Hall, D.F. Hurst, D.B. King, E.S. Kline, B.G. LaFleur, J. Lind, S. Lovitz, D.J. Mondeel, S.A. Montzka, F.L. Moore, J.D. Nance, J.L. Neu, P.A. Romashkin, A. Scheffer, and W.J. Snible, Halocarbons and other atmospheric trace species, in *Climate Monitoring and Diagnostics Laboratory: Summary Report No. 27, 2002-2003*, edited by R.C. Schnell, A.-M. Buggle,

and R.M. Rosson, 115-135, NOAA/Climate Monitoring and Diagnostics Laboratory, Boulder, Colo., 2004.

Thornton, B.F., D.W. Toohey, L.M. Avallone, H. Harder, M. Martinez, J.B. Simpas, W.H. Brune, and M.A. Avery, In situ observations of ClO near the winter polar tropopause, *J. Geophys. Res., 108* (D8), 8333, 2003.

Thuburn, J., and G.C. Craig, On the temperature structure of the tropical substratosphere, *J. Geophys. Res., 107* (D2), 4017, 2002.

Tiedtke, M., A comprehensive mass flux scheme for cumulus parameterization in large-scale models, *Mon. Wea. Rev., 117* (8),1779-1800, 1989.

Toon, G.C., J.-F. Blavier, B. Sen, and B.J. Drouin, Atmospheric $COCl_2$ measured by solar occultation spectrometry, *Geophys. Res. Lett., 28* (14), 2835-2838, 2001.

Trudinger, C.M., D.M. Etheridge, G.A. Sturrock, P.J. Fraser, P.B. Krummel, and A. McCulloch, Atmospheric histories of halocarbons from analysis of Antarctic firn air: Methyl bromide, methyl chloride, chloroform, and dichloromethane, *J. Geophys. Res., 109*, D22310, doi: 10.1029/2004JD004932, 2004.

Tucceri, M.E., D. Holscher, A. Rodriguez, T.J. Dillon, and J.N. Crowley, Absorption cross section and photolysis of OIO, *Phys. Chem. Chem. Phys., 8* (7), 834-846, 2006.

Tuck, A.F., S.J. Hovde, K.K. Kelly, S.J. Reid, E.C. Richard, E.L. Atlas, S.G. Donnelly, V.R. Stroud, D.J. Cziczo, D.M. Murphy, D.S. Thomson, J.W. Elkins, F.L. Moore, E.A. Ray, M.J. Mahoney, and R.R. Friedl, Horizontal variability 1-2 km below the tropical tropopause, *J. Geophys. Res., 109*, D05310, doi: 10.1029/2003JD003942, 2004.

Van Roozendael, M., T. Wagner, A. Richter, I. Pundt, D.W. Arlander, J.P. Burrows, M. Chipperfield, C. Fayt, P.V. Johnston, J.-C. Lambert, K. Kreher, K. Pfeilsticker, U. Platt, J.-P. Pommereau, B.-M. Sinnhuber, K.K. Tørnkvist, and F. Wittrock, Intercomparison of BrO measurements from ERS-2 GOME, ground-based and balloon platforms, *Adv. Space Res., 29* (11), 1661-1666, 2002.

Vaughan, G., and C. Timmis, Transport of near-tropopause air into the lower midlatitude stratosphere, *Quart. J. Roy. Meteorol. Soc., 124* (549), 1559-1578, 1998.

von Glasow, R., R. Sander, A. Bott, and P.J. Crutzen, Modeling halogen chemistry in the marine boundary layer 2. Interactions with sulfur and the cloud-covered MBL, *J. Geophys. Res., 107* (D17), 4323, 2002.

von Glasow, R., R. von Kuhlmann, M.G. Lawrence, U. Platt, and P.J. Crutzen, Impact of reactive bromine chemistry in the troposphere, *Atmos. Chem. Phys., 4*, 2481-2497, 2004.

Wagner, T., and U. Platt, Satellite mapping of enhanced BrO concentrations in the troposphere, *Nature, 395* (6701), 486-490, 1998.

Wagner, T., C. Leue, M. Wenig, K. Pfeilsticker, and U. Platt, Spatial and temporal distribution of enhanced boundary layer BrO concentrations measured by the GOME instrument aboard ERS-2, *J. Geophys. Res., 106* (D20), 24225-24235, 2001.

Wamsley, P.R., J.W. Elkins, D.W. Fahey, G.S. Dutton, C.M. Volk, R.C. Myers, S.A. Montzka, J.H. Butler, A.D. Clarke, P.J. Fraser, L.P. Steele, M.P. Lucarelli, E.L. Atlas, S.M. Schauffler, D.R. Blake, F.S. Rowland, W.T. Sturges, J.M. Lee, S.A. Penkett, A. Engel, R.M. Stimpfle, K.R. Chan, D.K. Weisenstein, M.K.W. Ko, and R.J. Salawitch, Distribution of halon-1211 in the upper troposphere and lower stratosphere and the 1994 total bromine budget, *J. Geophys. Res., 103* (D1), 1513-1526, 1998.

Wang, P.K., Moisture plumes above thunderstorm anvils and their contributions to cross-tropopause transport of water vapor in midlatitudes, *J. Geophys. Res., 108* (D6), 4194, 2003.

Warwick, N.J., G. Carver, X. Yang, N. Savage, F. O'Connor, R.A. Cox, and J.A. Pyle, Global modeling of natural bromocarbons, *J. Geophys. Res.*, in press, 2006.

Wennberg, P.O., J.W. Brault, T.F. Hanisco, R.J. Salawitch, and G.H. Mount, The atmospheric column abundance of IO: Implications for stratospheric ozone, *J. Geophys. Res., 102* (D7), 8887-8898, 1997.

Wernli, H., and M. Bourqui, A Lagrangian "1-year climatology" of (deep) cross-tropopause exchange in the extratropical Northern Hemisphere, *J. Geophys. Res., 107* (D2), 4021, 2002.

Wittrock, F., R. Müller, A. Richter, H. Bovensmann, and J.P. Burrows, Measurements of iodine monoxide (IO) above Spitsbergen, *Geophys. Res. Lett., 27* (10), 1471-1474, 2000.

WMO (World Meteorological Organization), *Scientific Assessment of Ozone Depletion: 1994, Global Ozone Research and Monitoring Project–Report No. 37*, Geneva, Switzerland, 1995.

WMO (World Meteorological Organization), *Scientific Assessment of Ozone Depletion: 1998, Global Ozone Research and Monitoring Project–Report No. 44*, Geneva, Switzerland, 1999.

WMO (World Meteorological Organization), *Scientific*

Assessment of Ozone Depletion: 2002, Global Ozone Research and Monitoring Project–Report No. 47, Geneva, Switzerland, 2003.

Worton, D.R., W.T. Sturges, J. Schwander, R. Mulvaney, J.-M. Barnola, and J. Chappellaz, 20th century trends and budget implications of chloroform and related tri- and dihalomethanes inferred from firn air, *Atmos. Chem. Phys., 6* (10), 2847-2863, 2006.

Wuebbles, D.J., and M.K.W. Ko, *Summary of EPA/NASA Workshop on the Stratospheric Impacts of Short-Lived Gases*, March 30-31, 1999, Washington D.C., available through the U.S. Environmental Protection Agency, Stratospheric Protection Division, Washington D.C., 1999.

Wuebbles, D.J., K.O. Patten, M.T. Johnson, and R. Kotamarthi, New methodology for Ozone Depletion Potentials of short-lived compounds: n-Propyl bromide as an example, *J. Geophys. Res., 106* (D13), 14551-14571, 2001.

Yang, X., R.A. Cox, N.J. Warwick, J.A. Pyle, G.D. Carver, and F.M. O'Connor, Tropospheric bromine chemistry and its impacts on ozone: A model study, *J. Geophys. Res., 110*, D23311, doi: 10.1029/2005JD006244, 2005.

Yano, J.I., F. Guichard, J.P. Lafore, J.L. Redelsperger, and P. Bechtold, Estimations of mass fluxes for cumulus parameterizations from high-resolution spatial data, *J. Atmos. Sci., 61* (7), 829-842, 2004.

Yin, Y., D.J. Parker, and K.S. Carslaw, Simulation of trace gas redistribution by convective clouds - Liquid phase processes, *Atmos. Chem. Phys., 1*, 19-36, 2001.

Yin, Y., K.S. Carslaw, and D.J. Parker, Redistribution of trace gases by convective clouds - mixed-phase processes, *Atmos. Chem. Phys., 2*, 293-306, 2002.

Yokouchi, Y., T. Inagaki, K. Yazawa, T. Tamaru, T. Enomoto, and K. Izumi, Estimates of ratios of anthropogenic halocarbon emissions from Japan based on aircraft monitoring over Sagami Bay, Japan, *J. Geophys. Res., 110*, D06301, doi: 10.1029/2004JD005320, 2005a.

Yokouchi, Y., F. Hasebe, M. Fujiwara, H. Takashima, M. Shiotani, N. Nishi, Y. Kanaya, S. Hashimoto, P. Fraser, D. Toom-Sauntry, H. Mukai, and Y. Nojiri, Correlations and emission ratios among bromoform, dibromochloromethane, and dibromomethane in the atmosphere, *J. Geophys. Res., 110*, D23309, doi: 10.1029/2005JD006303, 2005b.

Zhou, Y., R.K. Varner, R.S. Russo, O.W. Wingenter, K.B. Haase, R. Talbot, and B.C. Sive, Coastal water source of short-lived halocarbons in New England, *J. Geophys. Res., 110*, D21302, doi: 10.1029/2004JD005603, 2005.

Zingler, J., and U. Platt, Iodine oxide in the Dead Sea Valley: Evidence for inorganic sources of boundary layer IO, *J. Geophys. Res., 110*, D07307, doi: 10.1029/2004JD004993, 2005.